FIRST PRINCIPLES COMPUTATION OF ELECTRONIC STRUCTURE, DYNAMICAL AND SUPERCONDUCTING PROPERTIES OF PEROVSKITE LANTHANUM BARIUM CUPRATE ($LaBa_2Cu_3O_7$)

CHEROTICH SEVILLE

A Thesis Submitted to the Institute of Postgraduate Studies of Kabarak University in Partial Fulfilment of the Requirements for the Award of the Masters of Science in Physics Degree

KABARAK UNIVERSITY

AUGUST, 2025

DECLARATION

1. I do declare that:

i. This thesis is my original work and has not been presented for a degree in any other University or institution of higher learning or any other award.

ii. That the work has not incorporated material from other works or a paraphrase of such material without due and appropriate acknowledgement

iii. That the work has been subjected to processes of anti-plagiarism and has met Kabarak University's 15% similarity index threshold

2. I do understand that issues of academic integrity are paramount, and therefore, I may be suspended or expelled from the University, or my degree may be recalled for academic dishonesty or any other related academic malpractices.

Signed:_____ Date:_____

Cherotich Seville

GMP/M/0276/01/22

RECOMENDATION

To the Institute of Postgraduate Studies:

The thesis entitled "**First Principles Computation of Electronic Structure, Dynamical and Superconducting Properties of Perovskite Lanthanum Barium Cuprate ($LaBa_2Cu_3O_7$),"** written by **Cherotich Seville** is presented to the Institute of Postgraduate Studies of Kabarak University. We have reviewed the thesis and recommend it be accepted in partial fulfilment of the requirement for the award of the Master of Science in Physics Degree.

Signed:_____ Date:_____

Dr. Phillip Nyawere

Department of Physical & Biological Sciences

Kabarak University

Signed:_____ Date:_____

Dr. Peter Tanui

Department of Education Science

Kabarak University

COPYRIGHT

ACKNOWLEDGMENTS

I want to express my deepest gratitude to God for His grace, protection, and good health since I began this work.

I am also grateful to my research supervisors,Dr. Peter Tanui and Dr P.W.O. Nyawere, for their positive encouragement, timely guidance, and unwavering support throughout the duration of this project. Their expertise and insightful feedback have been instrumental in shaping this work.

Furthermore, I extend my appreciation to my family, Dad (Richard Langat), Mom (Josephine Langat), and my siblings for their prayers, financial support, love, patience, and moral support during this endeavour.

DEDICATION

I dedicate this thesis to my siblings, parents (Richard and Josephine), and friends in appreciation of their unwavering love, support, and motivation.

ABSTRACT

Nanoscale superconducting materials have garnered significant attention because they have the potential to develop new and enhanced properties for technological applications. High critical temperature superconductors (Tc) made from transition and lanthanide oxides are particularly promising due to their capability to produce strong currents in magnetic fields. Notably, research has shown that particle size plays a crucial role in enhancing the critical current density in these materials. Perovskite materials have attracted research because of their ability to transition from normal metals to superconductors. They are attractive for a wide range of applications due to their unique characteristics and properties, such as light-emitting diodes, power transmission cables, photovoltaic, and pressure-induced emission. Electronic structure and dynamical properties are key in understanding the behaviour of materials in relation to stability for superconductivity.Both theoretical and experimental approaches have been employed to make new discoveries in these endeavours. This research explored the electronic structure in depth, uncovering essential aspects like bandgaps and Fermi surfaces, as well as offering valuable insights into the material's behaviour. Furthermore, the dynamical properties through investigation of phonon spectra and lattice dynamics to analyse vibrational modes and their impacts on material stability and functionality have been studied.Superconducting properties of $LaBa_2Cu_3O_7$ have also been studied through analysis of critical temperature and superconducting gap through first-principles computation. The main objective of this research was to study externally applied pressure doping, phase transition behaviour, and superconducting properties of $LaBa_2Cu_3O_7$ using *ab initio* approach. The ground state energy was calculated within the framework of density functional theory (DFT), utilizing the plane wave self-consistent field (PWscf) and ultra-soft pseudopotential (USPP) method. This calculation was performed using the Perdew-Burke Ernzerhof (PBE) generalized gradient approximation and local density approximations, as implemented in the Quantum Espresso Code.Under electronic structure, the results showed that $LaBa_2Cu_3O_7$ is an orthorhombic structure with a band gap of 2.043 eV,indicating it’s a semiconductor. However, under pressure, it becomes a superconductor, thus metallic. $LaBa_2Cu_3O_7$ is dynamically stable, as there were no negative frequencies obtained on the phonon dispersion curve. When pressure was induced, it indicated that a pressure of 20 GPa resulted in the highest Tc. From pressure-induced doping, it was confirmed that pressure can induce doping, thereby enhancing the superconductivity transition temperature up to the optimal doping level. The optimal superconductivity transition temperature was found to be higher than the normal transition temperature.

Keywords: *Perovskite, Phase transition, and Orthorhombic*

TABLE OF CONTENTS

LIST OF TABLES

LIST OF FIGURES

LIST OF ACRONYMS AND ABBREVIATIONS

PWscf	Plane wave self-consistent field
HTSC	High temperature superconductors
DFT	Density functional theory
USPP	Ultrasoft pseudopotential
PBE	Perdew-Burke Ernzerhof
QE	Quantum Espresso
GGA	Generalized gradient approximation
PAW	Project Augmented Wave
XRD	X-Ray diffraction
T_c	Transition temperature
LDA	Local density functional approximation
LAPW	Linearized augmented plane wave
DFPT	Density functional perturbation theory
VASP	Vienna Ab initio Simulation Package
E_F	Fermi level
MRI	Magnetic resonance imaging
Jc	Critical current density
SCF	Self-consistent field
K-S	Kohn Sham
BCS	Bardeen-Cooper-Schrieffer
GPa	Gigapascal

OPERATIONAL DEFINITION OF TERMS

Electronic Properties: These are parameters and representations that describe the state and the behaviour of electrons in a material.

Electronic Band Structure of a Material: describes the relationship between the energy levels of electrons and their wavevectors (momentum) in the crystalline solid. It provides information on the allowed energy states that electrons can occupy and the band gaps.

Phonon Dispersion: refers to the relationship between the frequency (or energy) of phonons and their wavevector (momentum) as they propagate through a crystal lattice.

Phonons are quantized modes of vibration of the atoms in a crystal, playing a crucial role in determining the thermal, mechanical, and electronic properties of materials.

Density of States (DOS): represents the number of electronic states per unit energy interval at each energy level that are available to be occupied by electrons.

The Fermi surface is a surface of constant energy in momentum space, specifically at the Fermi energy (the highest occupied energy level at absolute zero temperature).

Debye temperature is a thermodynamic quantity in material science that is associated with the phonon vibrational modes in a crystal, the elastic constant, and specific heat.

Dynamical properties: refer to the behavior and characteristics of its lattice vibrations (phonons), how these vibrations interact with electrons, and how they influence various physical properties. These properties are crucial for understanding the mechanisms behind superconductivity, thermal conductivity, and other temperature-dependent behaviors of the material.

Electron-Phonon Coupling: is the interaction between electrons and phonons, which can affect electrical resistivity and superconducting properties.

Jc: refers to the current density.

CHAPTER ONE

INTRODUCTION

1.1 Introduction

This chapter discusses the background of the concepts on electronic structure, dynamical, and superconducting properties of perovskite materials. It additionally outlines the goals and enumerates the research queries that will direct this research. In addition, the justification, significance, scope of the research, and assumptions are also presented.

1.2 Background to the Study

The origin of superconductivity in cuprates based on perovskite has attracted a lot of interest among researchers in recent years. Superconducting materials obtained at the nanoscale level have attracted a great deal of attention, due to the possibility of generating new and improved properties for potential technological applications (Rivera *et al*, 2016). Superconductivity was discovered by Kamerlingh Onnes (Van, 2012) and is a remarkable macroscopic quantum phenomenon whereby significant efforts have been dedicated to elucidating the mechanism of superconductivity. Superconducting materials have the potential to revolutionize electric power and high-field magnet technology. They enable highly efficient power generation, can carry electricity with zero resistance, significantly reducing energy losses in power transmission, compact and lightweight electrical equipment, high-speed maglev transportation, and the generation of ultra-strong magnetic fields. These advancements can benefit high-resolution MRI systems, nuclear magnetic resonance (NMR) systems, future advanced high-energy particle accelerators, and nuclear fusion reactors.

A perovskite is any material with a crystal structure with the general formula $ABX_{3,}$where AB are positively charged ions, i.e., cations, and X is a negatively charged

ion (anion – oxide). It was discovered that the mineral called perovskite, which consists of calcium titanium oxide ($CaTiO_3$).

Perovskite structures are of significant interest for a wide range of applications due to their outstanding optoelectronic properties, such as light-emitting diodes due to tunable bandgap and colour emission properties suitable for lighting applications, power transmission cables because it can significantly reduce energy loss during transmission, and photovoltaics, and also pressure induced emission (Hung *et al.*, 2014). Perovskite solar cells have gained immense attention for their excellent photovoltaic properties. They offer high power conversion efficiencies, ease of fabrication, and potential for low-cost production, making them promising for next-generation solar energy harvesting. Their ionic bonding nature with soft metal lattices allows extensive phase transition behaviours, including expansion, lattice distortion, compression, and rearrangement under varied external environmental variables such as pressure and temperature.

Ion substitution has been widely employed to explore the mechanism of super-conductivity in cuprate superconductors, which provides vital information regarding the mechanism of the superconducting phase's lattice structure stability (Wang *et al.*, 2002). In this research, density functional theory calculations as implemented in the Quantum Espresso code will be used. This is done in order to investigate the phase transition and superconducting properties of the perovskite. The lattice structure of the $LaBa_2Cu_3O_7$ phase undergoes a phase transformation from orthorhombic to the tetragonal phase. In the high-Tc superconductor, the level of oxygen content plays a crucial role in the change of the orthorhombic to tetragonal structure.

1.3 Statement of the Problem

This research study sought to investigate the electronic structure and dynamical properties of $LaBa_2Cu_3O_7$ using first-principle calculations and to understand further the phase transition and superconducting behaviour properties of this material. Although research on the $LaBa_2Cu_3O_7$ compound has been done theoretically and experimentally, results on superconducting properties and phase transition tend to be limited. Thus, in this work, $LaBa_2Cu_3O_7$ was studied computationally considering the application of pressure in relation tothe phase transition.

1.4 Objectives of the Study

1.4.1 Main Objective

The main goal of this research was to study electronic, dynamical, and applied pressure doping on the phase transition behaviour of $LaBa_2Cu_3O_7$ using an *ab initio* approach.

1.4.2. Specific Objectives

i. To determine the electronic structure properties of the perovskite $LaBa_2Cu_3O_7$ by first principles.
ii. To investigate the dynamical properties of the perovskite $LaBa_2Cu_3O_7$ by first principles.
iii. To determine pressure-induced superconducting properties of the perovskite $LaBa_2Cu_3O_7$.
iv. To determine the pressure-induced doping properties of perovskite $LaBa_2Cu_3O_7$.

1.4 Research Questions

i. What are the electronic structure properties of the perovskite $LaBa_2Cu_3O_7$?
ii. What are the dynamical properties of the perovskite $LaBa_2Cu_3O_7$?
iii. What are the pressure-induced superconducting properties of $LaBa_2Cu_3O_7$?

iv. What are the pressure-induced doping properties of the perovskite $LaBa_2Cu_3O_7$?

1.5 Justification of the Study

Superconductor materials have garnered significant interest because of the potential to create enhanced properties for prospective technological applications. Thus, this research study is aimed at predicting the pressure-induced doping, phase transition, and superconducting properties of perovskite materials through first-principle computations to provide insights into the underlying physics and electronic structure.

1.6 Significance of the Study

This study will contribute to the foundational understanding of the phase transitions and superconducting properties of $LaBa_2Cu_3O_{7,}$which have more expansive implications for materials science, the development of advanced technologies, and condensed matter physics. Computational simulation is readily available and thus utilized in this research study.

1.7 Scope of the Study

This research focused on pressure-induced phase transition, superconducting properties, dynamical properties, and electronic properties of LaBa2Cu3O7perovskites. Computational modelling methods based on Density Functional Theory were used to obtain data. Quantum Espresso and siesta codes were used to simulate the results.

1.8 Assumptions

DFT is based on the Hohenberg-Kohn theorem, which states that the ground state density of a many-particle system uniquely determines its properties. DFT assumes that the total energy of a system can be expressed as a functional of the electron density, and that the ground state energy is minimized when the electron density is the actual ground state

density. Since DFT uses a DFT code like Quantum Espresso, it is assumed that the crystal structure of the material at 0 K is the same even at T> Tc.

This study assumed that the simulated results would reproduce the properties that will be implemented experimentally, and the results obtained would be a replica of the experimental data recorded. Additionally, the time allocated for research would be sufficient to yield the desired results, providing answers to the stated objectives.

CHAPTER TWO

LITERATURE REVIEW

2.1 Introduction

This section reviews the literature according to the objectives of the study and presents related work done by different scientists. In addition, it explains the theoretical and conceptual framework. A summary of the research gap is also presented.

2.2 Review of Relevant Literature

The review of literature is done according to the objectives of the study.

2.3 Electronic Structure Properties

Sun and Lin (2024) investigated the electronic band structure of $YBa_2Cu_3O_{6.9}$using a Fermi-liquid approach and found that the calculations give very similar Fermi surfaces. However, with 13 atoms in the orthorhombic unit cell, the calculated bands away from the Fermi level are a complex maze and differ in detail between the various calculations.

Hao and Fu (2024) studied the electronic structure of $Pb_9Cu(PO_4)_6O$ by DFT calculations using VASP with the GGA-PBESol exchange-correlation potential, giving lattice parameters and a volume contraction.The DFT electronic structure shows Cu^{2+}in a $3d^9$configuration with two extremely flat Cu bands crossing the Fermi energy. This puts $Pb_9Cu(PO_4)_6O$ in an ultra-correlated regime and suggests that, without doping, it is a Mott or charge transfer insulator. A slight doping is required to arrive at a metallic system, as observed in the experiment. In agreement with the experiment, the parent compound is insulating with a rather large gap of 2.3 eV between the O-p and Pb-p states in DFT.

Kaiser and Schneemeyer (2022) prepared and identified a single phase of the high-temperature superconducting compound in the chemical system Y-Ba-Cu-O, an

orthorhombic, distorted, oxygen-deficient perovskite ofstoichiometry $Ba_2YCu_3O_{9-\delta}$ (δ =2.1) employing single-phase polycrystalline samples. Samples exhibit zero resistance at 91 K, with a transition widthof 1.5 K. Their electronic properties have been characterized. The density of electronic states at E_F is substantially smaller than in (La, Sr) $_2CuO_4$, and its T_c is more than twice that in those materials.

2.4 Dynamical Properties

Chen (2017) performed first-principle calculations on the dynamical properties of $La_2Sr_xCuO_4$ using local density-functional approximation (LDA), and obtained phonon frequencies and eigenvectors in the full Brillouin zone. The calculations were performed using the LAPW ~linearized augmented plane-wave, which is a linear response method implemented with the Steinheimer approach. The use of LAPW basis functions facilitates the treatment of localized valence wave functions such as those derived from Cu(3d) and O(2p) orbitals.

2.5 Pressure-Induced Doping Properties

Takayama-Muromachi *et al*. (2010) and subsequently Bianconi *et al*. proposed that the charge carriers are doped mainly in the oxygen 2p orbitals of the O (3)atom. Harabor, Ana, *et al* (2023) investigated the effect of doping $YBa_2Cu_3O_{7-\delta,}$ a superconducting compoundwith 1 and 2 wt.% of Ag nanoparticles with different sizes and concentrations. The samples were characterized using XRD, SEM, and EDX measurements. Critical current measurement was performed using a standard four-probe technique at liquid nitrogen temperature by chemical reduction (Poon 1983). The results showed that the J_c increased monotonically by increasing the Ag nanoparticles' size up to 700 nm. Also, J_c is greater in samples with higher Ag concentration. The enhancement of critical current density is attributed to the improvements made through the PLD method. The

change in the silver doping concentration slightly affected the transition temperatures ($T_{c,zero}$), whereas the critical current densities (J_c) of the samples and their magnetic field (B) dependencies were noticeably affected.

Conducting in situ X-ray diffraction (XRD) at elevated temperatures on YBCO-Ag powders uncovered that the introduction of silver reduces the incongruent melting point of YBCO to 760°C. This alteration led to a polished surface morphology of YBCO films even at temperatures as low as 760°C. Additionally, the incorporation of silver was observed to enhance both grain growth and intergranular conductivity.

L. Gao *et al* (2022) experimentally investigated the superconducting transition temperatures (T_c's) of optimally doped $HgBa_2Ca_{m-1}$ $Cu_mO_{2m+2+\delta}$ (Hg 1:2:m—1:rn) with m =1, 2, and 3 and $Hg_{1-x}Pb_xBa_2Ca_2Cu_3O_{8+\delta}$ [Hg($_x$Pb) 1:2:2:3] under quasihydrostatic pressures up to 45 GPa. There seemed to be a universal upward shift of T_c under pressure, regardless of *m*, for all Hg 1:2:m—1:m, implying a common origin for all compounds. Record high T_c's of 164, 154, and 118K, respectively, and for Hg 1:2:2:3 at 31 GPa, Hg 1:2:1:2 at 29 GPa, and Hg 1:2:0:1 at 24 GPa. The universal T_c shift under pressure suggested a common origin for high-temperature superconductors in these compounds and was reached for the optimally doped Hg 1:2:m—1:m with m =3, 2, and 1, respectively. However, moderate Pb doping drastically depresses the enhancement for all members of the HTS family, suggesting a unique character for the HgO_δ layer.

Deng, Liangzi, *et al* (2019) investigated the bulk superconducting state through direct current (dc) magnetization measurements. The researchers observed a simultaneous increase in the superconducting transition temperatures (Tcs) for both monolayer $Bi_2Sr_2CuO_{6+\delta}$ (Bi2201) and bilayer $Bi_2Sr_2CaCu2O_{8+\delta}$ (Bi2212), surpassing the maximum Tcs (Tc-maxs) anticipated by the universal correlation between Tc and doping (p) or

pressure (P) under higher pressures. In the case of underdoped Bi2201, the initial Tc of 9.6 K at ambient pressure peaked at 23 K at 26 GPa, followed by a decline as predicted by the universal Tc-P relationship. However, at pressures exceeding 40 GPa, Tc exhibited a rapid and continuous increase, reaching 30 K at 51 GPa without any indication of saturation. Calculations show that the excess oxygen δ resides energetically favourably between the BiO layers.

2.6 The Pressure-Induced Superconducting Properties

Markert, John T., *et al* (1989) experimentally studied superconductivity in the LaBaCuO system to the K_2NiF_4 phase. By replacing Ba with Sr, they found that the LaSrCuO system, which has the K2NiF4 structure, generally exhibits a higher T_c and a sharper transition. A transition width of 2K and an onset T_c of 48.6K were obtained at ambient pressure. Pressure was found to enhance the T_c of the LaBaCuO system at a rate of greater than 10^{-3} $Kbar^{-1}$ and to raise the onset T_c to 57K with a zero-resistance reached at 40K. Pressure reduces the lattice parameters and enhances the Cu^{+3} /Cu^{+2} ratio in the compounds.

Sharma, R. G. (2021) conducted experimental investigations into the presence of superconductivity above 40K in the La-Ba-Cu-O compound system. A distinct superconducting transition, with an initiation temperature exceeding 40 K, was identified under pressure in the La-Ba-Cu-O compound system. This system was synthesized directly through a solid-state reaction involving La_2O_3, CuO, and $BaCO_3$, followed by decomposing the mixture in a reduced atmosphere. The researchers observed indications of non-bulk superconductivity above 40 K in the LBCO compound system under hydrostatic pressure, noting the most significant positive pressure effect on superconductivity.

2.7 Conceptual Framework

Figure 1

Conceptual Framework

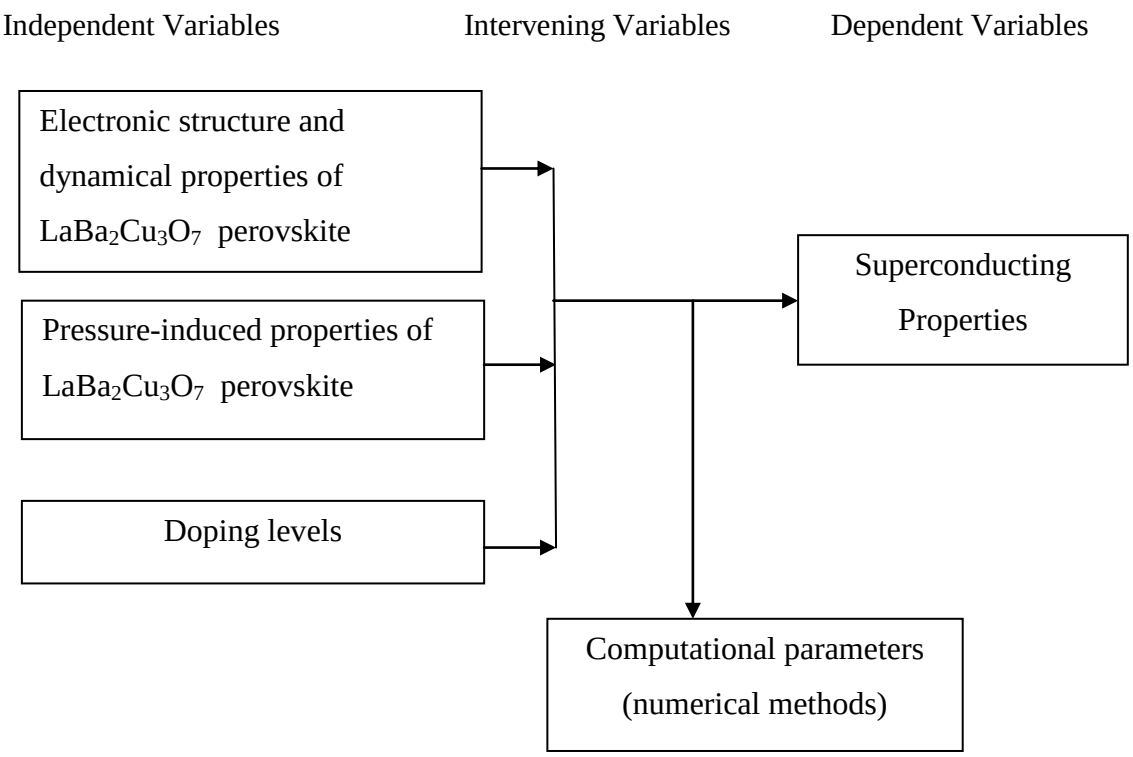

Figure 1 above illustrates the proposed conceptual framework. It consists of three variables: the independent variables, intervening variables, and the dependent variables. The independent variables entail the electronic structure and dynamical properties of $LaBa_2Cu_3O_7$ perovskite. The intervening variables are the computational parameters, while the dependent variable is the superconducting efficiency, which represents the outcome of the computational model influenced by the independent variables chosen for the study. The structural optimization will be obtained by doing a relaxation using an input file and implemented in Quantum Espresso for self-consistent fields. Electronic structure calculation is performed using the desired K-points, which provide the density of state calculation.

2.8 Research Gaps

Although much research has been done on the perovskite materials, there is limited information on the application of pressure in relation to phase transition, pressure-induced doping, and superconducting properties of the perovskite $LaBa_2Cu_3O_7$ material.

An experimental research study by Müller-Berdnordz *et al* presented in this paper on electronic properties, dynamical properties, and superconducting properties of $LaBa_2Cu_3O_7$ shows that $LaBa_2Cu_3O_7$ is a type-II superconductor with a critical temperature of 37 K. Subsequent magnetic studies confirmed that high-temperature superconductivity indeed exists in the system (Zi-Wen Dong *et al*, 1987). Thus, research on perovskite $LaBa_2Cu_3O_7$ will be done computationally, considering the application of pressure in relation to the phase transition.

A.M. Morales Rivera *et al*. (2016) reported the synthesis and characterization of a lanthanum–barium–copper oxide, based on a $LaBa_2Cu_3O_7$ system, using a wet chemical route that enables the combustion–polymerization of citrate species, to produce materials with enhanced morphological, surface, and textural properties for prospective applications. Structural analysis was performed through Rietveld refinement using X-ray diffraction data, and the outcomes affirmed the existence of an orthorhombic structure with a perovskite crystalline phase, belonging to space group Pmmm (47). Thus, using a computational method, the structural characterization and properties of $LaBa_2Cu_3O_7$ are studied.

Figure 2

Unit cell of $LaBa_2Cu_3O_7$ plotted from X-Ray Experimental Data and Plotted using PCW Software

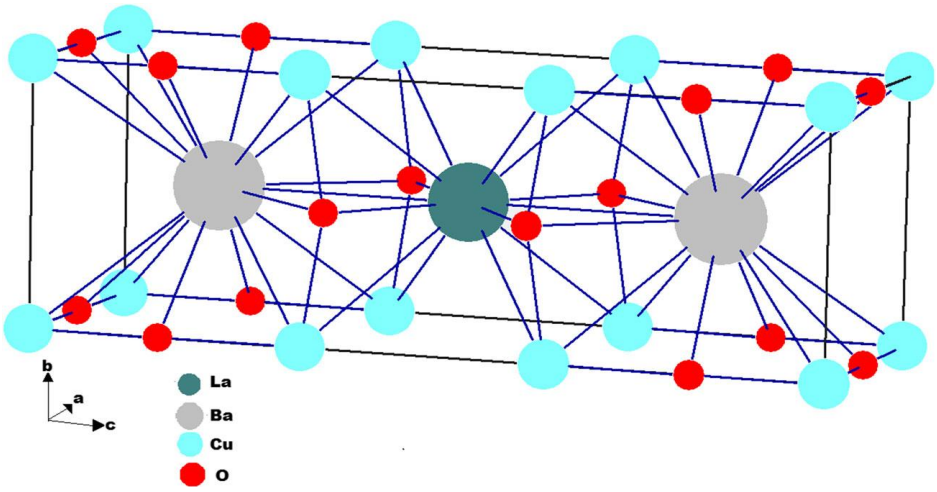

***Source**: A. M. Morales Rivera et al.*

Figure 2 above shows a unit cell of $LaBa_2Cu_3O_7$ obtained by X-ray diffraction data, where the results confirm the presence of a perovskite crystalline phase, with space group Pmmm (47); and is an orthorhombic structure with cell parameters*a* = 3.925 Å and with a preferential orientation along (1 1 0) facet.

CHAPTER THREE

RESEARCH DESIGN AND METHODOLOGY

3.1 Introduction

This chapter presents the research design, instrumentation, and methods that were used for the first-principles Computation of Electronic Structure, Dynamical, and pressure-induced superconducting properties of perovskite $LaBa_2Cu_3O_{7.}$ This was a computational study involving the use of computational modelling, which is a scientific design where the reproduction of the system takes place. Density functional theory (DFT) was used. The results were simulated using computer software, whereby data analysis was obtained by running computer programs in the code Quantum Espresso (QE).The software package used was Quantum Espresso, an open-source, multipurpose code. For heavy simulations, the Centre of High-Performance Computing system was used.GGA-PBE exchange-correlation functional was used to enhance the validity of the instrument, considering that it requires less computing power than advanced functionals (Prokopenko *et al*., 2019).

3.2 Data Collection Procedure

Quantum Espresso is an integrated suite of Open-Source computer codes for first-principles electronic-structure calculations, simulation, optimization, and materials modelling,based on density-functional theory, plane wave basis sets, and pseudopotentials. The PWscf (Plane-Wave self-consistent field) component provides the core plane wave DFT functions of QE. This allows for the calculation of electronic structure calculations within density functional theory and density functional perturbation theory, using plane wave basis sets and pseudopotentials.

Ground state energy calculations were carried out in the context of density functional theory (DFT) based on the plane wave self-consistent field (PWscf) and ultrasoft pseudopotential (USPP) method, as treated in the Perdew-Burke Ernzerhof (PBE) generalized gradient approximation and local density approximations, as implemented in the Quantum Espresso Code.

The Projected Augmented Wave (PAW) method, as implemented in the ABINIT code, was used to determine the electronic structure and the relaxation of the structure. The phonon package was implemented in the density-functional perturbation theory (DFPT) for the calculations of energy.

3.3 Electronic Structure Properties

First-principle calculations of the electronic structure of materials are typically performed using Density Functional Theory (DFT). DFT uses the first principles method to study the electronic structure of many-body systems. The first step involved obtaining the crystal structure of LaBaCuO, which includes lattice parameters and atomic positions within the unit cell. Project augmented methods and pseudopotentials, as implemented in the Quantum Espresso simulation package, were used to simplify the interaction between valence electrons and atomic cores.

The Perdew–Burke–Ernzerhof (PBE) parameterization of the Generalized Gradient Approximation (GGA) was employed for the exchange-correlation functional. The unit cell was optimized in terms of k-points and kinetic energy cut-off values, with the results graphed to ensure accuracy. Precise values were determined at the convergence of the ground state energy, achieving the minimum convergence threshold in calculations using appropriate basis sets. Appropriate K-points were selected for sampling the Brillouin Zone, whereby their density affected the accuracy and computational cost. Monkhorst -

Pack grid was used to generate the k points (Zanca, F *et al*, 2021). Higher cut-off energies were chosen, which resulted in more accurate calculations.

Self-consistent field calculations were performed to obtain the ground-state electron density, ensuring convergence of the total energy concerning the electron density. (Lehtola, S. *et al*, 2020). Electronic structure, including band gaps, Fermi surfaces, and effective masses, was analysed, and results obtained were compared with other data to validate the calculations.

3.4 Dynamical Properties

First-principles computations of the dynamical properties of $LaBa_2Cu_3O_7$ perovskite provide detailed insights into the lattice dynamics, stability, and interactions within the material. These calculations are fundamental for predicting material behaviour, guiding experimental studies, and developing new applications. These properties include phonon dispersion, vibrational modes, and electron-phonon interactions, which are essential for understanding the material's behaviour at the atomic level.

The phonon dispersion relations described the collective excitations in the lattice (phonons), calculated using the Quantum Espresso code based on density functional theory (DFT). Phonon dispersion curves provided information on the stability of the crystal structure and the interactions between atoms. Soft modes (negative frequencies) indicate structural instabilities or phase transitions.

The vibrational modes of the crystal are analysed to understand how atoms move in response to thermal energy. A specific frequency and atomic displacement pattern characterize each mode. The electron-phonon coupling constant, which measures the strength of this interaction, was calculated. Strong electron-phonon interactions lead to phenomena such as superconductivity, where electron pairs form and move through the

lattice without resistance. Conversely, weak interactions may result in higher thermal conductivity. Phonon calculations for each structure were performed with an 8 × 8 × 4 K-point mesh to sample the Brillouin zone.

3.5 Pressure-Induced Superconducting Properties

The BCS theory and McMillan's equation were used to calculate the TC of the material at different conditions of pressure developed from Eilenberg's theory. The strength of the electron-phonon interaction, quantified by the coupling constant λ, can be computed as a function of pressure. An increase in λ under pressure suggests stronger interactions between electrons and phonons, which relates to superconducting properties. Under pressure, a material undergoes various changes in elastic behavior due to the compression of interatomic orbitals, which in turn alters the electronic orbitals and the bonding order (J. O. Agora et al., 2020). The strength of a material can be understood through the phonons in its crystal lattice. These vibrational modes reduce the forces on atoms displaced from their equilibrium positions. Consequently, the frequency of their oscillations decreases, leading to periodic lattice distortions. This process lowers the crystal's energy and causes the energy distribution to the soft phonons to become negative. Therefore, the criterion for crystal stability is linked to the phonon frequencies; depending on their magnitude, instability can arise.

3.6 Pressure-Induced Doping Superconducting Properties

Doping superconductors is known to vary the superconducting transition temperature T_C depending on the degree of holes or electrons introduced in a system. One method that has been used is doping to alter the number of holes and electrons in the material's crystals, impacting the electronic charge behaviour and the structure at the Fermi level (D. LeBoeuf *et al*,2007). When cuprate superconductors are doped, their normal state behaves like an ordinary Fermi liquid, similar to metals, and their superconducting

properties can be explained by the Bardeen-Cooper-Schrieffer (BCS) theory. Doped $LaBa_2Cu_3O_7$ at different pressures is used to calculate the Debye constant from which the superconducting transition temperature is calculated.

3.7 Computational Details

Computational simulations rely on principles such as the Density Functional Theorem, Born-Oppenheimer approximations, Hohenberg and Kohn theorems, and Kohn equations, ultimately resulting in the resolution of the Schrödinger equations. Density functional theory has been used with great success to investigate the ground state properties of solids, both in the bulk form and at surfaces and interfaces, and it is the most widely used in first principles computations (Gross, A. E., Dobson, J. F., & Petersilka, M. (2005).

3.7.1 Many-Body Problem

The many-body problem involves finding a solution to the Schrödinger equation that accurately describes the quantum state of a system with multiple interacting particles. Various approximation methods and numerical techniques, such as density functional theory, are employed to address the challenges posed by the many-body problem and obtain meaningful results for practical systems. In 1964, Walter Kohn and Pierre Hohenberg proved that an exact solution to the many-body problem can be obtained by only using the electronic density of the systems as a variable, which is much simpler than the wave function.

To obtain the ground state wave function, we solve the many-body Schrödinger equation to determine the ground state energy. The time-independent many-body Schrödinger equation is mainly considered in DFT. The general Hamiltonian for the many-body system can be written as;

$$H = \sum_i -\frac{\hbar^2}{2M_i}\nabla_i + \frac{1}{2}\sum_{i,j}\frac{z_i z_j e^2}{\left(R_i - R_j\right)}\nabla_{rk} + \frac{1}{2}\sum_{kj}\frac{e^2}{r_k - r_l} - \sum_{k,i}\frac{Ze^2}{r_k - R_i} \quad \ldots (1)$$

Where, M_i represents the mass of the nucleus at position R

M_e represents the mass of an electron located at position r_i

Z represents the atomic number of the atom.

The equation above can be summarized as;

$$H = T_e + T_n + W_{ee} + W_{en} + W_{nn} \quad \ldots(2)$$

Schrödinger's equation was applied to the solution of the hydrogen atom since it has a single electron (Rob Maborn and Robert Oppenheimer, 1927).

Born Oppenheimer treats electrons only as quantum particles in the field of the fixed or slowly varying nuclei; therefore, there's no influence of the ionic motion on one electronic surface (Gerbrand Ceder 2005). In the Born Oppenheimer approximation, the atomic nucleus within a molecule possesses a significantly greater mass than that of an electron, leading to the nuclei exhibiting much slower movement compared to electrons.

The nuclei, nevertheless, can remain stationary at various positions, allowing the electronic wave function to be influenced by the nuclei's positions, despite their motion being disregarded. The solution tothe electronic Schrödinger equation is given in the equation below:

$$\phi_v(r_i, R_a) = \theta(r_i, R_a) \times (R_a) \quad \ldots (3)$$

The function $x(R_a)$It is the vibrational wavefunction, which is a function of the nuclear coordinates R and depends upon both the vibrational and electronic quantum numbers or states, *n* and *e*, respectively. The electronic function, $\phi_v(r_i, R_a)$, is a function of both the

nuclear and electronic coordinates, but only depends upon the electronic quantum number or electronic state, *e*.

3.7.2 Hartree-Fock Approximation

Hartree-Fock approximation explains the electron–electron repulsion by one electron moving in the average field of the remaining N−1 electrons. This determines the wave function and energy of a given system in a stationary state. The many-electron problem is reduced to a single-electron problem. It is assumed that all electrons are independent, so the equations do not satisfy the Pauli Exclusion Principle, and a given electron interacts with the other electrons only through the mean field Coulomb potential. The Hartree wave function is generalized to be provided by the antisymmetric feature via a Slater determinant of the one-electron wave function (N Salami, A. Shokri, 2021).

The many-body wave function in the Hartree approximation is given by:

$$V_i^{HF}(r) = e^2 \int \frac{n(r^{'}) - n_i^{HF}(r, r')}{|r - r'|} dr' \qquad \ldots (4)$$

3.7.3 Density Functional Theory

Density functional theory was developed in 1964 by Hohenberg & Kohn (GS Manyali *et al*, 2014). For many years, wavefunction functional theory (Schrödinger theory) has been the method of choice when performing electronic structure calculations on chemical systems. However, within the last few years, density functional theory DFT has experienced a rise in its popularity for the simulation of periodic systems, calculating structures and properties of chemical systems. Not only does DFT provide computational advantages over wavefunction functional theory (WFT),but quantities of interest to chemists (such as softness, hardness, reactivity indices, and electronegativity) are readily defined. Density functional theory is equivalent to solving Schrödinger's equation and is, therefore, an exact theory for describing the electronic structure and properties of matter.

(Libero J Bartolotti, Ken Flurchick 1996). It is the most widely used method for first-principle calculations of the structure of atoms, molecules, crystals, surfaces, and their interactions.

3.7.4 Hohenberg and Kohn Theorem

This theorem states that the ground-state electron density uniquely determines the external potential within an electronic system. It enables the development of a practical approximation known as the Kohn-Sham method to solve electronic structure problems efficiently. The ground state charge density thus determines the ground state energy

$$E_{GS} = F[n(r)] + \int V_{ext}(r)\,\mathrm{n(r)\,dr} - \mu[\int n(r)d^3r - N] \quad \ldots (5)$$

$F\,[\mathrm{n(r)}]$ is the universal functional known as the Hohenberg-Kohn functional.

$V_{ext}(\mathrm{r})\mathrm{n}(\mathrm{r})\mathrm{dr}$ is the external potential

$\mu\,[\int \mathrm{n}(\mathrm{r})\mathrm{d}^3\,\mathrm{r} - \mathrm{N}]$ is the ground state electron density.

3.7.5 Kohn and Sham Equation

Kohn and Sham (KS) form the foundation for practical approaches in density functional calculations and have provided chemistry and physics with an independent particle model featuring desirable characteristics (EJ Baerends, 2001). The Kohn-Sham equations consist of a set of non-interacting single-particle Schrödinger-like equations for a set of fictitious non-interacting electrons. These equations are expressed as follows:

$$E[\eta(r) = E_k[\eta(r) + E_{e-e}[\eta(r)] + U_{e-i}[\eta(r)] + E_{XC}[\eta(r)] \quad \ldots (6)$$

Where:

$E_{\mathrm{k}}\,[\eta\,(\mathrm{r})]$ is the kinetic energy of the electrons,

$E_{\mathrm{e\text{-}e}}\,[\eta(\mathrm{r})]$ is electron-electron energy

$U_{\mathrm{e\text{-}}i}\,[n\,(\mathrm{r})]$ electron-ion interaction potential and

Solving these Kohn-Sham equations self-consistently provides the electron density and, subsequently, the electronic structure of the system. The Kohn-Sham method makes DFT computationally feasible for a broad spectrum of materials and systems. Fig. 3 is the flowchart for solving the Kohn-Sham equation as shown in Figure 3 below;

Figure 3

Flowchart for Solving Kohn-Sham Equation

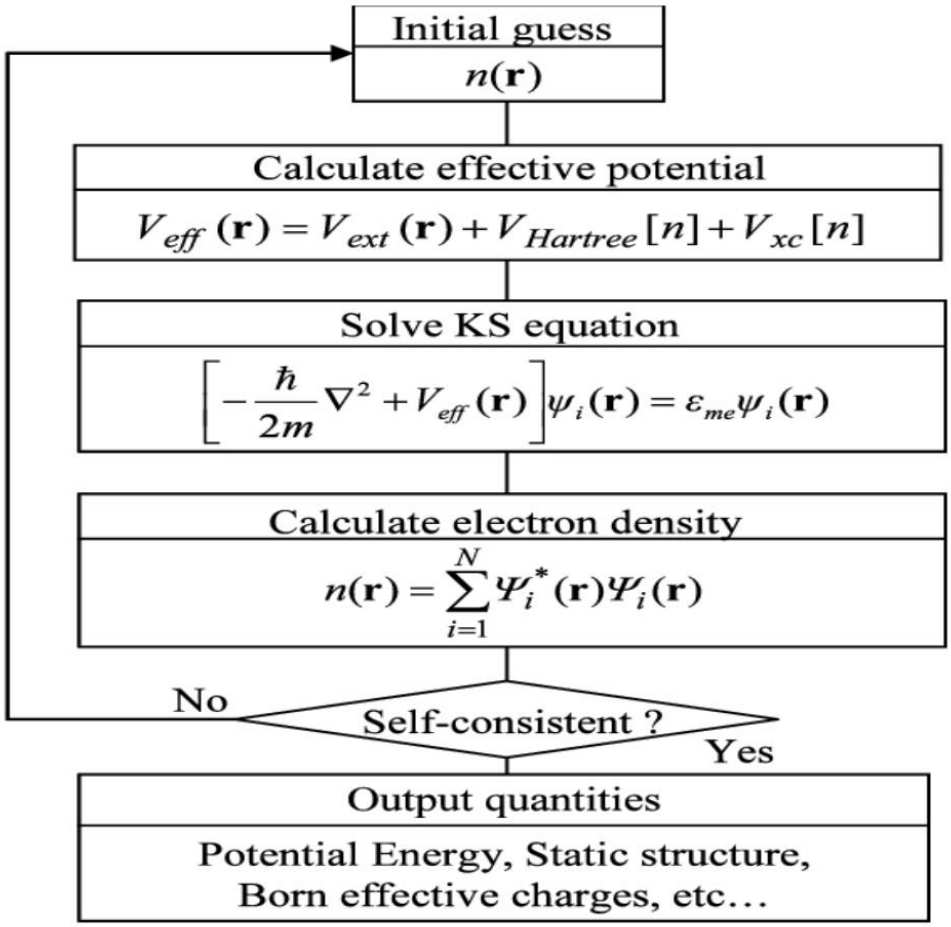

Source: *Bickelhaupt, F. M et al, (2000)*

3.7.6 Exchange-Correlation Approximation

It is a quantity in the Kohn-Sham equation. It involves approximating the exchange and correlation energy functional, which is a part of the total energy functional in DFT. It is expressed as a functional of the density E_{xc} [n].

$$E_{xc}(n) = T(n) - T_o(n) + \mathrm{U}_{xc} \quad \ldots (7)$$

Where:

T_o(n) is the exact Kinetic energy functional,

T_o(n) is the non-interacting Kinetic energy functional

U_{xc} is the interaction of the electrons with their exchange-correlation hole

Various approximations are used since the exact forms of exchange and correlation functionals are unknown.These approximations are categorized into: Local Density Approximation (LDA), Generalized Gradient Approximation (GGA), and Hybrid functional.

3.7.7 Local Density Approximation

Walter Kohn and Lu Jeu Sham first introduced the local-density approximation in 1965(Bagayoko, Diola, 2014). The Local Density Approximation (LDA) is a widely used method in density functional theory (DFT) for approximating the exchange-correlation energy functional. This approximation simplifies the complex many-body problem of electron-electron interactions.

Mathematically, the LDA expression for the exchange-correlation energy density is given by:

$$E_{xc}^{LDA}\,[\mathrm{n(r)}] = \epsilon_{xc}^{hom}\big(n(r)\big)dr \quad \ldots(8)$$

Where, ϵ_{xc}^{hom} is a function of the electron density n(r)

The LDA is computationally efficient, making it suitable for a wide range of systems. However, it has limitations, particularly in describing strongly correlated electron systems and the non-local nature of exchange and correlation effects, and underestimation of band gap (Mathieu Lewin *et al*, 2019).

3.7.8 Generalized Gradient Approximation

The GGA uses the spatial variation of the electrons to determine the exchange correlation energy, and it is expressed as:

$$E_{xc}^{GGA}[\mathrm{n(r)}] = \int \epsilon_{xc}(\mathrm{n(r)}, \nabla \mathrm{n(r)})\mathrm{n(r)dr} \quad \ldots(9)$$

GGA functionals are computationally more demanding than LDA but offer improved accuracy, especially for molecular systems and materials with varying electron densities. Generalized gradient approximation (GGA) methods for electronic structure calculations may underestimate bandgaps by over 50% for some materials (Janotti and Van de Walle, 2011).

3.7.9 Hybrid Functionals

These combine a fraction of Hartree-Fock exchange with the exchange-correlation functionals. They are often a convenient and computationally efficient way of obtaining band structures with improved accuracy. The hybrid functional, the GLLBSC Gritsenko *et al.* (GLLB) functional (Kuisma *et al.*, 2010), accurately replicates bandgaps for a diverse array of materials, closely aligning with experimental values. This method explicitly includes the derivative discontinuity of the exchange-correlation functional at integral particle numbers, a crucial aspect for achieving precise band structure results in a DFT calculation. The combination can be justified by the ab initio adiabatic formula in which the exchange correlation energy is written as:

$$E_{xc} = \int_0^1 U_{xc}^{\xi} d\xi \quad \ldots (10)$$

Where ξ is an inter-electronic coupling strength parameter.

U_{xc} is the exchange correction potential energy at the intermediate coupling strength .

3.8 The Perdew, Burke, Ernzerhof Exchange Correlation Functional

When used to calculate atomic positions, it tends to overestimate bond lengths, leading to an average error and a mean absolute error of around 0.01(Perdew *et al*., 1998). As a result, its usefulness is significantly reduced compared to LDA, which has a mean error of 0.001. The PBE method is often used to determine bond energies because it has been shown to considerably lower the average absolute error to a level close to chemical accuracy. It was chosen for this study because its design ensures that both the correlation and exchange components retain several physical characteristics. Additionally, it is well-suited for the closed system being examined in this article.

3.8.1 Plane Waves

The interactions between the nucleus and electrons were studied using Density Functional Theory and the Born-Oppenheimer approximation. This method enabled the formulation of the single-particle problem for a system of 60 stationary nuclei moving within an effective potential. The expansion of plane waves in the Kohn-Sham wave function is crucial for computing the total energy of periodic solids. Bloch's theorem, which describes the solutions to the Schrödinger equation for a single particle with a periodic potential and periodicity, provides the foundation for this approach. This Bloch's theorem is given by;

$$\phi_{kj}(r) = e^{ikr} u_{kj}(r) \quad \ldots (11)$$

The electronic states are classified using the same **k** vector, defined within the first Brillouin zone. This segment can be expanded using a basis set of plane waves, which exhibit the periodicity characteristic of a crystal structure.

$$u_{kj}(r) = \sum_G C_{JG} + k e^{i(k+G)r} \quad \ldots (12)$$

Where;

$$\mu_{kj}(r) = \sum_G C_{jk} + Ge^{ikr}\mu_{kj}(r) \quad \ldots (13)$$

Kohn-Sham equations are given as;

$$[-\frac{\hbar^2}{2m}\nabla^2 + V_{eff}(r)]\phi_{kj}(r) = \in_{kj}(r) \quad \ldots (14)$$

Where;

$$V_{eff}(r) = V_{ext}(r) + V_H(r) + V_{xc}(r) \quad \ldots (15)$$

And

$$n(r) = 2\frac{\Omega_c}{2\pi^3}\sum_j \int \left|\psi_{kj}(r)\right|^2 \Theta(E_F - C_{kj})\,\mathrm{d}^3 k \quad \ldots (16)$$

Here, V_{ext}, V_H, V_{xc}They respectively represent the nuclei's exterior, Hartree, and exchange-correlation potentials of the nuclei. The factor of 2 in the expression accounts for the spin, and the step function θ\can be either 0 or 1. The Fermi energy, E_F, is determined by the number of electrons, N_e, within a single cell, representing the highest occupied energy level for a single particle. This energy level is represented as;

$$\int \Omega C_n(r) d^{3r} r \quad \ldots (17)$$

Bloch's theorem allows the extension of electronic wave functions at each K-point using a discrete set of plane waves. This theorem has been used to solve the problem of computing an infinite number of electronic states at an unlimited number of K-points within a single unit cell. The current method still requires an endless number of computations for the various K-points, leading to only a slight improvement. Due to the similarity of electronic states at neighbouring k-points, the wave functions at a specific point can be represented by a wave function at a single k-point in k-space (Yang & Whitfield, 2023).

3.8.2 Energy Cut-off

In material analysis, the Plane Wave Basis Energy is calculated using DFT. The optimization of the cut-off energy was investigated using a constant k-point mesh. Experimental lattice parameters are obtained from crystallographic databases. The convergence test for the k-point grid and plane-wave energy cut-off was conducted at specific lattice constants, with atomic positions relaxed at 0 Kelvin. Adjusting the volume while relaxing atomic coordinates was crucial in each DFT computation. A k-point grid was selected to ensure convergence of results, and the system was then simulated in QE by gradually increasing the energy cut-off values. The Energy cutoff values and cell parameters are shown in the figure below:

Figure 4

Energy cut-off against Cell Parameters

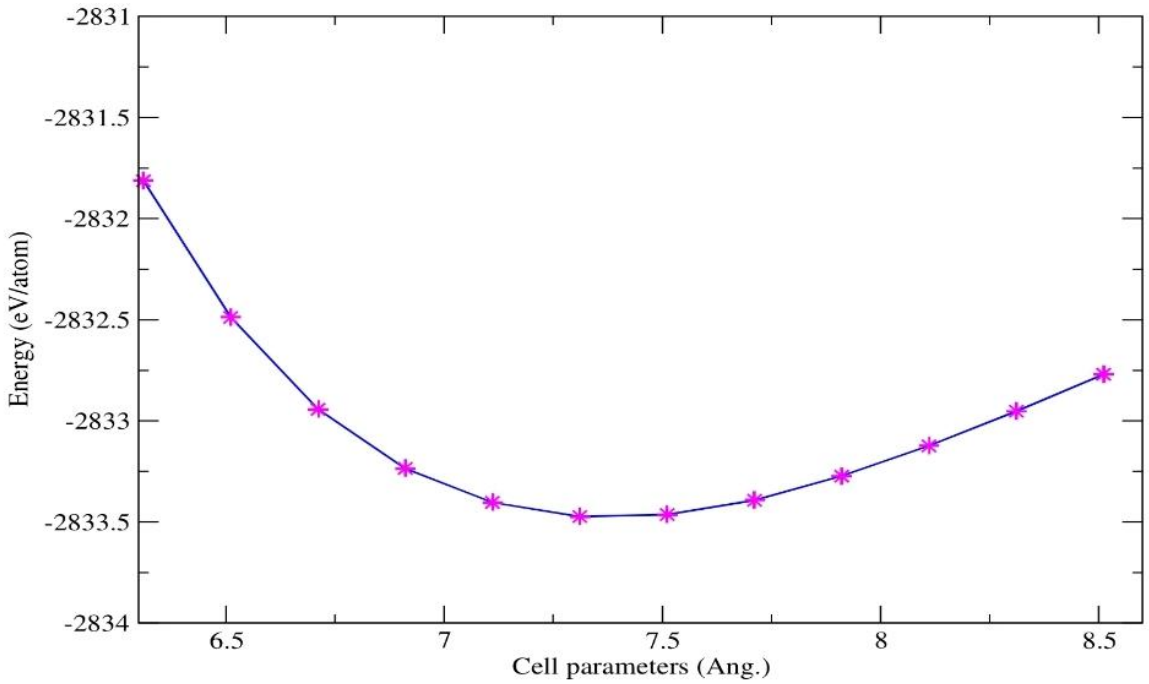

The figure indicates that an energy cut-off below 30 Ry is inadequate; therefore, values above 30 Ry should be used. However, increasing the energy cut-off beyond this point

does not enhance accuracy but rather extends CPU time, thereby increasing the computational cost.

3.8.3 K-Points

Electronic states are only permitted at specific k-points, defined by the boundary conditions of the bulk solid. The number of allowed k-points is directly proportional to the volume of the solid. However, it is essential to note that each of the infinitely many k-points corresponds to an infinite number of electrons in the solid. Bloch's theorem is used to address periodicity, replacing the need to compute an endless set of electronic wave functions with the computation of a finite set of electronic wave functions at an infinite number of k-points.

The occupied states determine the electronic potential in a bulk solid. In theory, an infinite number of calculations would be necessary for an accurate computation of this potential. K-points that are nearby have almost identical electronic wave functions. The electronic wave functions can be represented in a specific region of k-space using the wave functions from a single k-point. In this context, the electronic potential and, consequently, the total energy of the solid can be determined using a limited set of electronic states (k points). In this work, the generation of non-standard k-points was automated using the Monkhorst-Pack method. This approach involves integrating the irreducible part of the Brillouin Zone. Given the need for dense k-point grids in transition metals, a thorough optimization technique was applied. The k-point mesh utilized in the irreducible high-symmetry points of the Brillouin zone was 8x8x4 for evaluating integrals in reciprocal space. This Monkhorst pack grid gives a well-converged electronic structure. The K-point size for $LaBa_2Cu_3O_7$ upon convergence is depicted below;

Figure 5

Energy vs. K-Points Graph

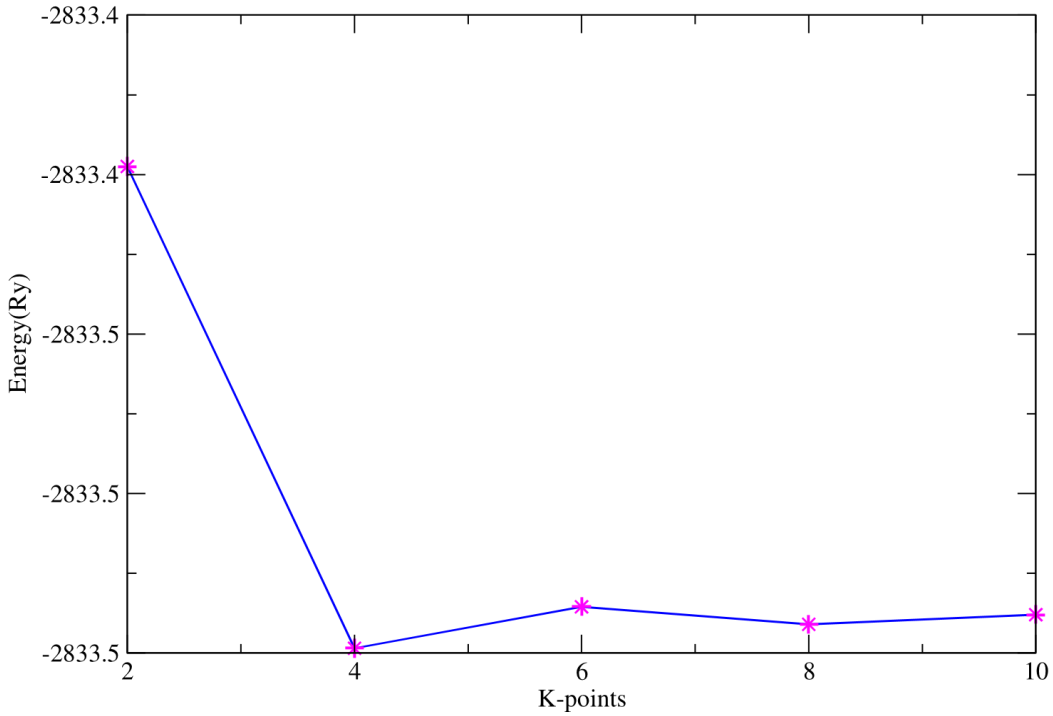

3.8.4 Pseudopotential Approximation

Pseudopotentials (Vps) are employed to enhance computational efficiency by replacing the potential at the nucleus of an atom with an effective one. It is widely accepted that the chemical and physical properties of an atom are primarily determined by its valence electrons, which has led to the formulation of the pseudopotential approximation. This technique assumes that core electrons are fixed and that ionic interactions are purely electrostatic. Pseudopotential approximations take advantage of this assumption to exclude the central states of the atom. Instead of dealing with the strong nuclear potential, a reduced "pseudopotential" is applied to a set of pseudo-wave functions alongside the proper valence wave functions. The pseudopotential approximation is an excellent tool for focusing on the essential contributions of the outermost electrons in electronic structure calculations.

Electrons in the inner regions of an atom tend to be firmly bound to the nucleus, making them relatively unaffected by external disturbances. This stability is due to the smooth nature of their wave functions when they are farther from the nucleus. However, as these electrons approach the nucleus, their wave functions exhibit rapid fluctuations. The valence of an atom is primarily determined by the wave functions located at the outer edge of the nucleus. It is assumed that the core remains static, as its electric density cancels itself out, even though it acts as a boundary constraint on the wave functions outside its region. The true Coulomb potential is more complex and refined than any approximation. Instead, pseudopotentials that mimic the behavior of all-electron potentials are used. The pseudopotentials (Vps) used in this study were relatively soft. While these pseudopotentials relax the norm conservation requirement to some extent, they still require the scattering properties to align over a wider energy range. The charge augmentation mechanism is included in the pseudopotential to restore the principle of norm conservation, ensuring that valence charges are appropriately distributed within the core region. In addition to enhancing smoothness and transferability, this approach allows for the previous goal to be achieved.

3.8.5 Norm Conserving Pseudopotential

The statements above aim to simplify the understanding of core electrons by directly highlighting their characteristics and properties. A norm-preserving pseudopotential is used to ensure that the motion of the non-periodic core electrons is normalized. Introducing periodicity into the electron motion allows for a Gaussian distribution to be achieved through normalization, which in turn promotes faster convergence. In terms of forces and stresses, even slight changes in magnitude or direction can cause disruptions within the system.

3.8.6 Ultra Soft Pseudo-Potential

The use of pseudopotentials that include ion cores, containing deep inner core electrons and nuclei, allows for the efficient use of planewave basis sets in electronic structure calculations. This approach is practical even though ions have a minimal impact on the properties of solids. Practical solutions to the self-consistent Kohn-Sham equation require numerous approximations. Consequently, various techniques have been developed to achieve rapid convergence with minimal loss of accuracy (Pickett, 1989). Pseudo-potential approaches share standard theoretical foundations, but their production methods vary, leading to different types. Most plane-wave electronic structure codes employ either norm-conserving or ultra-soft pseudopotentials. These allow for accurate numerical convergence using a basis set with significantly lower cut-off values, efficiently representing the electron wave-function with reasonable computational resources (H.-Y. Lee et al., 2012). Ultra-soft pseudopotentials achieve convergence faster than norm-conserving pseudopotentials.

3.8.7 Self-consistent Field (scf) Cycle

The SCF method is used to find a stable solution to the Kohn-Sham equations in density functional theory (DFT). These equations describe the electronic structure of a material by solving for the electron density that minimizes the total energy of the system. The SCF method iterates to achieve self-consistency between the electron density and the potential field created by this density.

In computational techniques, the Schrodinger equation is expressed as;

$$H\psi_i(r) = \left[-\frac{1}{2}\nabla^2 + V_{eff} \right] \psi_i(r) = \varepsilon_i \psi_i(r) \qquad \text{... (18)}$$

The V_{eff} is expressed as;

$$V_{eff}(r) = V_{ion}(r) + V_H[n(r)] + V_{xc}[n(r)] \quad \text{... (19)}$$

The Hamiltonian operator, denoted as H, encompasses the operator for kinetic energy as well as an effective potential based on the equation; $e = me = 1$. The electron density n(r) is calculated using the wave function,$H\psi_i(r)$,Hence, it follows that it relies on itself. The Kohn-Sham equations for a single particle were solved using a computer program that runs an executable command to calculate the Hamiltonian and potential, resulting in a new electron density. The process is repeated until the desired energy level is reached. Once convergence is achieved, the system's energy level decreases to its minimum value, and the interatomic forces reach their minimum magnitude. This result was made possible by setting a convergence threshold. Below is a diagram that gives the steps for it.

Figure 6

Shows the Computational Schematic Representation of the S-C Loop For the Solution of the K-S Equation

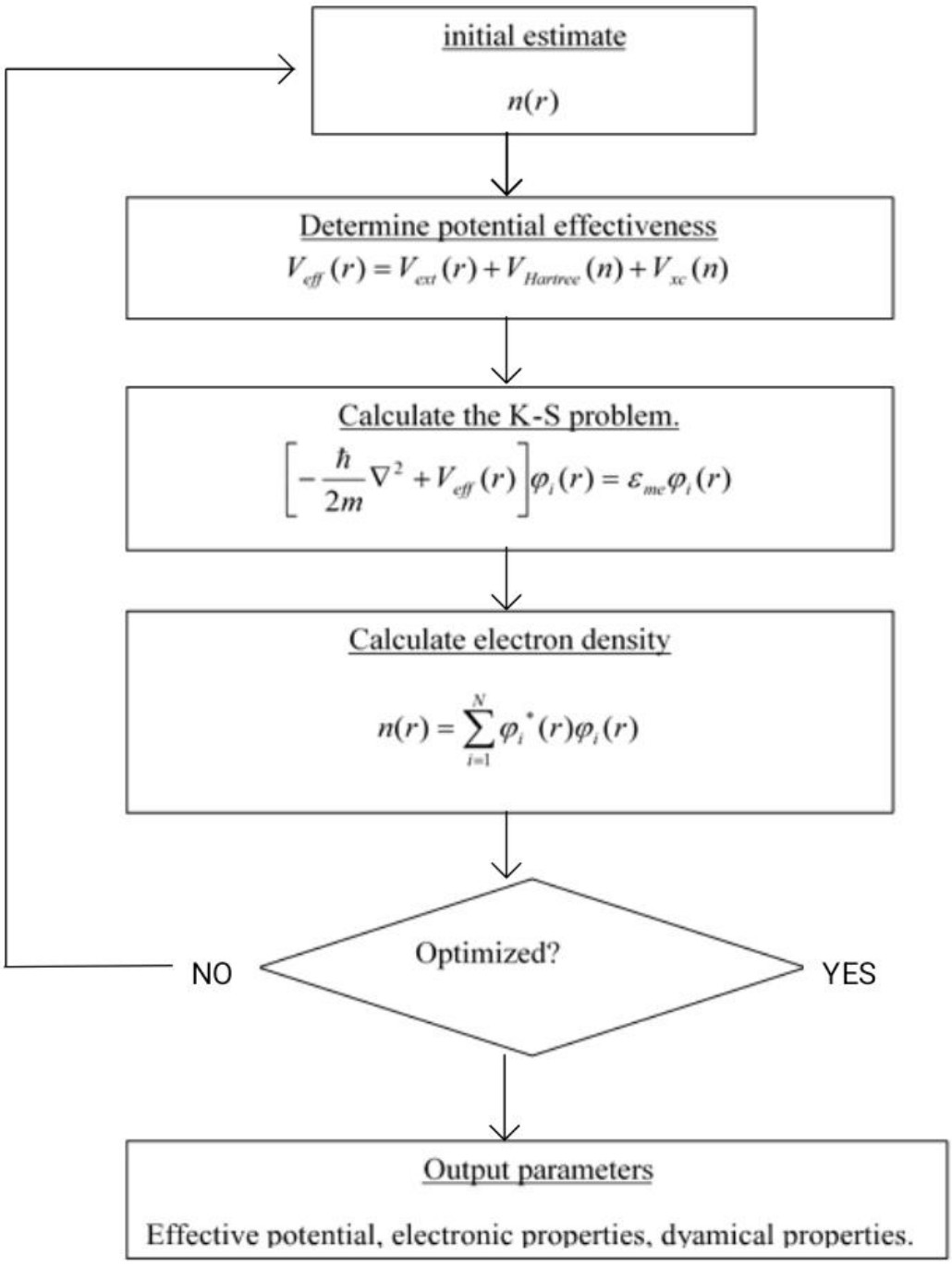

CHAPTER FOUR

DATA ANALYSIS, PRESENTATION AND DISCUSSION

4.1 Introduction

This chapter discusses the results, data on the structural properties, the electronic, dynamical, and superconducting properties of perovskite $LaBa_2Cu_3O_7$. Also, it compares the results obtained from this work and other research on perovskite materials from first principles and other works.

4.2 Structural Properties

The structure belongs to the space group of Pmmm (#47) that consists of thirteen atoms per primitive cell. Structural optimization was performed by minimizing the total energy of $LaBa_2Cu_3O_7$ to varying unit cell volume to obtain lattice parameters and ground state energy. These structural parameters are key to understanding the material's geometry and its influence on electronic properties. The optimized parameters include the cell dimensions, kinetic cut-off energy, and K-points. These optimizations confirmed that $LaBa_2Cu_3O_7$ is a simple orthorhombic crystal in a stable state. This orthorhombic structure was generated using the Quantum Espresso code using the Xcrysden program. The optimized primitive unit cell is given in Figure 7 below:

Figure 7

The Optimized Orthorhombic Structure of Laba$_2$cu$_3$o$_7$ (Xcrysden)

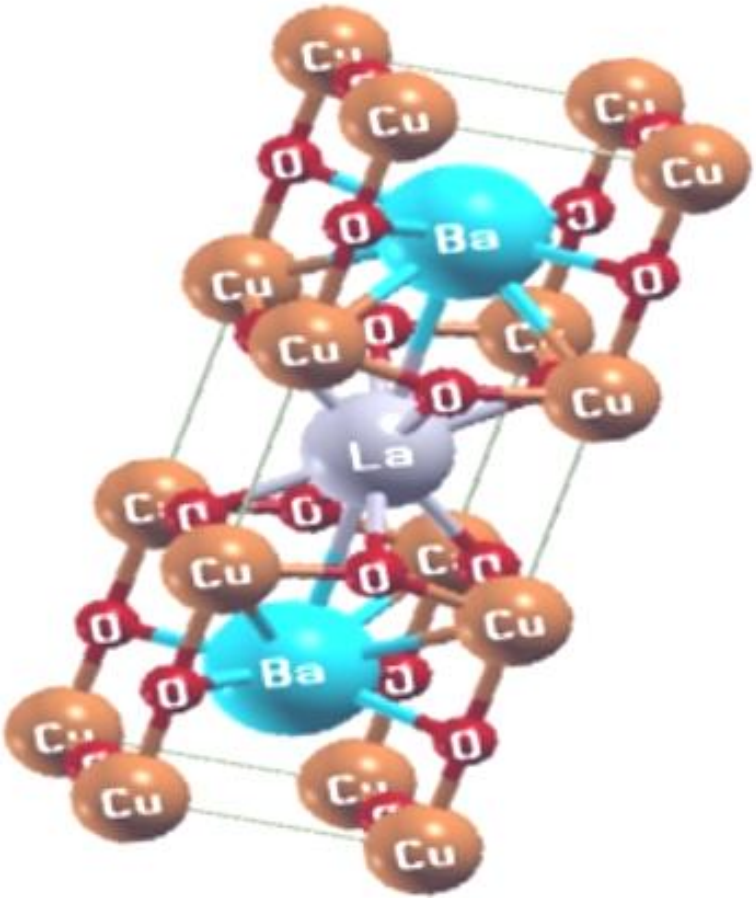

Structural properties consist of lattice parameters and bond length. The calculated lattice parameters compared to other works are presented in Table 1 below:

Table 1

Comparison of the Lattice Parameters, Volume, Methodology, and Reference with Other Works

Compound	a(Å)	b(Å)	c(Å)	Ref
YBCO	3.8227	3.8872	11.6802	[13]
GdBCO	3.837	3.677	11.7860	[13]
NdBCO	3.911	3.9183	11.7250	[14]
LaBaCuO	3.878	3.9183	11.8909	Present
Expt.	3.821	3.8840	11.6770	[13]

The difference between our present work results and experimental work results is less than 1.5% thus showing that the computational methodology employed in this work is reliable for lattice parameter simulation.

4.3 Electronic Structure Properties

Understanding the electronic structure behaviour of materials hinges significantly on their electronic properties, like band gap and density of states. The electronic band structure was plotted in high symmetry directions in the first Brillouin zone. Interactions between Cu 3d and O 2p states with strong electron correlations characterized the electronic structure of LaBa2Cu3O7 perovskite. The Cu 3d and O 2p orbitals hybridize, leading to the formation of bonding and antibonding molecular orbitals forming bands near the Fermi level. O 2p states typically dominated the valence band, while the conduction band involved Cu 3d states. The on-site Coulomb repulsion between Cu 3d electrons leads to the Mott insulating behavior in the undoped state.

Upon doping, the system undergoes a transition to metallic behavior, and the electrons in the Cu 3d band form mobile quasiparticles that interact strongly with the spin fluctuations, enabling superconductivity. A higher E_F indicated more available states for Cooper pair formation. The band structures for $LaBa_2Cu_3O_7$are shown in Fig. 8 below. As seen in Figure 8, the Fermi level (E_F) was set at zero energy and specified by a horizontal dashed red line. The band gap was observed between the highest valence band and the lowest conduction band, resulting in a band gap value of 2.04 eV, which indicates that it’s a semiconductor. However, under pressure, it becomes a superconductor, suggesting it is a metal.

Figure 8

Shows the Band Structure of $LaBa_2Cu_3O_7$

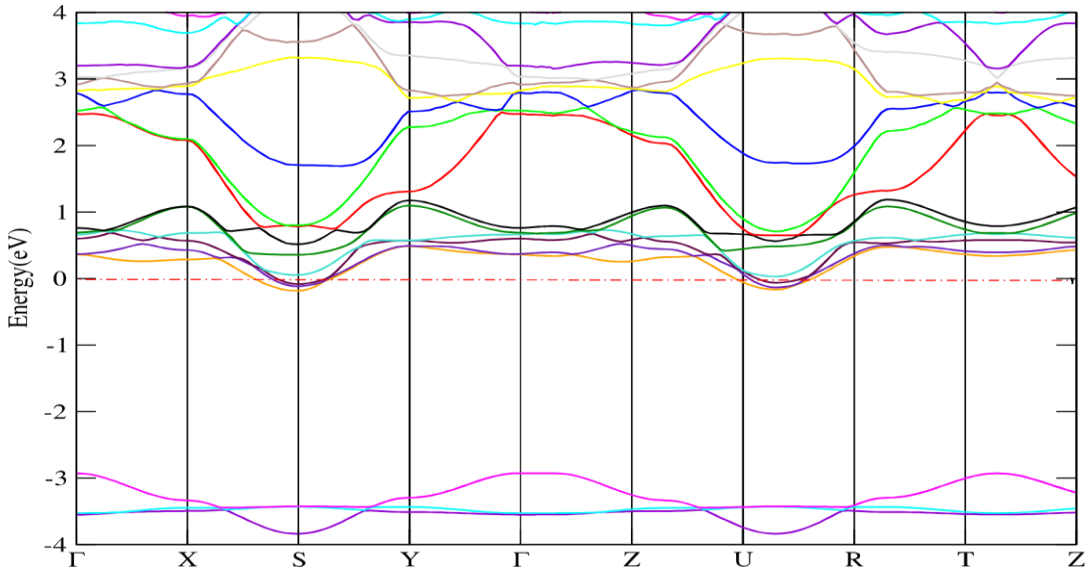

Table 2

Comparison of the Band Gaps, Methodology, and Reference with Other Works

Perovskite	Band gaps eV	Methodology	Reference
$LaBa_2Cu_3O_7$	2.043	QE	This work
Ba_2LaTaO_6	2.030	Exp (Vienna ab)	Premlata Kumari *et al*

4.4 Dynamical Properties

It involves investigating phonon spectra and lattice dynamics to analyse vibrational modes and their impacts on material stability and functionality. The electron-phonon coupling constant (λ) provides a measure of the interaction strength between electrons and lattice vibrations (phonons). λ often decreases slightly under pressure, due to phonon hardening, reducing the denominator more than the numerator in the integrand and reducing phonon DOS at lower frequencies. However, in some pressure ranges, non-monotonic behavior is seen; phonon softening in specific modes (especially buckling modes under uniaxial pressure) could cause local increases in λ. The coupling constant

λ=2.74 indicates strong electron-phonon interaction, which is a key feature in high-temperature superconductivity. Under pressure, changes in the phonon frequencies and lattice dynamics affect the electron-phonon coupling, leading to a pressure dependence of λ.

In the phonon dispersion relation, there are two branches: the lower branch is the acoustic mode, characterized by in–phase vibrations, and the upper branch is the optical mode, associated with out-of-phase vibrations. Acoustic modes vibrate at lower frequencies and are always in phase with the unit cell, while the optical modes have higher frequencies. In optical modes, adjacent atoms vibrate in out-of-phase directions, whereas in acoustic modes, adjacent atoms vibrate in the in-phase directions.

The phonon dispersions were calculated using the Density functional perturbation theory as implemented in the plane wave self-consistent field. If an element cell has n atoms, then there exists a total of 3n modes, consisting of 3 acoustic modes and thirty-six optical modes. The primitive unit cell of $LaBa_2Cu_3O_7$ contains 13 atoms, thus 39 modes of vibration. The optical modes are 36, and the acoustic modes are three. The acoustic modes converge at the gamma high symmetry point, as shown in the phonon dispersion curve in Figure 9. The graph shows the optical mode differentiated from the acoustic mode. These phonon calculations show that the compound is dynamically stable, as there are no negative frequencies observed.

Figure 9

Phonon Dispersion Curves

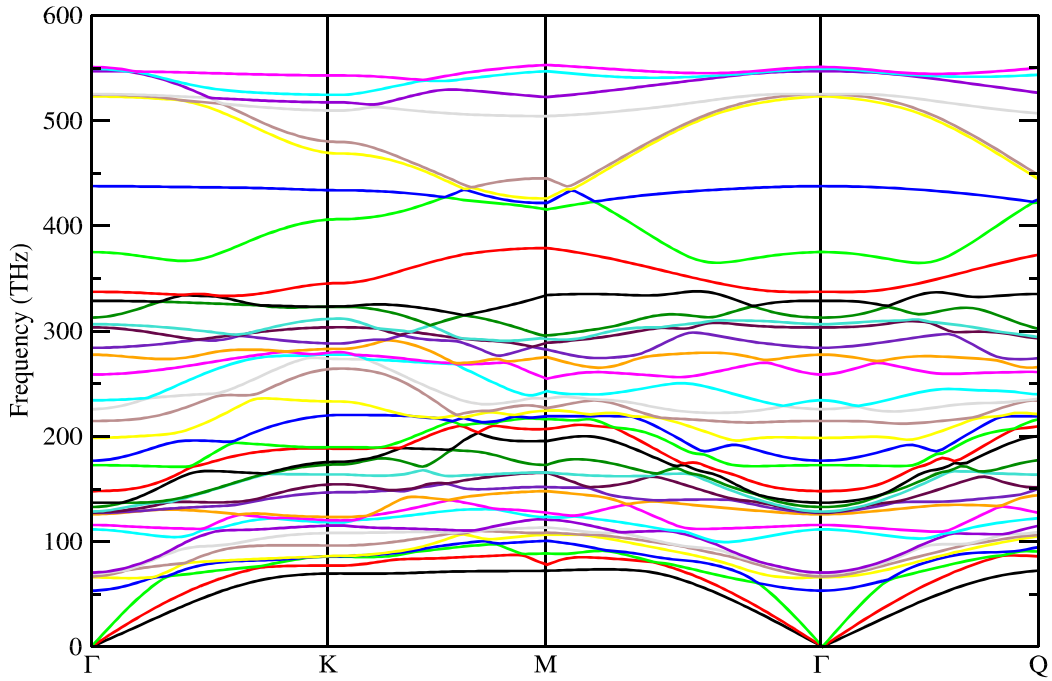

Phonons should have non-negative and real frequencies for stability, which means that a system is considered dynamically stable at equilibrium if the potential energy continuously increases with any displacement of atoms. Phonon frequencies emerge from the displacement of atoms in a crystal from their equilibrium positions, causing an increase in forces. Negative frequencies indicate that the potential energy decreases, leading to an unstable system**.**

4.5 Pressure-Induced Superconducting Properties

The superconducting transition temperature was based on the McMillan equation of superconducting transition temperature developed from Eilenberg's theory and given by:

$$T_c = \frac{\theta_D}{1.45} \exp\left[\frac{-1.04(1+\lambda)}{\lambda - \mu^*(1+0.62\lambda)}\right] \qquad \ldots\ldots\ldots\ldots\ldots\ldots\ldots\ldots (20)$$

Where θ_D is the Debye temperature, $\mu*$ is the renormalized Coulomb repulsion, and its value is chosen to range from 0.1 to 0.2, and λ is the electron-phonon coupling constant.

The use of McMillan's formula required the application of the Debye temperature calculated from the elastic constants. Elastic properties were calculated to obtain the Debye temperature. Debye temperature is a thermodynamic quantity in material science that is associated with the phonon vibrational modes in a crystal, the elastic constant, and specific heat. The orthorhombic crystal structure of $LaBa_2 Cu_3 O_7$ has nine independent elastic constants: $C_{1\ 1}$, $C_{2\ 2}$, $C_{3\ 3}$, $C_{1\ 2}$, $C_{1\ 3}$, $C_{2\ 3}$, $C_{4\ 4}$, $C_{5\ 5}$, and $C_{6\ 6}$ [Nyawere]. These constants are utilized to determine the elastic modulus, shear modulus, and bulk modulus, which are presented as a function of pressure. The calculated elastic constants, Cij, were used to derive the bulk and shear moduli as a function of pressure. The calculated Debye values were used to calculate the superconducting transition temperature using the McMillan equation.

Figure 10

Pressure (GPa) vs Transition Temperature (T_c)

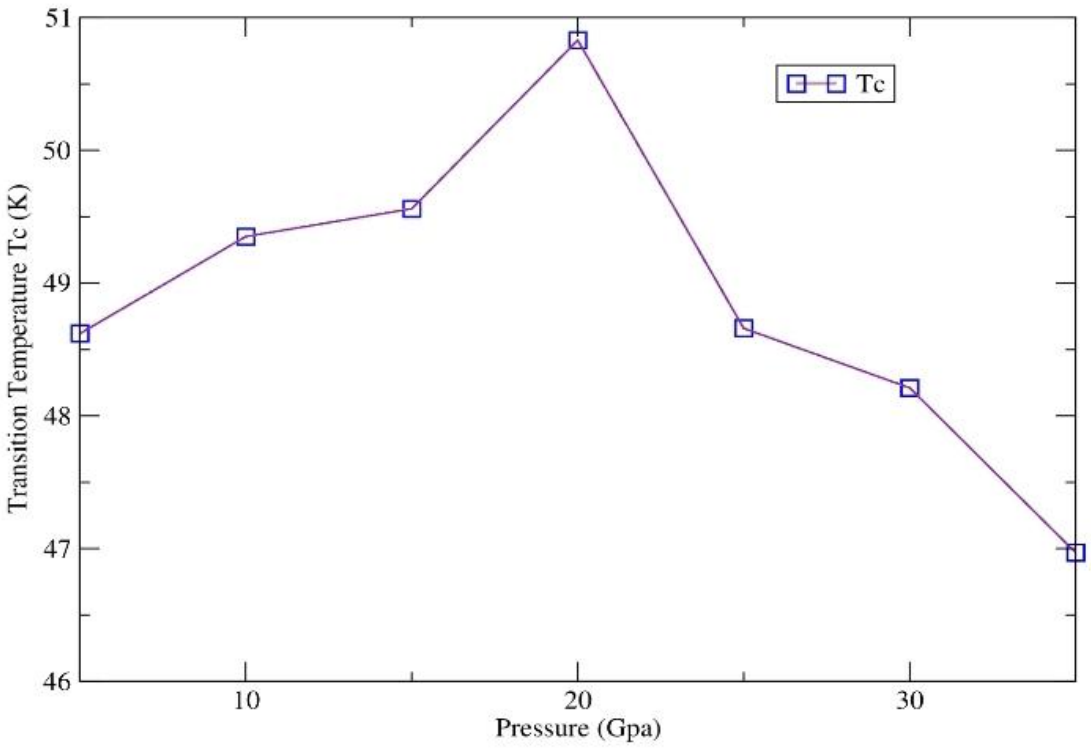

At 20 GPa, pressure compresses the lattice, modifying the Cu-O bond, thus resulting in a higher T_c. The peak suggests that the electronic bands near the Fermi level are reached, enhancing the electronic density available for superconductivity. The material undergoes a structural phase transition in which the stable orthorhombic phase changes to the tetragonal phase when subjected to a pressure of more than 20 GPa, leading to soft phonons, and thus, above that pressure, the stability criterion of the orthorhombic phase may not be satisfied since the material undergoes distortion. At ≈25 GPa, $LaBa_2 Cu_3 O_7$ undergoes a phonon-driven orthorhombic→tetragonal transition as in Fig. 10 above. The associated soft B_1 g mode both marks the structural change and amplifies electron–phonon coupling, pushing λ upward and thus enhancing $T_(c)$ within a conventional Eliashberg framework. Pressure changes phonon frequencies and electron phonon coupling constants, impacting superconductivity.

4.6 Pressure-Induced Doping Superconducting Properties

The condition for applying the BCS theory and the McMillan equation in the cuprate superconductor is that they must undergo doping to populate the holes in the CuO_2 layer. The BCS theory is specifically relevant for doped cuprate superconductors. In this scenario, when superconducting electrons move towards the Cu^{2+} ion, they repel electrons in the O^{2-} ion, pushing them towards another Cu^{2+} ion, which results in the creation of a hole (doping). Doping can be accomplished by either decreasing the concentration of oxygen atoms or applying pressure to the crystal.

When external pressure is applied, the charge concentration near the Fermi level of the crystal lattice increases, altering the electronic structure. In these types of materials, superconductivity depends on polar ionic and doping effects. This process enhances the mobility of oxygen ions between layers, thereby affecting superconductivity and the

transition temperature for superconductivity. The superconductivity transition temperature resulting from pressure-induced doping is represented in Table 3. The electron-phonon coupling constant used for the study was $\lambda = 2.74$.

Table 3

The Calculated Debye Temperature (ΘD) and the Superconductivity Transition Temperature (TC) for LaBa2Cu3O7 and GdBa2Cu3O7- x

$Ba_2Cu_3O_7$ [*this work*]			GdBa2Cu3O7- x [Agora *et al*]	
P(GPa)	$\Theta_D(K)$	T_C (K)	$\Theta_D(K)$	T_C (K)
0	315.21	42.68	409.00	67.92
5	359.08	48.61	463.11	77.08
10	364.49	49.35	495.99	82.20
15	366.11	49.56	511.42	84.86
20	375.45	50.83	850.39	141.16
25	359.37	48.66	465.44	83.59
30	356.04	48.21	403.35	77.47
35	346.91	46.97	334.54	60.32
40	286.10	38.74	225.10	54.33

Figure 11

A Plot Graph for Hole Doping for Laba$_2$cu$_3$o$_7$

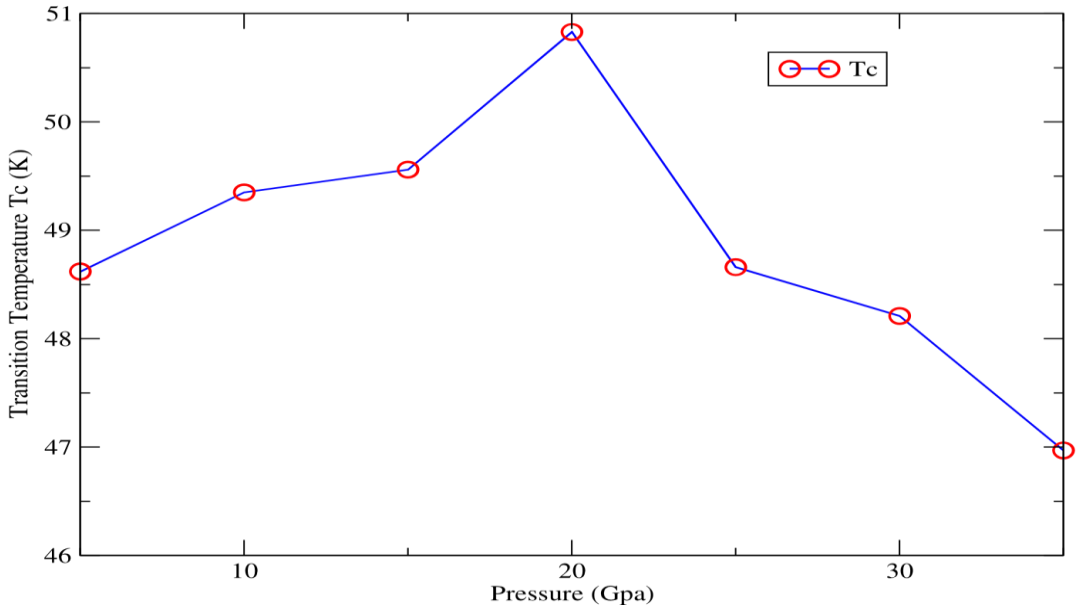

Induced holes under pressure and the superconductivity transition temperature for the cuprate superconductors are related by the equation of the inverted parabola expressed by the equation:

$$T_c = T_c(\max)\left[1 - B(n_{op} - n)^2\right] \quad \ldots (21)$$

Where n_{op} is the hole concentration in which the $T_C$attains its maximum value T_C(max). The constant$B$ = $(n_{op}-n_{min})^{-2}$, where n_{min} is the minimum hole concentration when superconductivity starts to appear. Equation 21 can be modified to include pressure and can be presented by:

$$T_c(P) = T_c(\max)(\mathrm{P})\left[1 - B(n_{op} - n(P))^2\right] \quad \ldots (22)$$

Where (P), (max)(P), and n(P) are measured at pressure (P). The model assumes that nop and $B$are independent of the pressure. By taking (op)(P) to be pressure-dependent T_C at maximum hole concentration, then equation 21 can be written as:

$$T_C(P) = \frac{T_C(op)^{(P)}\left[1 - B(n_{op} - n(P))^2\right]}{\left[1 - B(n_{op} - n_{op}(p))^2\right]} \quad \ldots (23)$$

Equation 23 represents the under-doped crystal. As pressure increases, (P) may approach n_{op} and thus the T_C will be maximum under the conditions of doping by inducing pressure. In this work, it is approximated to happen at around 20GPa (Table 2). The increase of T_C (Table 2) as a result of pressure-induced doping up T(max)can be attributed to the increase in charge carriers in the CuO_2 Planes of $BaLa_2Cu_3O_{7,}$ as it happens for all cuprate superconductors (C. Ambrosch-Draxl *et al*, 2004). The charge carrier increases the density of state near the Fermi level and thus increases the Fermi energy up to the over-doping limit (Table 2). The calculated values of T_C show that the material is a good high-temperature superconductor, and this is supported by the fact that

the values for the Debye temperature are also high. Better $T_C$means the material is stable (R. L. Barns *et al*, 1987; W. Klose et al,1970) and can be evidenced by the stability criterion.

In Figure 11 above, beyond 20GPa, Tc drops because there are structural distortions weakening superconductivity, and excess pressure suppresses phonon interactions, reducing Tc. The materials achieve optimal doping at around 20 GPa. The results indicate that pressure can induce doping, thereby increasing the superconductivity transition temperature to its optimal level. This optimal transition temperature is higher than the standard transition temperature.

CHAPTER FIVE

SUMMARY, CONCLUSION, AND RECOMMENDATIONS

5.1 Introduction

This chapter provides a detailed summary of the study done to employ first-principles computational modelling using the Quantum Espresso program, which is based on density functional theory. Conclusion and recommendations on the study of orthorhombic $LaBa_2Cu_3O_7$ are presented.

5.2 Summary

The main goal of this research was to study externally applied pressure doping, phase transition behaviour of $LaBa_2Cu_3O_7$using an *ab initio* approach through the analysis of electronic, dynamical, and superconducting properties. The electronic structure results showed that $LaBa_2Cu_3O_7$ has an orthorhombic structure with a lattice parameter calculated to be 3.925 Å, which compares well with other works and a band gap of 2.043eV obtained using the Quantum Espresso code in the framework of DFT based on PWscf and USSP.

The phonon dispersions were calculated using the Density functional perturbation theory as implemented in the plane wave self-consistent field. The primitive unit cell of $LaBa_2Cu_3O_{7\ \text{contains}}$ 13 atoms, thus 39 modes of vibration. The optical modes are 36, and the acoustic modes are three. The acoustic modes converge at the gamma high symmetry point, as shown in the phonon dispersion curve. The graph showed the optical mode clearly differentiated from the acoustic mode. These phonon calculations showed that the compound is dynamically stable, as there were no negative frequencies observed.

When external pressure was applied, the charge concentration near the Fermi level of the crystal lattice increased, thus altering the electronic structure. Inducing high pressure

showed changes in lattice parameters and atomic positions, leading to a phase transition. The alteration enhances the density of states at the Fermi level, which is correlated with superconducting behaviour.

The condition for applying the BCS theory and the McMillan equation in the cuprate superconductor is that they must undergo doping to populate the holes in the CuO_2 layer. The BCS theory is specifically relevant for doped cuprate superconductors. When external pressure is applied, the charge concentration near the Fermi level of the crystal lattice increases, altering the electronic structure. The results suggested that pressure of more than 20 GPa gave rise to the highest T_C in the study.

5.3 Conclusion

The calculations suggest that the strong electron-phonon coupling in the CuO_2 planes primarily drives the high Tc in $LaBa_2Cu_3O_7$. Furthermore, the anisotropy in the electronic structure and the presence of charge carriers in the CuO_2 planes are critical for achieving superconductivity. These insights not only enhance our understanding of $LaBa_2Cu_3O_7$ but also contribute to the broader knowledge of high-temperature superconductors, potentially guiding the design of new materials with improved superconducting properties.

5.4 Recommendations

This research on the properties of $LaBa_2Cu_3O_7$ recommends the following:

1. Thermo-electric properties for $LaBa_2Cu_3O_7$ are significant properties that could be investigated for more interesting applications. Understanding and optimizing the thermoelectric properties of $LaBa_2Cu_3O_7$ can lead to its application in thermoelectric devices, where waste heat is converted into electrical energy. These recommend the following: Electronic Structure - Analysis Utilize Density

Functional Theory (DFT) to compute the electronic band structure, focusing on the density of states near the Fermi level. This analysis helps in understanding carrier concentrations and effective masses, which are crucial for thermoelectric performance. Boltzmann Transport Calculations - Implement Boltzmann transport theory to estimate the Seebeck coefficient, electrical conductivity, and thermal conductivity. These parameters are vital for determining the thermoelectric figure of merit (ZT). Defect Engineering involves investigating the role of oxygen vacancies and doping on thermoelectric properties. Introducing controlled defects can modulate carrier concentrations and scattering mechanisms, potentially enhancing thermoelectric efficiency.

2. Optical properties and refractive index are significant properties that could be investigated for more interesting applications, such as absorption spectra, which can be influenced by defects or doping. The tunable optical properties of $LaBa_2Cu_3O_7$ make it a candidate for applications in optical detectors, photodetectors, and other optoelectronic devices. The ability to engineer its optical response through defect manipulation adds versatility to its functional applications.

REFERENCES

Abdulrahman, M. W., & Hussain, F. I. (2019, July).Synthesis of Y3Ba5Cu8O18 superconductor by auto-combustion reaction.In AIP Conference Proceedings (Vol. 2123, No. 1).AIP Publishing.

Agora, J. O., Otieno, C., Nyawere, P. W., & Manyali, G. S. (2020). Ab initio study of pressure-induced phase transition, structural and electronic structure properties of superconducting perovskite compound GdBa2Cu3O7-x. Computational Condensed Matter, 23, e00461.

Agora, J. O., Otieno, C., Nyawere, P. W., & Manyali, G. S. (2022). Elastic behavior, pressure-induced doping, and superconducting transition temperature of GdBa2Cu3O7−x. Journal of Physics Communications, 6(1), 015004.

Ahmad, S., Nadeem, S., & Muhammad, N. (2019). Boundary layer flow over a curved surface embedded in a porous medium—c*ommunications in Theoretical Physics*, *71*(3), 344.

Arslan, E. (2017). SrauSi3 ve SrAu2Si2 Kristallerinin Fiziksel ÖZelliklerinin Teorik Olarak Hesaplanmasi (Master's thesis, Sakarya Universitesi (Turkey).

Bagayoko, D. (2014). Understanding density functional theory (DFT) and completing it in practice. *AIP Advances*, *4*(12).

Chen, W., Semenok, D. V., Troyan, I. A., Ivanova, A. G., Huang, X., Oganov, A. R., & Cui, T. (2020). Superconductivity and equation of state of lanthanum at megabar pressures.Physical Review B, 102(13), 134510.

Chu, C. W. (2021). Room-temperature superconductivity: What more needs to be further studied?In IEEE CSC & ESAS Superconductivity News Forum (Vol. 14, p. 49).

Chu, C. W., Deng, L. Z., & Lv, B. (2015).Hole-doped cuprate high-temperature superconductors. *Physica C: Superconductivity and its Applications*, *514*, 290-313.

Chu, C. W., Deng, L. Z., & Lv, B. (2015).Hole-doped cuprate high-temperature superconductors. *Physica C: Superconductivity and its Applications*, *514*, 290-313.

Dynes, R. C. (1972). McMillan's equation and the Tc of superconductors. *Solid State Communications*, *10*(7), 615–618. https://doi.org/10.1016/0038-1098(72)90603-5

Emetere, M. E. (2020). Experimental validation of structural sequencing of La0.2Sr0. 1Dy0.1Cu0. 2Oy. Applied Physics A, 126(1), 21.

Greene, R. L. (2023). The Strange Metal State of the high-Tc Cuprates. *arXiv preprint arXiv:2306.14794*.

Grotjahn, R., Furche, F., & Kaupp, M. (2019).Development and implementation of excited-state gradients for local hybrid functionals. Journal of Chemical Theory and Computation, 15(10), 5508-5522.

Gui, X., Lv, B., & Xie, W. (2021). Chemistry in superconductors.*Chemical Reviews*, *121*(5), 2966-2991.

Hao, L. Y., & Fu, E. G. (2024).First-principles calculation on the electronic structures, phonon dynamics, and electrical conductivities of Pb10 (PO4) 6O and Pb9Cu (PO4) 6O compounds. Journal of Materials Science & Technology, 173, 218-224.

Hao, L. Y., & Fu, E. G. (2024).First-principles calculation on the electronic structures, phonon dynamics, and electrical conductivities of Pb10 (PO4) 6O and Pb9Cu (PO4) 6O compounds. *Journal of Materials Science & Technology*, *173*, 218-224.

Hung, C. M., Tu, C. S., Xu, Z. R., Chang, L. Y., Schmidt, V. H., Chien, R. R., & Chang, W. C. (2014).Effect of diamagnetic barium substitution on magnetic and photovoltaic properties in multiferroic BiFeO3.*Journal of Applied Physics*, *115*(17).

Hung, W. S., An, Q. F., De Guzman, M., Lin, H. Y., Huang, S. H., Liu, W. R., ...& Lai, J. Y. (2014). Pressure-assisted self-assembly technique for fabricating composite membranes consisting of highly ordered selective laminate layers of amphiphilic graphene oxide. *Carbon*, *68*, 670-677.

Kandyel, E., & Sekkina, M. A. (2002).Influence of Co, Ni, and Zn substitution for Cu on the structural and superconducting properties of (Hg0. 7Cr0. 3) Sr2CuO4+ δ. *Journal of Physics and Chemistry of Solids*, *63*(10), 1815-1822.

Knoop, F., Shulumba, N., Castellano, A., Alvarinhas Batista, J. P., Farris, R., Verstraete, M. J., ... & Hellman, O. (2024). TDEP: Temperature-dependent effective potentials. Journal of Open Source Software, 9(94).

Koretsune, T., & Arita, R. (2017).Efficient method to calculate the electron–phonon coupling constant and superconducting transition temperature. Computer Physics Communications, 220, 239-242.

LeBoeuf, D., Doiron-Leyraud, N., Vignolle, B., Sutherland, M., Ramshaw, B. J., Levallois, J., ...& Taillefer, L. (2011). Lifshitz critical point in the cuprate superconductor YBa 2 CuO y from high-field Hall effect measurements. *Physical Review B—Condensed Matter and Materials Physics*, *83*(5), 054506.

Lehtola, S., Blockhuys, F., & Van Alsenoy, C. (2020). An overview of self-consistent field calculations within finite basis sets. *Molecules*, *25*(5), 1218.

Li, W. M., Zhao, J. F., & Jin, C. Q. (2023). Enhanced cuprate superconductivity from elongated to compressed coordination. *Physica C: Superconductivity and its Applications*, *615*, 1354373.

Maina, D. N. (2024). Ab initio calculations of electronic, elastic, and superconductivity properties of hexagonal antiperovskite-type carbides XCCr3 (X= Al, Ga, or Zn) materials (Doctoral dissertation).

Nyawere, P. W. O. (2024). Density functional calculations of the mechanical, electronic, and dynamical properties of antiperovskite Ca3BO (B= Pb, Ge, Sn). Open Journal of Microphysics, 14(1), 1-12.

Ortiz, J. V., & Zalik, R. A. (2020). Eigenvalues of uncorrelated, density-difference matrices and the interpretation of Δ-self-consistent-field calculations. The Journal of Chemical Physics, 153(11).

Poole, C. P., Zasadinsky, J. F., Zasadinsky, R. K., & Allen, P. B. (1999).Electron-phonon coupling constants. Handbook of Superconductivity, 478-483.

Pressures Phys. Rev. B 102, 134510 (2021)

Rahangdale, K. K., & Ganguly, S. (2023). Magneto-dielectric properties of B-site doped (Fe3+, Zr4+) BiMnO3 perovskite ceramic. Materials Science and Engineering: B, 289, 116225.

Rahman, M. A., Rahaman, M. Z., & Samsuddoha, M. N. (2015).A review on cuprate-based superconducting materials, including characteristics and applications.*American Journal of Physics and Applications*, *3*(2), 39-56.

Ramshaw, B. J., Sebastian, S. E., McDonald, R. D., Day, J., Tam, B., Zhu, Z., ...& Harrison, N. (2014). A quantum critical point at the heart of high-temperature superconductivity.arXiv preprint arXiv:1409.3990, 5.

Rivera, A. M., Cuaspud, J. G., Várgas, C. P., & Ramirez, M. B. (2016).Synthesis and characterization of LaBa2Cu3O7− δ system by the combustion technique.*J. Supercond. Nov. Magn*, *29*(5), 1163-1171.

Rivera, A. M., Cuaspud, J. G., Várgas, C. P., & Ramirez, M. B. (2016).Synthesis and characterization of LaBa2Cu3O7− δ system by the combustion technique. *J. Supercond. Nov. Magn*, *29*(5), 1163-1171.

Setty, C., Baggioli, M., & Zaccone, A. (2020).Understanding the Effects of Pressure, Anharmonicity, and Phonon Softening on the Superconducting Critical Temperature. *arXiv preprint arXiv:2007.04981*.

Solovjov, A. L. (2012). Pseudogap and local pairs in high-Tc superconductors. *Superconductors—Materials, Properties and Applications*, 137.

Song, Y., Golben, J. P., Chittipeddi, S., Lee, S. I., McMichael, R. D., Chen, X. D., ...& Epstein, A. J. (1988). X-ray and neutron-diffraction study of La 1 Ba 2 Cu 3 O 9− δ: Influence of the Cu-O structure on T c. *Physical Review B*, *37*(1), 607.

Sun, Z., & Lin, H. Q. (2024).Exploring high-temperature superconductivity in the extended Hubbard model with antiferromagnetic tendencies. *Physical Review B*, *109*(3), 035107.

Van Delft, D. (2012). History and significance of the discovery of superconductivity by Kamerlingh Onnes in 1911. *Physica C: Superconductivity*, *479*, 30-35.

Waldram, J. R. (2017). *Superconductivity of metals and cuprates*.CRC Press.

Wang, Z. H., Zou, X. W., Fang, J., Yang, T., Tang, Y. L., Huang, Z., ...& Ding, S. Y. (2002). The effect of Er-substitution on the superconducting properties of MTG-YBaCuO crystals.*Superconductor Science and Technology*, *15*(2), 183.

Wesche, R. (2013). *High-temperature superconductors: materials, properties, and applications* (Vol. 6). Springer Science & Business Media.

Wu, H., Tan, S., Wang, W., & Zhang, Y. (2005). Superconductivity in La 1.85− 4⁄3 x Sr 0.15+ 4⁄3 x Cu 1 Mn x O 4 with x up to 0.2. *Physical Review B—Condensed Matter and Materials Physics*, *71*(14), 144520.

Yao, C., & Ma, Y. (2021). Superconducting materials: Challenges and opportunities for large-scale applications. Iscience, 24(6).

Yu, J., Deng, Z., Li, H., Ma, S., Zhao, J., & Wang, L. (2019). Vibration suppression of high-temperature superconducting maglev system via electromagnetic shunt damper. Journal of Superconductivity and Novel Magnetism, 32, 2819-2828.

Zanca, F., Glasby, L. T., Chong, S., Chen, S., Kim, J., Fairen-Jimenez, D., ...& Moghadam, P. Z. (2021). Computational techniques for characterisation of electrically conductive MOFs: quantum calculations and machine learning approaches. *Journal of Materials Chemistry C*, *9*(39), 13584-13599.

APPENDICES

Appendix I: Input and output files for PWSCF Code

Input

```
& control
calculation = 'scf'
restart_mode='from_scratch',
prefix='BaLaCuO',
pseudo_dir ='./',
outdir='./tmp'
/
&system
ibrav= 8,
celldm(1) = 7.3962,
celldm(2) = 1.01020408163,
celldm(3) = 3.0663265,
nat=  13,
ntyp= 4,
ecutwfc =15,
occupations='smearing',smearing='marzari-vanderbilt', degauss=0.1
ecutrho=300.0,
/
&electrons
diagonalization='david'
mixing_mode = 'plain'
mixing_beta = 0.5
conv_thr =  1.0d-8
/
&ions
ion_dynamics='bfgs',
/
&cell
cell_dynamics = 'bfgs'
```

/

ATOMIC_SPECIES

Ba 137.327 Ba.pbe-spn-kjpaw_psl.1.0.0.UPF

La 138.905 La.pbe-spfn-kjpaw_psl.1.0.0.UPF

Cu 63.546 Cu_pbe_v1.2.uspp.F.UPF

O 15.99   O.pbe-n-kjpaw_psl.0.1.UPF

ATOMIC_POSITIONS (crystal)

Ba 0.5000000000 0.5000000000 0.1800261782

Ba 0.5000000000 0.5000000000 0.8199738218

Cu 0.0000000000 0.0000000000 0.0000000000

Cu 0.0000000000 0.0000000000 0.3358903234

Cu 0.0000000000 0.0000000000 0.6641096766

La 0.5000000000 0.5000000000 0.5000000000

O 0.0000000000 0.0000000000 0.1595006994

O 0.0000000000 0.0000000000 0.8404993006

O 0.0000000000 0.5000000000 0.3674702691

O 0.0000000000 0.5000000000 0.6325297309

O 0.5000000000 0.0000000000 0.3672392735

O 0.5000000000 0.0000000000 0.6327607265

O 0.0000000000 0.5000000000 0.0000000000

!CELL_PARAMETERS (angstrom)

! 3.91735712438023 -0.00000000000000 0.00000000000000

! 0.00000000000000 3.96247794916463 0.00000000000000

! 0.00000000000000 0.00000000000000 12.01828059166546

K_POINTS automatic

8 8 4 0 0 0

Output

Program PWSCF v.6.7MaX starts on 22Mar2023 at 11:48: 6

This program is part of the open-source Quantum ESPRESSO suite

for quantum simulation of materials; please cite

"P. Giannozzi et al., J. Phys.:Condens. Matter 21 395502 (2009);

"P. Giannozzi et al., J. Phys.:Condens. Matter 29 465901 (2017);

URL http://www.quantum-espresso.org",
in publications or presentations arising from this work. More details at
http://www.quantum-espresso.org/quote
Serial version
Waiting for input
Reading input from standard input
Warning: card &CELL ignored
Warning: card   CELL_DYNAMICS = 'BFGS' ignored
Warning: card / ignored

Current dimensions of program PWSCF are:
Max number of different atomic species (ntypx) = 10
Max number of k-points (npk) = 40000
Max angular momentum in pseudopotentials (lmaxx) = 3
file Ba.pbe-spn-kjpaw_psl.1.0.0.UPF: wavefunction(s) 5S 6S renormalized
file La.pbe-spfn-kjpaw_psl.1.0.0.UPF: wavefunction(s) 5S 5D 4F renormalized
file O.pbe-n-kjpaw_psl.0.1.UPF: wavefunction(s) 2P renormalized
G-vector sticks info
---
sticks: dense smooth   PW   G-vecs: dense   smooth   PW
Sum   1313   261   89   109985   9795   1909
bravais-lattice index   =   8
lattice parameter (alat) =   7.3962 a.u.
unit-cell volume   =   1253.2954 (a.u.)^3
number of atoms/cell   =   13
number of atomic types   =   4
number of electrons   =   130.00
number of Kohn-Sham states   =   78
kinetic-energy cutoff   =   15.0000 Ry
charge density cutoff   =   300.0000 Ry
scf convergence threshold =   1.0E-08
mixing beta   =   0.5000
number of iterations used =   8 plain   mixing

Exchange-correlation= SLA PW   PBX PBC

(1 4 3 4 0 0 0)

celldm(1)= 7.396200 celldm(2)= 1.010204 celldm(3)= 3.066327

celldm(4)= 0.000000 celldm(5)= 0.000000 celldm(6)= 0.000000

crystal axes: (cart. coord. in units of alat)

a(1) = (1.000000 0.000000 0.000000)

a(2) = (0.000000 1.010204 0.000000)

a(3) = (0.000000 0.000000 3.066327)

reciprocal axes: (cart. coord. in units 2 pi/alat)

b(1) = (1.000000 0.000000 0.000000)

b(2) = (0.000000 0.989899 0.000000)

b(3) = (0.000000 0.000000 0.326123)

PseudoPot. # 1 for Ba read from file:

./Ba.pbe-spn-kjpaw_psl.1.0.0.UPF

MD5 check sum: c432291d3e53af55f19d5e8866385beb

Pseudo is Projector augmented-wave + core cor, Zval = 10.0

Generated using "atomic" code by A. Dal Corso v.5.1

Shape of augmentation charge: PSQ

Using radial grid of 1251 points,seven beta functions with:

l(1) = 0

l(2) = 0

l(3) = 0

l(4) = 1

l(5) = 1

l(6) = 2

l(7) = 2

Q(r) pseudized with 0 coefficients

PseudoPot. # 2 for La read from file:

./La.pbe-spfn-kjpaw_psl.1.0.0.UPF

MD5 checksum: 1b39010b0ab9e8c18b47286845cf5387

Pseudo is Projector augmented-wave + core cor, Zval = 11.0

Generated using "atomic" code by A. Dal Corso v.6.2.2

Shape of augmentation charge: PSQ

Using radial grid of 1253 points, 8 beta functions with:

l(1) = 0

l(2) = 0

l(3) = 1

l(4) = 1

l(5) = 2

l(6) = 2

l(7) = 3

l(8) = 3

Q(r) pseudized with 0 coefficients

PseudoPot. # 3 for Cu read from file:

./Cu_pbe_v1.2.uspp.F.UPF

MD5 check sum: 6e991ff952a84172a2a52a1c1e996048

Pseudo is Ultrasoft + core correction, Zval = 19.0

Generated by new atomic code, or converted to UPF format

Using radial grid of 867 points, 6 beta functions with:

l(1) = 0

l(2) = 0

l(3) = 1

l(4) = 1

l(5) = 2

l(6) = 2

Q(r) pseudized with 8 coefficients, rinner = 1.150 1.150 1.150

1.150 1.150

PseudoPot. # 4 for O read from file:

./O.pbe-n-kjpaw_psl.0.1.UPF

MD5 check sum: 0234752ac141de4415c5fc33072bef88

Pseudo is Projector augmented-wave + core cor, Zval = 6.0

Generated using "atomic" code by A. Dal Corso v.5.0.99 svn rev. 10869

Shape of augmentation charge: BESSEL

Using radial grid of 1095 points, 4 beta functions with:

l(1) = 0

l(2) = 0

l(3) = 1

l(4) = 1

Q(r) pseudized with 0 coefficients

atomic species valence mass pseudopotential

Ba 10.00 137.32700 Ba(1.00)

La 11.00 138.90500 La(1.00)

Cu 19.00 63.54600 Cu(1.00)

O 6.00 15.99000 O (1.00)

8 Sym. Ops., with inversion, found

Cartesian axes

site n. atom positions (alat units)

1 Ba tau(1) = (0.5000000 0.5051020 0.5520190)

2 Ba tau(2) = (0.5000000 0.5051020 2.5143075)

3 Cu tau(3) = (0.0000000 0.0000000 0.0000000)

4 Cu tau(4) = (0.0000000 0.0000000 1.0299494)

5 Cu tau(5) = (0.0000000 0.0000000 2.0363771)

6 La tau(6) = (0.5000000 0.5051020 1.5331633)

7 O tau(7) = (0.0000000 0.0000000 0.4890812)

8 O tau(8) = (0.0000000 0.0000000 2.5772453)

9 O tau(9) = (0.0000000 0.5051020 1.1267838)

10 O tau(10) = (0.0000000 0.5051020 1.9395427)

11 O tau(11) = (0.5000000 0.0000000 1.1260755)

12 O tau(12) = (0.5000000 0.0000000 1.9402510)

13 O tau(13) = (0.0000000 0.5051020 0.0000000)

number of k points= 75 Marzari-Vanderbilt smearing, width (Ry)= 0.1000

cart. coord. in units 2pi/alat

k(1) = (0.0000000 0.0000000 0.0000000), wk = 0.0078125

k(2) = (0.0000000 0.0000000 0.0815308), wk = 0.0156250

k(3) = (0.0000000 0.0000000 -0.1630616), wk = 0.0078125

k(4) = (0.0000000 0.1237374 0.0000000), wk = 0.0156250

k(5) = (0.0000000 0.1237374 0.0815308), wk = 0.0312500

k(6) = (0.0000000 0.1237374 -0.1630616), wk = 0.0156250

k(7) = (0.0000000 0.2474747 0.0000000), wk = 0.0156250
k(8) = (0.0000000 0.2474747 0.0815308), wk = 0.0312500
k(9) = (0.0000000 0.2474747 -0.1630616), wk = 0.0156250
k(10) = (0.0000000 0.3712121 0.0000000), wk = 0.0156250
k(11) = (0.0000000 0.3712121 0.0815308), wk = 0.0312500
k(12) = (0.0000000 0.3712121 -0.1630616), wk = 0.0156250
k(13) = (0.0000000 -0.4949495 0.0000000), wk = 0.0078125
k(14) = (0.0000000 -0.4949495 0.0815308), wk = 0.0156250
k(15) = (0.0000000 -0.4949495 -0.1630616), wk = 0.0078125
k(16) = (0.1250000 0.0000000 0.0000000), wk = 0.0156250
k(17) = (0.1250000 0.0000000 0.0815308), wk = 0.0312500
k(18) = (0.1250000 0.0000000 -0.1630616), wk = 0.0156250
k(19) = (0.1250000 0.1237374 0.0000000), wk = 0.0312500
k(20) = (0.1250000 0.1237374 0.0815308), wk = 0.0625000
k(21) = (0.1250000 0.1237374 -0.1630616), wk = 0.0312500
k(22) = (0.1250000 0.2474747 0.0000000), wk = 0.0312500
k(23) = (0.1250000 0.2474747 0.0815308), wk = 0.0625000
k(24) = (0.1250000 0.2474747 -0.1630616), wk = 0.0312500
k(25) = (0.1250000 0.3712121 0.0000000), wk = 0.0312500
k(26) = (0.1250000 0.3712121 0.0815308), wk = 0.0625000
k(27) = (0.1250000 0.3712121 -0.1630616), wk = 0.0312500
k(28) = (0.1250000 -0.4949495 0.0000000), wk = 0.0156250
k(29) = (0.1250000 -0.4949495 0.0815308), wk = 0.0312500
k(30) = (0.1250000 -0.4949495 -0.1630616), wk = 0.0156250
k(31) = (0.2500000 0.0000000 0.0000000), wk = 0.0156250
k(32) = (0.2500000 0.0000000 0.0815308), wk = 0.0312500
k(33) = (0.2500000 0.0000000 -0.1630616), wk = 0.0156250
k(34) = (0.2500000 0.1237374 0.0000000), wk = 0.0312500
k(35) = (0.2500000 0.1237374 0.0815308), wk = 0.0625000
k(36) = (0.2500000 0.1237374 -0.1630616), wk = 0.0312500
k(37) = (0.2500000 0.2474747 0.0000000), wk = 0.0312500
k(38) = (0.2500000 0.2474747 0.0815308), wk = 0.0625000
k(39) = (0.2500000 0.2474747 -0.1630616), wk = 0.0312500

k(40) = (0.2500000 0.3712121 0.0000000), wk = 0.0312500
k(41) = (0.2500000 0.3712121 0.0815308), wk = 0.0625000
k(42) = (0.2500000 0.3712121 -0.1630616), wk = 0.0312500
k(43) = (0.2500000 -0.4949495 0.0000000), wk = 0.0156250
k(44) = (0.2500000 -0.4949495 0.0815308), wk = 0.0312500
k(45) = (0.2500000 -0.4949495 -0.1630616), wk = 0.0156250
k(46) = (0.3750000 0.0000000 0.0000000), wk = 0.0156250
k(47) = (0.3750000 0.0000000 0.0815308), wk = 0.0312500
k(48) = (0.3750000 0.0000000 -0.1630616), wk = 0.0156250
k(49) = (0.3750000 0.1237374 0.0000000), wk = 0.0312500
k(50) = (0.3750000 0.1237374 0.0815308), wk = 0.0625000
k(51) = (0.3750000 0.1237374 -0.1630616), wk = 0.0312500
k(52) = (0.3750000 0.2474747 0.0000000), wk = 0.0312500
k(53) = (0.3750000 0.2474747 0.0815308), wk = 0.0625000
k(54) = (0.3750000 0.2474747 -0.1630616), wk = 0.0312500
k(55) = (0.3750000 0.3712121 0.0000000), wk = 0.0312500
k(56) = (0.3750000 0.3712121 0.0815308), wk = 0.0625000
k(57) = (0.3750000 0.3712121 -0.1630616), wk = 0.0312500
k(58) = (0.3750000 -0.4949495 0.0000000), wk = 0.0156250
k(59) = (0.3750000 -0.4949495 0.0815308), wk = 0.0312500
k(60) = (0.3750000 -0.4949495 -0.1630616), wk = 0.0156250
k(61) = (-0.5000000 0.0000000 0.0000000), wk = 0.0078125
k(62) = (-0.5000000 0.0000000 0.0815308), wk = 0.0156250
k(63) = (-0.5000000 0.0000000 -0.1630616), wk = 0.0078125
k(64) = (-0.5000000 0.1237374 0.0000000), wk = 0.0156250
k(65) = (-0.5000000 0.1237374 0.0815308), wk = 0.0312500
k(66) = (-0.5000000 0.1237374 -0.1630616), wk = 0.0156250
k(67) = (-0.5000000 0.2474747 0.0000000), wk = 0.0156250
k(68) = (-0.5000000 0.2474747 0.0815308), wk = 0.0312500
k(69) = (-0.5000000 0.2474747 -0.1630616), wk = 0.0156250
k(70) = (-0.5000000 0.3712121 0.0000000), wk = 0.0156250
k(71) = (-0.5000000 0.3712121 0.0815308), wk = 0.0312500
k(72) = (-0.5000000 0.3712121 -0.1630616), wk = 0.0156250

k(73) = (-0.5000000 -0.4949495 0.0000000), wk = 0.0078125
k(74) = (-0.5000000 -0.4949495 0.0815308), wk = 0.0156250
k(75) = (-0.5000000 -0.4949495 -0.1630616), wk = 0.0078125
Dense grid: 109985 G-vectors FFT dimensions: (45, 45, 125)
Smooth grid: 9795 G-vectors FFT dimensions: (20, 20, 60)
Estimated max dynamical RAM per process > 1.12 GB
Check: negative core charge= -0.000005
Initial potential from superposition of free atoms
starting charge 126.93619, renormalised to 130.00000
Starting wfcs are 97 randomized atomic wfcs
Total CPU time spent up to now is 32.7 secs
Self-consistent Calculation
iteration # 1 ecut= 15.00 Ry beta= 0.50
Davidson diagonalization with overlap
ethr = 1.00E-02, avg # of iterations = 6.3
total cpu time spent up to now is 143.9 secs
total energy = -2665.96788765 Ry
estimated scf accuracy < 189.98029868 Ry
iteration # 2 ecut= 15.00 Ry beta= 0.50
Davidson diagonalization with overlap
ethr = 1.00E-02, avg # of iterations = 4.4
total cpu time spent up to now is 270.6 secs
total energy = -2746.51593456 Ry
estimated scf accuracy < 176.73452940 Ry
iteration # 3 ecut= 15.00 Ry beta= 0.50
Davidson diagonalization with overlap
ethr = 1.00E-02, avg # of iterations = 6.7
total cpu time spent up to now is 399.3 secs
total energy = -2741.57906323 Ry
estimated scf accuracy < 487.86651194 Ry
iteration # 4 ecut= 15.00 Ry beta= 0.50
Davidson diagonalization with overlap
ethr = 1.00E-02, avg # of iterations = 5.5

total cpu time spent up to now is 505.9 secs

total energy = -2765.01022296 Ry

estimated scf accuracy < 22.95434571 Ry

iteration # 5 ecut= 15.00 Ry beta= 0.50

Davidson diagonalization with overlap

ethr = 1.00E-02, avg # of iterations = 2.0

total cpu time spent up to now is 569.2 secs

total energy = -2765.09818442 Ry

estimated scf accuracy < 8.40267414 Ry

iteration # 6 ecut= 15.00 Ry beta= 0.50

Davidson diagonalization with overlap

ethr = 6.46E-03, avg # of iterations = 1.5

total cpu time spent up to now is 626.0 secs

total energy = -2764.71606184 Ry

estimated scf accuracy < 4.59744703 Ry

iteration # 7 ecut= 15.00 Ry beta= 0.50

Davidson diagonalization with overlap

ethr = 3.54E-03, avg # of iterations = 1.5

total cpu time spent up to now is 680.4 secs

total energy = -2764.19135033 Ry

estimated scf accuracy < 1.94998487 Ry

iteration # 8 ecut= 15.00 Ry beta= 0.50

Davidson diagonalization with overlap

ethr = 1.50E-03, avg # of iterations = 5.1

total cpu time spent up to now is 753.9 secs

total energy = -2764.53622822 Ry

estimated scf accuracy < 1.59705300 Ry

iteration # 9 ecut= 15.00 Ry beta= 0.50

Davidson diagonalization with overlap

ethr = 1.23E-03, avg # of iterations = 2.3

total cpu time spent up to now is 816.2 secs

total energy = -2764.46961277 Ry

estimated scf accuracy < 1.36806255 Ry

iteration # 10 ecut= 15.00 Ry beta= 0.50
Davidson diagonalization with overlap
ethr = 1.05E-03, avg # of iterations = 2.0
total cpu time spent up to now is 876.3 secs
total energy = -2764.60887313 Ry
estimated scf accuracy < 0.28465896 Ry
iteration # 11 ecut= 15.00 Ry beta= 0.50
Davidson diagonalization with overlap
ethr = 2.19E-04, avg # of iterations = 3.1
total cpu time spent up to now is 936.4 secs
total energy = -2764.62439479 Ry
estimated scf accuracy < 0.04512837 Ry
iteration # 12 ecut= 15.00 Ry beta= 0.50
Davidson diagonalization with overlap
ethr = 3.47E-05, avg # of iterations = 6.2
total cpu time spent up to now is 1003.7 secs
total energy = -2764.62681079 Ry
estimated scf accuracy < 0.02239502 Ry
iteration # 13 ecut= 15.00 Ry beta= 0.50
Davidson diagonalization with overlap
ethr = 1.72E-05, avg # of iterations = 3.0
total cpu time spent up to now is 1063.3 secs
total energy = -2764.62697041 Ry
estimated scf accuracy < 0.00596651 Ry
iteration # 14 ecut= 15.00 Ry beta= 0.50
Davidson diagonalization with overlap
c_bands: 1 eigenvalues not converged
ethr = 4.59E-06, avg # of iterations = 3.6
total cpu time spent up to now is 1125.2 secs
total energy = -2764.62743790 Ry
estimated scf accuracy < 0.00026849 Ry
iteration # 15 ecut= 15.00 Ry beta= 0.50
Davidson diagonalization with overlap

c_bands: 1 eigenvalues not converged
ethr = 2.07E-07, avg # of iterations = 2.7
total cpu time spent up to now is   1190.4 secs
total energy   =   -2764.62746657 Ry
estimated scf accuracy   <   0.00008460 Ry
iteration # 16   ecut=   15.00 Ry   beta= 0.50
Davidson diagonalization with overlap
ethr = 6.51E-08, avg # of iterations = 2.1
total cpu time spent up to now is   1252.5 secs
total energy   =   -2764.62747756 Ry
estimated scf accuracy   <   0.00000691 Ry
iteration # 17   ecut=   15.00 Ry   beta= 0.50
Davidson diagonalization with overlap
ethr = 5.32E-09, avg # of iterations = 3.1
total cpu time spent up to now is   1318.9 secs
total energy   =   -2764.62747885 Ry
estimated scf accuracy   <   0.00000167 Ry
iteration # 18   ecut=   15.00 Ry   beta= 0.50
Davidson diagonalization with overlap
ethr = 1.28E-09, avg # of iterations = 2.5
total cpu time spent up to now is   1379.6 secs
total energy   =   -2764.62747909 Ry
estimated scf accuracy   <   0.00000008 Ry
iteration # 19   ecut=   15.00 Ry   beta= 0.50
Davidson diagonalization with overlap
ethr = 6.31E-11, avg # of iterations = 3.5
total cpu time spent up to now is   1450.2 secs
total energy   =   -2764.62747911 Ry
estimated scf accuracy   <   0.00000003 Ry
iteration # 20   ecut=   15.00 Ry   beta= 0.50
Davidson diagonalization with overlap
ethr = 2.58E-11, avg # of iterations = 2.0
total cpu time spent up to now is   1512.6 secs

total energy = -2764.62747912 Ry

estimated scf accuracy < 0.00000001 Ry

iteration # 21 ecut= 15.00 Ry beta= 0.50

Davidson diagonalization with overlap

ethr = 8.19E-12, avg # of iterations = 2.0

Total CPU time spent up to now is 1574.8 secs

End of self-consistent calculation

k = 0.0000 0.0000 0.0000 (1255 PWs) bands (eV):

-134.6374-134.5445-134.3606 -87.1635 -86.7884 -86.6970 -86.6952 -86.4789

-86.4095 -85.6026 -85.3778 -84.7336 -19.8067 -14.1124 -14.0752 -11.3529

-10.9277 -10.5082 -10.2977 -10.1585 -10.0622 -9.8526 -3.4315 -3.4052

-2.8106 0.4670 0.5979 0.7885 0.8310 0.8631 0.9130 0.9634

3.3768 3.7624 4.2122 4.6691 4.9233 5.0626 5.0968 5.4501

5.5650 5.7334 5.8584 6.5110 6.6030 7.0728 7.1296 7.2910

7.5064 7.7344 7.7755 7.8349 8.1726 8.1930 8.3589 8.5920

8.6960 9.0633 9.2653 9.2689 10.0417 10.0907 10.1623 10.1825

10.6946 10.7546 10.8346 10.8914 13.2205 13.5199 15.0672 15.1763

15.5063 16.7108 16.8489 16.8744 17.7939 17.9466

k = 0.0000 0.0000 0.0815 (1246 PWs) bands (ev):

-134.6059-134.3376-134.2969 -86.7585 -86.7416 -86.4991 -86.2358 -86.2231

-85.9289 -85.6178 -85.3831 -84.7752 -19.8068 -14.1150 -14.0722 -11.3547

-10.9233 -10.4878 -10.2795 -10.1477 -10.0560 -9.8672 -3.4297 -3.4068

-2.8112 0.5544 0.5871 0.8301 0.8672 0.9104 0.9668 3.3163

3.4123 3.8556 3.8820 4.2493 4.7891 5.3791 5.4431 5.8513

5.8820 6.0809 6.5964 6.6673 6.8742 7.2838 7.3712 7.5368

7.5448 7.7498 8.2805 8.3765 8.5291 8.6755 8.8965 9.0590

9.3742 9.5048 9.5065 9.7988 9.9578 9.9784 10.1659 10.2843

10.5358 10.5690 10.9071 11.4203 12.6883 13.9643 15.1302 15.2877

15.4960 16.3847 16.7145 17.1318 17.7820 18.0094

k = 0.0000 0.0000-0.1631 (1260 PWs) bands (ev):

-134.7434-134.5484-134.4940 -86.8446 -86.6780 -86.6232 -86.5805 -86.3929

-86.3016 -86.2136 -85.9347 -85.4208 -19.8071 -14.1175 -14.0702 -11.3434

-10.9230 -10.5125 -10.2993 -10.1759 -10.0650 -9.8737 -3.4323 -3.4097

-2.8222 0.5632 0.5800 0.8246 0.8668 0.9044 0.9662 2.9877

3.0729 3.2971 3.5560 5.0163 5.0318 5.0398 5.0817 5.2838

5.4837 5.5292 5.5325 5.9518 6.4222 6.4589 6.5097 6.8688

6.9173 7.3200 7.6064 7.6968 8.1280 8.3599 8.3872 8.9810

8.9901 9.0637 9.0926 9.4152 9.5270 9.7253 9.8471 10.0306

10.1371 10.2408 10.2744 11.7301 12.1691 14.3258 15.1432 15.1964

15.6367 16.1443 16.7128 16.8675 17.6700 18.1113

k = 0.0000 0.1237 0.0000 (1249 PWs) bands (ev):

-134.7891-134.3682-134.2090 -86.9790 -86.5922 -86.4685 -86.2191 -86.2146

-86.1070 -86.0808 -85.3483 -84.7349 -19.7960 -14.0890 -14.0515 -11.2791

-10.9389 -10.4859 -10.3383 -10.2109 -10.0769 -9.9002 -3.4265 -3.3958

-2.8641 0.5546 0.6067 0.7868 0.8286 0.9476 0.9974 1.9966

3.3605 4.4740 4.4876 4.9621 5.0951 5.1932 5.3897 5.4914

5.8489 5.9127 6.0414 6.0626 6.5200 6.6930 6.7271 7.2493

7.6745 8.0636 8.0975 8.4542 8.5721 8.7917 8.9050 9.0777

9.2988 9.3186 9.4981 9.6286 9.6708 9.9018 10.0823 10.1126

10.1404 10.2739 10.9059 11.7563 13.7005 13.7052 15.3525 15.4912

15.8051 16.6255 17.0475 17.0526 17.4247 17.8820

k = 0.0000 0.1237 0.0815 (1249 PWs) bands (ev):

-134.6975-134.4408-134.2275 -86.7601 -86.5084 -86.4405 -86.3043 -86.2621

-86.1615 -86.0664 -85.5132 -84.7930 -19.7961 -14.0910 -14.0489 -11.2880

-10.9359 -10.4870 -10.3317 -10.2049 -10.0771 -9.9108 -3.4223 -3.3972

-2.8649 0.5632 0.5973 0.7810 0.8303 0.9444 0.9997 2.7537

3.5488 3.8265 4.1556 4.3171 5.0659 5.1397 5.4823 5.6147

5.7866 5.8221 6.2680 6.3559 6.6257 6.7385 7.1172 7.2746

7.4654 7.5958 7.9097 8.0621 8.6060 8.8290 8.8703 8.9744

9.1442 9.3912 9.4875 9.5165 9.8220 9.9234 10.0538 10.1647

10.3593 10.3950 11.0640 12.0247 13.1154 14.4416 15.4317 15.6071

15.7700 16.6223 16.6268 17.2024 17.4839 17.8626

k = 0.0000 0.1237-0.1631 (1248 PWs) bands (ev):

-134.5852-134.4518-134.3048 -86.7125 -86.6933 -86.4849 -86.2344 -86.1772

-85.8233 -85.8136 -85.5468 -85.2238 -19.7961 -14.0932 -14.0463 -11.2945

-10.9337 -10.4873 -10.3269 -10.2025 -10.0738 -9.9158 -3.4207 -3.3967

-2.8690 0.5806 0.5893 0.7831 0.8320 0.9404 1.0028 3.5039
3.7008 3.7885 4.3077 4.4442 4.9372 5.1178 5.3195 5.4843
5.8333 5.8690 6.1180 6.1883 6.7107 6.7444 7.4674 7.5856
7.7383 8.0491 8.1106 8.4559 8.4788 8.4899 8.7994 8.9331
9.0908 9.3020 9.3573 9.4456 9.5190 9.9080 9.9545 10.0689
10.1520 10.5856 10.7299 12.2226 12.7906 14.7065 15.4849 15.5331
15.9256 16.4153 16.6215 16.9578 17.5803 17.8922
k = 0.0000 0.2475 0.0000 (1237 PWs) bands (ev):
-134.5879-134.2683-134.1127 -86.7136 -86.2700 -85.9852 -85.9352 -85.8620
-85.7786 -85.7035 -85.4093 -84.8127 -19.7694 -14.0282 -13.9919 -11.1626
-10.9409 -10.4407 -10.3881 -10.3340 -10.1239 -10.0208 -3.3976 -3.3732
-2.9848 0.6129 0.6206 0.6882 0.7554 1.0327 1.0824 4.0383
4.1752 4.3192 4.4484 4.5175 5.2427 5.5896 5.7474 6.1103
6.2164 6.7710 6.8237 6.8788 7.1763 7.3808 7.5279 7.6885
8.0119 8.2054 8.3112 8.4260 8.6332 8.7715 9.0654 9.0844
9.0895 9.1501 9.2583 9.4761 9.4884 9.7420 9.8421 9.9142
10.1004 11.5253 11.7301 13.4727 13.9944 15.3387 16.0350 16.2713
16.4059 16.6274 17.0302 17.4323 17.5583 18.1464
k = 0.0000 0.2475 0.0815 (1240 PWs) bands (ev):
-134.6226-134.2962-134.1534 -86.6513 -86.6079 -86.0538 -85.9349 -85.8040
-85.6896 -85.6719 -85.5454 -85.1290 -19.7693 -14.0297 -13.9900 -11.1604
-10.9415 -10.4492 -10.4114 -10.3207 -10.1322 -10.0110 -3.4049 -3.3689
-2.9856 0.6064 0.6128 0.6932 0.7489 1.0301 1.0844 3.2246
4.0629 4.1453 4.3180 4.5081 4.9767 5.6725 5.7263 5.9611
6.0766 6.4768 6.5461 6.8639 7.0938 7.2512 7.3383 7.5173
7.9080 7.9303 8.2804 8.3446 8.6612 8.7861 8.8888 9.0030
9.0372 9.1810 9.3028 9.3872 9.5944 9.9418 10.0351 10.1014
10.2022 11.0427 11.7349 13.4968 13.8950 15.5683 16.1377 16.3079
16.4084 16.5592 16.9759 17.2224 17.5170 18.2137
k = 0.0000 0.2475-0.1631 (1232 PWs) bands (ev):
-134.3936-134.2725-134.0868 -86.3462 -86.3339 -86.0064 -85.8992 -85.7710
-85.3956 -85.3861 -85.3595 -84.9930 -19.7693 -14.0306 -13.9886 -11.1474
-10.9470 -10.4347 -10.4209 -10.3104 -10.1248 -9.9982 -3.4000 -3.3685

-2.9840 0.6158 0.6161 0.6963 0.7431 1.0293 1.0880 3.8512

4.3577 4.3765 4.6569 4.6634 4.9538 5.2286 5.3379 5.9313

6.1676 6.7283 6.8720 6.8885 6.9905 7.7491 7.8032 7.9857

8.1335 8.3799 8.4992 8.5991 8.6371 8.8647 8.9714 9.0826

9.3092 9.3101 9.4192 9.8676 9.9081 10.0020 10.2143 10.7192

10.8693 11.7088 12.8361 13.5546 13.9902 15.9527 16.3037 16.3194

16.4139 16.6844 16.7320 17.0670 17.5856 17.6817

k = 0.0000 0.3712 0.0000 (1231 PWs) bands (eV):

-134.5057-134.1586-134.0678 -86.5652 -86.1268 -85.8369 -85.7943 -85.7266

-85.7263 -85.5314 -85.0855 -84.8008 -19.7421 -13.9646 -13.9305 -10.9675

-10.9612 -10.5100 -10.4949 -10.3492 -10.1862 -10.1394 -3.3834 -3.3412

-3.1029 0.5952 0.6109 0.6625 0.7098 1.1215 1.1714 3.3520

3.8622 3.9744 4.0661 4.9539 5.7162 5.9221 5.9257 6.1291

6.5272 6.5339 6.9454 7.0392 7.4558 7.5172 7.8617 7.9239

8.0856 8.1337 8.1821 8.3023 8.6230 8.7240 9.0022 9.0852

9.0910 9.1550 9.1846 9.2509 9.5717 9.9122 10.2334 10.4021

10.7359 11.7551 13.7036 14.6833 14.8389 16.1637 16.2681 16.7361

17.0270 17.2045 17.4059 17.5968 17.7646 18.4152

k = 0.0000 0.3712 0.0815 (1229 PWs) bands (ev):

-134.3863-134.1730-134.0607 -86.5237 -86.3307 -85.9128 -85.8464 -85.7488

-85.3294 -85.2671 -84.8795 -84.8542 -19.7421 -13.9653 -13.9294 -10.9707

-10.9610 -10.5139 -10.4930 -10.3315 -10.1931 -10.1364 -3.3769 -3.3424

-3.1015 0.5927 0.6212 0.6692 0.7031 1.1195 1.1734 3.5765

3.6368 4.2699 4.5046 4.7028 5.3155 5.6232 6.1891 6.3157

6.3842 6.6891 6.9883 7.4531 7.4937 7.7136 7.8611 8.0640

8.3346 8.3899 8.4821 8.5473 8.8735 9.0056 9.0275 9.1346

9.2686 9.2779 9.4155 9.5034 9.7077 9.8341 10.3674 10.3734

10.4552 11.2689 13.1579 14.8040 15.0180 16.1589 16.3142 16.8345

16.9789 17.0933 17.4792 17.6165 17.8727 18.2345

k = 0.0000 0.3712-0.1631 (1232 PWs) bands (ev):

-134.3989-134.2709-134.0393 -86.3908 -86.2161 -86.1011 -86.0305 -85.7586

-85.3236 -85.2667 -85.0799 -85.0368 -19.7421 -13.9664 -13.9281 -10.9764

-10.9628 -10.5304 -10.4917 -10.3340 -10.1880 -10.1168 -3.3720 -3.3450

-3.1033 0.5944 0.6231 0.6779 0.6906 1.1191 1.1761 3.4863
3.9163 4.2860 4.4391 4.7348 4.7610 5.2180 5.2668 6.2350
6.3062 6.5823 6.6917 7.0209 7.3517 7.4228 7.7095 7.8502
8.0351 8.3531 8.3700 8.7720 8.7997 8.9168 9.0276 9.1674
9.2586 9.3205 9.5964 9.7281 9.7909 9.8131 10.1514 10.3821
10.7112 12.0886 12.9165 14.8701 14.9829 16.1706 16.4764 16.7539
16.9418 17.1928 17.2688 17.5409 17.6495 18.1771
k = 0.0000-0.4949 0.0000 (1206 PWs) bands (ev):
-134.0719-133.8823-133.7795 -86.3319 -85.9217 -85.4987 -85.2072 -85.1907
-85.0397 -84.4037 -84.3915 -83.8646 -19.7301 -13.9368 -13.9038 -10.9701
-10.7405 -10.7116 -10.5094 -10.2726 -10.2058 -10.1931 -3.3612 -3.3248
-3.1418 0.5782 0.6127 0.6774 0.7093 1.1611 1.2104 3.5968
4.1781 4.6002 4.7321 5.9706 6.1291 6.2278 6.3347 6.5141
6.6627 6.7184 7.3304 7.5331 7.9006 7.9619 8.5469 8.5575
8.6217 8.7431 8.7591 8.9041 9.1979 9.2135 9.2799 9.3484
9.4794 9.8137 9.9529 10.5836 10.7220 11.2305 11.3023 12.7548
12.9585 13.3971 14.5395 15.8338 16.0646 16.2034 16.2836 17.2781
17.5155 17.9493 18.0760 18.1870 18.5918 18.7159
k = 0.0000-0.4949 0.0815 (1210 PWs) bands (ev):
-134.0898-133.9476-133.8114 -86.3043 -86.0205 -85.7261 -85.6893 -85.2466
-84.9059 -84.4446 -84.2435 -83.9647 -19.7301 -13.9377 -13.9031 -10.9728
-10.7439 -10.7142 -10.5076 -10.2604 -10.2089 -10.2007 -3.3602 -3.3280
-3.1396 0.5743 0.6151 0.6788 0.7055 1.1591 1.2119 3.5681
4.1625 4.5549 4.7008 5.6167 5.6294 5.9867 6.2208 6.4289
6.6226 7.1444 7.1636 7.2453 7.7819 7.8529 8.5754 8.5781
8.6805 8.7729 8.7933 8.9569 9.0294 9.2661 9.3583 9.3843
9.6388 9.6706 9.9163 10.3071 10.8939 11.3020 11.4923 12.1971
12.2937 12.8506 14.3869 15.9114 16.0513 16.0677 16.2545 17.2663
17.3503 17.4943 18.1427 18.1958 18.3314 18.5856
k = 0.0000-0.4949-0.1631 (1212 PWs) bands (ev):
-134.1970-134.0394-133.6896 -86.0170 -86.0096 -85.9516 -85.6637 -85.0257
-84.9885 -84.7885 -84.5307 -83.9877 -19.7302 -13.9398 -13.9023 -10.9578
-10.7543 -10.7158 -10.5037 -10.2471 -10.2134 -10.2072 -3.3624 -3.3242

-3.1414 0.5644 0.6246 0.6869 0.7038 1.1583 1.2144 3.3955
3.9662 4.4968 5.2404 5.6873 5.7843 5.9318 6.0556 6.0643
6.3606 6.5605 6.6144 6.6362 7.4537 7.5480 7.8713 8.0693
8.6946 8.8023 8.8219 8.9364 9.0109 9.0405 9.1709 9.2445
9.4947 10.3448 10.4351 10.9113 10.9168 11.2032 11.2251 11.5013
13.5511 13.9231 13.9339 16.0807 16.1335 16.1404 16.1848 17.1079
17.2058 17.3925 18.1342 18.1596 18.2597 18.3055
k = 0.1250 0.0000 0.0000 (1245 PWs) bands (ev):
-134.5318-134.4234-134.2706 -86.6825 -86.2985 -86.2808 -86.2494 -86.2124
-86.1930 -85.6695 -85.6162 -84.8935 -19.7948 -14.0840 -14.0498 -11.2851
-10.9306 -10.5143 -10.3351 -10.2009 -10.0802 -9.8684 -3.4186 -3.3975
-2.8699 0.5102 0.6195 0.8678 0.8988 0.8990 0.9032 3.1085
3.8404 4.0885 4.2573 5.0710 5.1052 5.1345 5.5271 5.6426
5.8563 6.1693 6.3086 6.4672 6.5675 7.2597 7.4603 7.7087
7.9081 7.9653 8.1138 8.2014 8.4420 8.5649 8.7970 8.8172
9.0523 9.0876 9.1368 9.6707 9.8746 9.9098 10.0091 10.0459
10.4525 10.4618 10.9553 12.1325 13.6398 13.8831 15.4731 15.5049
15.7591 16.6112 17.0267 17.2414 17.8390 17.8607
k = 0.1250 0.0000 0.0815 (1245 PWs) bands (ev):
-134.6969-134.3422-134.1819 -86.7745 -86.6163 -86.5331 -86.2674 -86.0577
-86.0572 -85.7581 -85.2314 -84.7308 -19.7948 -14.0865 -14.0473 -11.2898
-10.9277 -10.5169 -10.3372 -10.1982 -10.0747 -9.8770 -3.4207 -3.3974
-2.8689 0.5128 0.6079 0.8634 0.8980 0.9015 0.9057 2.8836
3.7623 4.1833 4.6027 4.6048 5.2692 5.5189 5.6395 5.8826
6.1423 6.1714 6.2539 6.4280 6.6023 6.8871 7.2548 7.3788
7.4637 7.6992 7.8838 8.2730 8.4344 8.8985 8.9397 9.0779
9.1059 9.2924 9.4340 9.6513 9.7426 9.7865 10.0073 10.0938
10.3479 10.5849 11.2145 12.1885 13.2654 14.4519 15.5126 15.5720
15.7835 16.6119 16.6484 17.4275 17.6646 17.8735
k = 0.1250 0.0000-0.1631 (1242 PWs) bands (ev):
-134.5203-134.3847-134.2408 -86.4256 -86.2622 -86.2298 -86.1864 -86.1050
-85.8475 -85.8128 -85.5514 -85.1150 -19.7949 -14.0888 -14.0450 -11.2937
-10.9191 -10.5157 -10.3348 -10.1943 -10.0708 -9.8821 -3.4180 -3.3980

-2.8747 0.5280 0.6034 0.8616 0.8977 0.9044 0.9051 3.8103
3.9144 4.4697 4.9403 4.9888 5.3004 5.3294 5.4628 5.9957
6.1256 6.1632 6.5402 6.6098 6.7082 6.9584 7.5618 7.6805
7.8161 7.8420 8.1213 8.4007 8.4845 8.6439 9.0531 9.2956
9.3535 9.4078 9.5351 9.5570 9.6577 9.8501 9.9735 10.1126
10.1285 10.2356 10.8191 12.4251 12.8452 14.6912 15.3907 15.5831
15.9854 16.4516 16.6239 17.1815 17.6149 18.1931
k = 0.1250 0.1237 0.0000 (1237 PWs) bands (ev):
-134.5923-134.2828-134.0705 -86.4509 -86.4012 -86.3078 -86.2638 -86.1643
-85.6396 -85.6006 -85.1525 -84.4454 -19.7838 -14.0614 -14.0271 -11.2466
-10.9184 -10.4924 -10.3671 -10.2364 -10.0868 -9.9102 -3.4178 -3.3736
-2.9208 0.5388 0.6238 0.7550 0.7805 0.9715 0.9893 3.6215
4.4013 4.4305 4.5940 4.6090 4.8486 5.6926 5.8983 6.1688
6.2105 6.2579 6.6197 6.7588 6.7611 7.1511 7.1892 7.4497
8.1147 8.1528 8.7254 8.7311 8.8002 8.9323 9.0187 9.3348
9.3845 9.5067 9.6189 9.6473 9.8204 10.2071 10.3400 10.4753
10.5700 11.2478 11.2890 12.3429 13.7873 14.2609 15.6955 15.7613
16.0557 16.4035 17.0062 17.2414 17.3835 17.8841
k = 0.1250 0.1237 0.0815 (1246 PWs) bands (ev):
-134.6038-134.4167-134.2477 -86.6581 -86.5396 -86.5002 -86.2187 -86.1132
-86.0745 -85.7088 -85.4740 -84.9742 -19.7840 -14.0639 -14.0255 -11.2471
-10.9277 -10.5039 -10.3810 -10.2342 -10.1004 -9.9101 -3.4208 -3.3781
-2.9249 0.5353 0.6171 0.7519 0.7822 0.9697 0.9872 3.0808
3.8803 4.0491 4.2892 4.4887 4.8690 5.4122 5.5600 5.8456
5.9215 6.1451 6.5105 6.6308 6.7357 6.9907 7.2673 7.4448
7.6102 7.6485 8.0596 8.2002 8.6389 8.7300 8.9142 9.0108
9.0745 9.1820 9.3170 9.4180 9.6579 9.7279 9.8773 10.0929
10.4111 10.6557 10.9093 12.4696 13.3411 14.6009 15.7250 15.8206
15.9712 16.4110 16.7771 17.2268 17.3656 17.8600
k = 0.1250 0.1237-0.1631 (1246 PWs) bands (ev):
-134.5588-134.3761-134.3434 -86.5556 -86.4333 -86.4180 -86.2967 -86.0036
-85.9788 -85.8175 -85.4267 -85.4175 -19.7840 -14.0657 -14.0241 -11.2357
-10.9325 -10.5086 -10.3768 -10.2394 -10.1021 -9.9102 -3.4229 -3.3792

-2.9261 0.5402 0.6200 0.7510 0.7821 0.9694 0.9854 3.2500

3.5796 4.0354 4.4518 4.9041 5.0436 5.0787 5.5075 5.8731

6.1760 6.1857 6.4446 6.5978 6.6836 6.7895 6.9478 7.3189

7.5770 7.8288 8.1271 8.4991 8.5106 8.5588 8.9265 9.0083

9.0936 9.1642 9.3466 9.4652 9.6655 9.7657 9.9322 9.9973

10.4459 10.5299 10.6720 12.6368 12.9766 14.9363 15.6816 15.7934

16.2156 16.3911 16.5550 17.1280 17.3740 17.9469

k = 0.1250 0.2475 0.0000 (1236 PWs) bands (ev):

-134.4247-134.2961-134.1941 -86.4508 -86.4300 -86.2273 -85.8886 -85.7586

-85.7372 -85.4896 -85.4597 -84.8563 -19.7574 -14.0048 -13.9732 -11.1172

-10.9318 -10.4791 -10.4273 -10.3444 -10.1437 -10.0031 -3.4014 -3.3454

-3.0509 0.5872 0.6117 0.6237 0.7007 1.0057 1.0229 3.5568

3.7115 4.0803 4.5699 4.7416 4.9872 5.4754 5.8704 6.1385

6.2483 6.7121 6.7378 6.9856 7.1532 7.3142 7.5253 7.7028

8.0312 8.0961 8.3459 8.4433 8.7515 8.7964 9.0645 9.2104

9.2419 9.2928 9.4877 9.5950 9.6050 9.8185 10.3414 10.4527

10.6307 11.4811 11.7231 13.5993 13.9416 15.4053 15.9763 16.2153

16.4266 16.8325 16.8688 17.2944 17.6462 17.9768

k = 0.1250 0.2475 0.0815 (1236 PWs) bands (ev):

-134.4238-134.2969-134.1869 -86.4033 -86.3448 -86.2641 -85.9159 -85.7890

-85.6244 -85.5283 -85.4220 -84.9743 -19.7573 -14.0064 -13.9714 -11.1200

-10.9344 -10.4747 -10.4322 -10.3386 -10.1407 -10.0052 -3.4016 -3.3454

-3.0497 0.5859 0.6117 0.6241 0.6983 1.0075 1.0212 3.6603

3.9065 4.2169 4.4659 4.6118 4.9464 5.2973 5.6915 5.9293

6.1782 6.5661 6.8315 7.0810 7.3654 7.5529 7.6036 7.7618

8.0648 8.2177 8.3500 8.4981 8.7039 8.7584 9.0913 9.1304

9.1603 9.3403 9.3628 9.6501 9.8024 9.9305 10.1645 10.4887

10.7014 11.1619 11.9995 13.6138 13.9234 15.5629 15.9262 16.2836

16.4550 16.8106 16.8937 17.1027 17.4274 17.9971

k = 0.1250 0.2475-0.1631 (1244 PWs) bands (ev):

-134.5135-134.3375-134.3347 -86.6505 -86.6042 -86.5437 -85.8751 -85.8078

-85.7393 -85.7237 -85.4833 -85.3923 -19.7573 -14.0084 -13.9698 -11.1223

-10.9415 -10.4681 -10.4564 -10.3409 -10.1551 -10.0020 -3.4037 -3.3482

-3.0519 0.5835 0.6132 0.6215 0.6973 1.0083 1.0195 3.3639
3.6946 3.9259 4.0316 4.3857 4.8408 5.0682 5.4024 5.5132
5.8489 6.2715 6.3823 6.7255 6.7627 7.3078 7.3840 7.4992
7.5713 8.1161 8.2611 8.3038 8.6762 8.7241 8.8574 8.8927
9.0735 9.2539 9.2802 9.3603 9.5234 9.6382 9.8055 10.4833
10.5575 10.9704 11.7123 13.6188 13.8253 15.7918 15.8682 16.4194
16.4658 16.6975 16.8785 17.0608 17.1612 17.8482
k = 0.1250 0.3712 0.0000 (1227 PWs) bands (ev):
-134.2984-134.1728-134.0498 -86.3319 -86.1996 -86.1374 -85.8944 -85.5747
-85.1568 -85.0269 -84.9869 -84.8726 -19.7300 -13.9465 -13.9153 -10.9528
-10.9323 -10.5423 -10.5026 -10.3571 -10.1805 -10.1201 -3.3673 -3.3266
-3.1747 0.5247 0.5552 0.6385 0.7159 1.0129 1.0239 3.5810
4.0952 4.3898 4.6097 5.0313 5.0978 5.5890 5.8564 6.0527
6.5383 6.7876 7.3094 7.4327 7.5702 7.6046 7.8298 7.9815
8.4120 8.4731 8.5644 8.6283 8.7092 8.9817 9.0268 9.1930
9.1986 9.3707 9.3907 9.8660 9.9763 10.1529 10.5252 10.8001
10.8812 12.0687 13.1341 14.6060 15.0221 15.9130 16.1602 16.9725
17.0055 17.2238 17.3776 17.7577 17.9114 18.4124
k = 0.1250 0.3712 0.0815 (1224 PWs) bands (ev):
-134.2950-134.1607-133.9642 -86.2936 -86.2472 -85.9896 -85.8951 -85.5167
-85.1115 -84.9528 -84.8828 -84.7100 -19.7301 -13.9476 -13.9142 -10.9493
-10.9305 -10.5341 -10.5131 -10.3501 -10.1820 -10.1138 -3.3676 -3.3233
-3.1728 0.5245 0.5574 0.6442 0.7047 1.0137 1.0240 3.5994
4.2750 4.3848 4.5850 4.8380 4.8974 5.7532 6.1144 6.2953
6.4505 6.7601 6.9586 7.2188 7.4628 7.7298 7.8906 8.1952
8.2792 8.3931 8.6593 8.7788 8.8655 9.1953 9.2867 9.3555
9.4989 9.5387 9.9147 9.9471 10.3233 10.5375 10.8529 11.0668
11.5419 11.6566 13.2513 14.6641 15.0577 15.7178 16.1722 16.9153
16.9588 17.2242 17.4890 17.7541 17.9129 18.2468
k = 0.1250 0.3712-0.1631 (1226 PWs) bands (ev):
-134.3182-134.1968-133.9595 -86.5093 -86.4615 -86.0158 -85.6554 -85.6099
-85.1415 -85.1175 -84.9023 -84.5472 -19.7300 -13.9486 -13.9134 -10.9474
-10.9293 -10.5328 -10.5237 -10.3438 -10.1921 -10.1170 -3.3663 -3.3219

-3.1735 0.5211 0.5593 0.6487 0.6972 1.0169 1.0242 3.4968
4.0263 4.1265 4.3514 4.4991 4.8383 5.5621 6.0583 6.1064
6.2738 6.4333 6.9437 7.0165 7.4170 7.9406 8.0877 8.1248
8.1297 8.4439 8.7497 8.8171 9.0129 9.0699 9.2206 9.2428
9.4824 9.5678 9.9803 10.0896 10.2196 10.7796 10.8070 10.8453
10.9561 11.4949 14.0449 14.8029 15.0442 15.5096 16.1905 16.8638
16.9549 17.1950 17.5410 17.8134 17.9674 17.9685
k = 0.1250-0.4949 0.0000 (1218 PWs) bands (ev):
-134.1770-134.0096-133.9914 -86.0718 -85.9117 -85.7892 -85.7102 -85.3040
-85.2992 -85.0312 -84.7216 -84.5020 -19.7186 -13.9210 -13.8910 -10.9624
-10.7328 -10.6993 -10.5656 -10.2764 -10.2226 -10.2007 -3.3545 -3.3143
-3.2196 0.4978 0.5385 0.6544 0.7175 1.0124 1.0198 3.4547
4.1463 4.3437 4.8271 4.9204 5.6957 5.7348 5.8438 6.3285
7.0405 7.0818 7.4666 7.7185 7.7261 7.8796 8.1543 8.2113
8.6925 8.6932 8.7475 8.9504 8.9805 9.1865 9.1955 9.3229
9.3884 9.4989 9.8181 9.9603 10.5260 10.8867 10.9142 11.0837
11.1641 11.8815 13.6260 15.3066 15.7619 15.9175 16.5439 17.0427
17.5407 17.5455 17.7688 18.0661 18.2987 18.9251
k = 0.1250-0.4949 0.0815 (1224 PWs) bands (ev):
-134.3586-134.1774-133.8330 -86.4354 -86.3253 -85.9663 -85.8063 -85.3046
-85.2403 -85.0366 -84.6886 -84.5671 -19.7187 -13.9220 -13.8903 -10.9674
-10.7419 -10.7084 -10.5636 -10.2705 -10.2249 -10.2050 -3.3525 -3.3224
-3.2225 0.4903 0.5414 0.6636 0.7107 1.0130 1.0216 3.4250
4.1670 4.1923 4.3951 4.8253 5.0748 5.3087 5.6548 6.2965
6.6487 6.9079 6.9751 7.1055 7.7102 7.8389 7.8535 7.9149
8.4709 8.6426 8.6546 8.7313 8.9337 8.9695 9.3648 9.3991
9.5389 9.5674 9.8598 9.8894 10.0631 10.3692 10.9149 10.9847
11.4368 12.2797 13.6002 15.1954 15.4891 15.9757 16.4277 16.9823
17.2623 17.3509 17.8531 18.1246 18.2118 18.5910
k = 0.1250-0.4949-0.1631 (1220 PWs) bands (ev):
-134.2575-134.1504-133.8338 -86.3267 -86.2742 -85.7841 -85.6935 -85.3367
-84.9733 -84.8301 -84.7679 -84.6466 -19.7187 -13.9224 -13.8894 -10.9598
-10.7454 -10.7111 -10.5587 -10.2635 -10.2230 -10.2080 -3.3486 -3.3218

-3.2205 0.4855 0.5488 0.6798 0.6965 1.0145 1.0233 3.5444

4.2283 4.2872 4.7769 5.1279 5.3205 6.0763 6.2888 6.6657

6.7635 6.9469 7.1837 7.5453 7.7567 7.8184 7.8961 7.9439

8.4307 8.4500 8.7479 8.8450 8.9722 9.2951 9.4294 9.6310

9.6798 9.9389 9.9616 9.9690 10.0628 10.4322 10.7736 10.8731

10.9430 11.1182 14.2468 15.1952 15.5289 16.1308 16.2752 16.9494

17.1968 17.6193 17.6914 18.0104 18.2700 18.5259

k = 0.2500 0.0000 0.0000 (1237 PWs) bands (ev):

-134.6707-134.2369-134.0689 -86.7432 -86.2893 -86.2784 -85.9335 -85.9053

-85.6332 -85.5861 -85.3462 -84.7250 -19.7654 -14.0149 -13.9876 -11.1594

-10.9111 -10.5750 -10.4432 -10.3266 -10.1211 -9.8939 -3.3919 -3.3768

-3.0046 0.4666 0.6676 0.7657 0.8376 0.9586 0.9879 3.9568

4.0690 4.2308 4.6255 5.0184 5.1277 6.0301 6.2166 6.2543

6.3041 6.5287 6.5797 6.5997 7.0958 7.5174 7.7019 7.7300

8.1585 8.3684 8.4282 8.5020 8.6623 8.7461 8.9783 8.9951

9.1658 9.3383 9.3594 9.5052 9.5819 9.6749 9.7263 9.9794

10.1291 10.1571 11.3461 13.1080 13.9562 15.3180 16.0849 16.3376

16.3545 16.4826 16.9270 17.6618 17.8852 18.1138

k = 0.2500 0.0000 0.0815 (1239 PWs) bands (ev):

-134.7662-134.2441-134.0364 -86.9617 -86.7642 -86.1677 -85.8785 -85.7441

-85.5445 -85.5026 -85.4476 -84.8645 -19.7653 -14.0159 -13.9860 -11.1558

-10.9147 -10.5739 -10.4514 -10.3197 -10.1222 -9.8993 -3.3900 -3.3753

-3.0045 0.4642 0.6633 0.7621 0.8426 0.9571 0.9905 2.8061

3.7216 4.1648 4.1961 4.9580 5.0676 5.5741 5.9097 5.9522

6.2925 6.5391 6.5633 6.9554 7.1723 7.3062 7.4912 7.6011

7.9648 8.1105 8.2946 8.5159 8.7832 8.8378 8.9528 9.0786

9.3097 9.4167 9.5183 9.5272 9.6154 9.8157 9.8549 10.1415

10.1433 10.3671 11.1871 13.3777 13.9651 15.4636 16.2167 16.3257

16.3529 16.4528 16.9248 17.5940 17.6873 18.0279

k = 0.2500 0.0000-0.1631 (1240 PWs) bands (ev):

-134.5326-134.4425-134.0985 -86.6986 -86.6040 -86.0814 -85.9565 -85.8059

-85.7557 -85.6332 -85.3864 -85.2123 -19.7653 -14.0174 -13.9849 -11.1453

-10.9210 -10.5770 -10.4581 -10.3129 -10.1322 -9.8877 -3.3872 -3.3796

-3.0048 0.4698 0.6621 0.7619 0.8448 0.9552 0.9913 3.2998
3.6022 3.9984 4.2565 5.1652 5.3312 5.4930 5.6453 6.2368
6.3049 6.5266 6.6535 6.8788 7.2589 7.4305 7.4497 7.5545
7.6759 7.8822 8.2956 8.3961 8.4636 8.7579 9.0020 9.0161
9.2075 9.2355 9.3385 9.5418 9.5930 9.6892 9.7681 9.8636
10.2517 10.3771 10.5431 13.4455 14.0458 15.4935 16.0296 16.2977
16.3414 16.7279 16.9876 17.3880 17.5609 18.1343
k = 0.2500 0.1237 0.0000 (1238 PWs) bands (ev):
-134.5619-134.3306-134.1149 -86.5219 -86.3488 -86.2997 -86.1169 -85.8680
-85.6634 -85.6591 -85.4696 -84.7711 -19.7546 -13.9954 -13.9703 -11.1269
-10.9097 -10.5509 -10.4841 -10.3376 -10.1377 -9.9181 -3.3970 -3.3456
-3.0656 0.4775 0.6631 0.6830 0.7209 0.9636 0.9719 3.5212
3.9046 3.9760 4.3644 4.6115 4.9547 5.5180 5.8523 6.1120
6.2882 6.6625 6.7763 6.7932 7.2234 7.4671 7.5107 7.5408
7.7238 8.0811 8.2668 8.6367 8.6508 8.8511 8.9147 9.2478
9.2511 9.3183 9.3707 9.5477 9.7093 9.7803 10.0297 10.2853
10.4950 10.6844 11.3252 13.4506 13.9122 15.3960 15.8144 16.3520
16.5262 16.6379 16.6817 17.6842 17.7093 18.0039
k = 0.2500 0.1237 0.0815 (1235 PWs) bands (ev):
-134.4609-134.2864-134.1405 -86.5858 -86.1667 -86.1013 -85.9895 -85.7537
-85.7033 -85.5326 -85.3548 -84.8878 -19.7544 -13.9964 -13.9681 -11.1166
-10.9095 -10.5448 -10.4839 -10.3363 -10.1411 -9.9190 -3.3988 -3.3460
-3.0632 0.4770 0.6623 0.6815 0.7239 0.9658 0.9716 3.6407
3.9269 4.1670 4.7828 4.8856 5.1554 5.3131 5.9500 6.2617
6.4974 6.7789 7.0214 7.0541 7.2950 7.4905 7.7041 7.7859
8.1090 8.1456 8.2741 8.4482 8.6636 8.9374 9.0366 9.0984
9.1778 9.2699 9.3910 9.5056 9.7412 10.0805 10.3672 10.4286
10.6115 10.9346 11.1958 13.5000 13.9226 15.5058 15.8005 16.3870
16.4276 16.7257 16.8339 17.3766 17.6866 18.0678
k = 0.2500 0.1237-0.1631 (1242 PWs) bands (ev):
-134.5110-134.3919-134.2339 -86.5981 -86.5979 -86.2180 -85.9955 -85.9267
-85.7408 -85.5580 -85.4918 -85.3477 -19.7544 -13.9975 -13.9666 -11.1109
-10.9161 -10.5489 -10.4901 -10.3466 -10.1484 -9.9230 -3.3999 -3.3487

-3.0668 0.4684 0.6593 0.6824 0.7245 0.9654 0.9705 3.2421
3.6171 3.6251 4.0015 4.1134 4.9531 5.0977 5.5136 5.6001
6.2491 6.4065 6.7806 6.9272 7.2681 7.3502 7.5675 7.8397
7.9249 8.1040 8.3962 8.4365 8.6237 8.7455 8.9064 8.9350
9.2514 9.4256 9.4460 9.5192 9.5293 9.8948 10.0368 10.2381
10.2560 10.7113 10.8699 13.6240 13.7928 15.5013 15.7646 16.3615
16.4395 16.7268 16.9527 17.3358 17.3449 18.4280
k = 0.2500 0.2475 0.0000 (1223 PWs) bands (ev):
-134.3176-134.1216-133.9663 -86.0696 -85.9938 -85.8758 -85.7462 -85.6861
-85.3878 -85.2677 -84.9142 -84.5497 -19.7281 -13.9493 -13.9245 -11.0048
-10.9079 -10.5743 -10.4706 -10.3893 -10.1562 -9.9839 -3.3770 -3.3116
-3.2041 0.4559 0.4875 0.5968 0.7183 0.8609 0.8774 3.8428
4.1454 4.3132 4.4353 4.7426 4.8460 6.1178 6.2031 6.6779
6.7665 7.0413 7.2456 7.6590 7.7830 7.8768 7.9583 8.1161
8.3186 8.6308 8.6389 8.8944 8.9511 9.2156 9.3351 9.5291
9.6265 9.7451 9.7666 10.0279 10.0395 10.0633 10.8321 11.5367
11.9240 12.4202 12.5194 13.9165 14.1230 15.3721 15.8397 16.3699
16.7888 17.1565 17.2492 17.5216 17.7544 17.9335
k = 0.2500 0.2475 0.0815 (1230 PWs) bands (ev):
-134.3706-134.2224-134.0880 -86.1422 -86.1061 -85.9739 -85.9073 -85.7046
-85.5731 -85.4880 -85.0337 -85.0119 -19.7280 -13.9504 -13.9233 -10.9947
-10.9143 -10.5788 -10.4746 -10.4087 -10.1624 -9.9901 -3.3806 -3.3131
-3.2109 0.4547 0.4872 0.5916 0.7168 0.8573 0.8860 3.7050
4.0566 4.2285 4.5257 4.5833 4.8727 5.5414 5.9002 6.4350
6.6809 6.9285 7.0424 7.2854 7.4636 7.7388 7.9631 8.0494
8.2651 8.3631 8.4707 8.6668 8.7287 8.9418 9.0933 9.2666
9.3973 9.6019 9.6646 9.8483 10.1783 10.3390 10.5609 10.9904
11.4441 11.6936 11.9310 13.9456 14.0973 15.1938 15.6976 16.5439
16.7702 17.0052 17.1591 17.3786 17.6469 18.0452
k = 0.2500 0.2475-0.1631 (1228 PWs) bands (ev):
-134.3295-134.2193-134.0761 -86.1903 -86.0987 -86.0617 -85.7117 -85.5868
-85.4637 -85.3310 -85.1173 -85.0576 -19.7279 -13.9511 -13.9224 -10.9955
-10.9088 -10.5848 -10.4762 -10.4042 -10.1638 -9.9888 -3.3796 -3.3126

-3.2094 0.4562 0.4878 0.5906 0.7135 0.8561 0.8923 3.7168
3.8048 4.1220 4.2805 4.8287 4.9668 5.0771 6.0914 6.1419
6.6506 6.9146 7.1857 7.3746 7.7293 7.8034 8.0401 8.1398
8.4952 8.6268 8.6952 8.8211 8.8560 8.9754 9.2316 9.3265
9.4639 9.6079 9.7234 10.0236 10.1892 10.5699 10.6310 10.6990
11.7162 11.7923 12.4998 14.1261 14.1473 15.1297 15.6841 16.7567
16.7998 16.8348 17.1124 17.2967 17.5958 18.0784
k = 0.2500 0.3712 0.0000 (1218 PWs) bands (ev):
-134.1977-134.0456-133.9437 -85.9254 -85.8619 -85.8113 -85.6957 -85.4279
-85.2499 -85.0028 -84.8066 -84.5616 -19.7011 -13.9021 -13.8781 -10.9240
-10.8449 -10.6566 -10.5128 -10.3767 -10.1743 -10.0903 -3.3465 -3.3411
-3.2929 0.3659 0.3854 0.5858 0.6817 0.7561 0.7742 3.4229
4.0778 4.1159 4.5322 5.0112 5.5561 6.4147 6.5442 6.7273
6.7927 7.1175 7.2755 7.3784 7.7833 8.1064 8.2515 8.5691
8.6440 8.7156 8.8526 9.0281 9.0870 9.2450 9.2825 9.4983
9.6109 9.7914 10.1761 10.3177 10.3765 10.7723 11.0970 11.3202
11.9669 12.7310 12.8011 14.2990 14.8025 15.8801 16.3266 16.6228
16.8416 17.2088 17.7646 17.8738 18.0720 18.2310
k = 0.2500 0.3712 0.0815 (1226 PWs) bands (ev):
-134.2838-134.1028-134.0879 -86.4248 -85.9997 -85.7876 -85.6376 -85.5419
-85.4023 -85.3955 -84.9736 -84.8246 -19.7012 -13.9027 -13.8777 -10.9343
-10.8493 -10.6605 -10.5194 -10.3720 -10.1840 -10.0995 -3.3503 -3.3439
-3.2949 0.3618 0.3832 0.5858 0.6690 0.7590 0.7738 3.3363
3.5521 3.9591 4.2551 4.7529 5.0782 5.4872 6.0874 6.2432
6.7987 7.0269 7.1408 7.2297 7.5359 7.8446 7.9294 8.1317
8.2067 8.4893 8.7232 8.8313 8.9357 9.1120 9.2229 9.3874
9.5734 9.6977 9.7780 9.9197 10.2901 10.6059 10.7047 10.9270
12.0347 12.6375 12.7149 14.3461 14.6465 15.6746 16.2196 16.7704
17.0076 17.2446 17.5129 17.7516 18.1507 18.3563
k = 0.2500 0.3712-0.1631 (1228 PWs) bands (ev):
-134.3120-134.1534-134.0952 -86.0291 -85.9892 -85.8987 -85.8569 -85.7445
-85.4479 -85.4143 -85.0526 -84.9468 -19.7013 -13.9033 -13.8771 -10.9310
-10.8554 -10.6614 -10.5213 -10.3702 -10.1848 -10.1097 -3.3486 -3.3472

-3.2964 0.3633 0.3824 0.5887 0.6575 0.7660 0.7736 3.5547
3.5606 4.0483 4.5980 4.7874 5.2228 5.6134 5.8787 6.3046
6.7275 6.9320 7.0463 7.3674 7.4668 7.4919 7.8836 8.1902
8.2484 8.4032 8.5825 8.8306 8.8917 9.0145 9.1575 9.2198
9.4604 9.4991 9.7203 9.8334 9.8506 10.3094 10.7347 10.8521
11.8022 12.1210 13.3694 14.2708 14.3806 15.5321 16.1670 16.8042
17.1198 17.2128 17.4312 17.5434 18.2766 18.3295
k = 0.2500-0.4949 0.0000 (1236 PWs) bands (ev):
-134.4307-134.2857-134.1007 -86.5596 -86.2827 -85.9933 -85.8659 -85.7678
-85.7431 -85.7066 -85.3821 -84.6574 -19.6899 -13.8827 -13.8590 -10.9553
-10.7135 -10.6995 -10.6635 -10.2561 -10.2474 -10.2044 -3.4094 -3.3227
-3.3015 0.3240 0.3662 0.5709 0.5709 0.7031 0.7878 2.9514
3.4646 3.8844 3.9315 4.2133 4.2635 4.3115 5.5433 5.9825
6.3872 6.5715 6.7330 6.7467 7.0750 7.2272 7.2635 7.5499
7.9749 8.1993 8.2584 8.5270 8.6516 8.9104 8.9263 8.9833
9.2069 9.5245 9.7830 9.8273 9.9173 10.2532 10.5264 11.0858
12.2311 12.3794 12.6465 14.2846 15.0685 16.1162 16.5707 17.0076
17.2326 17.5365 17.5480 17.9690 18.2972 18.8386
k = 0.2500-0.4949 0.0815 (1228 PWs) bands (ev):
-134.4363-134.0912-133.9977 -86.5929 -86.1643 -86.0166 -85.7539 -85.4949
-85.2859 -85.1970 -85.0349 -84.7389 -19.6899 -13.8830 -13.8584 -10.9438
-10.7104 -10.6899 -10.6597 -10.2497 -10.2383 -10.1984 -3.4053 -3.3224
-3.2975 0.3262 0.3688 0.5681 0.5861 0.7133 0.7809 2.9457
3.3856 3.6479 3.8270 4.2661 5.0744 5.6660 6.2691 6.5140
6.6106 6.6453 6.9050 7.0064 7.3241 7.7492 7.8120 7.9993
8.2440 8.4267 8.7141 8.9469 8.9718 9.0645 9.3169 9.5030
9.5639 9.6788 9.9608 10.0108 10.2758 10.7607 11.0545 11.3528
11.6297 12.4196 12.8116 14.2399 14.8849 16.2310 16.7069 17.0330
17.2196 17.4014 17.5150 17.6186 18.0167 18.6902
k = 0.2500-0.4949-0.1631 (1228 PWs) bands (ev):
-134.3272-134.1466-134.0700 -86.4607 -86.2720 -86.0965 -85.6797 -85.3897
-85.2460 -85.2026 -85.1147 -84.9241 -19.6901 -13.8832 -13.8581 -10.9404
-10.7115 -10.6904 -10.6587 -10.2441 -10.2361 -10.2028 -3.4040 -3.3202

-3.2951 0.3168 0.3741 0.5664 0.5902 0.7281 0.7654 3.2190
3.4214 3.4897 3.9361 4.6285 5.3911 6.1992 6.2851 6.4978
6.8041 6.9649 6.9713 7.0103 7.7089 7.7299 7.8191 7.8789
7.9037 8.0705 8.2869 8.9439 9.0220 9.1905 9.4333 9.4896
9.5824 9.7493 9.9448 10.2475 10.2476 10.4138 10.4962 10.9473
11.5081 12.2211 12.6770 14.1494 14.2728 16.4667 16.6882 16.8111
17.3621 17.3681 17.4850 17.6445 17.8080 18.5910
k = 0.3750 0.0000 0.0000 (1213 PWs) bands (ev):
-134.1450-133.9922-133.9528 -86.0768 -85.6278 -85.4723 -85.4468 -85.4087
-85.2834 -85.1575 -84.7506 -84.3378 -19.7347 -13.9385 -13.9225 -10.9523
-10.9028 -10.6134 -10.5379 -10.4919 -10.1743 -9.8872 -3.3564 -3.3502
-3.1283 0.4554 0.6370 0.7399 0.7488 1.0608 1.0810 4.1987
4.5622 4.8396 5.0720 6.4002 6.4291 6.4435 6.8839 7.0109
7.1642 7.2895 7.4066 7.6870 7.9768 8.1290 8.3646 8.4433
8.4571 8.5783 8.8748 9.0747 9.1431 9.1500 9.3893 9.4408
9.5157 9.6487 9.7900 9.8432 9.8609 10.6488 10.6692 10.7706
11.0090 11.7766 12.0163 14.7220 15.2332 15.9439 16.1375 17.0318
17.0654 17.1535 17.3821 17.8705 17.9813 18.4112
k = 0.3750 0.0000 0.0815 (1228 PWs) bands (ev):
-134.3560-134.1955-134.0820 -86.3106 -86.2345 -85.9170 -85.6968 -85.6844
-85.5148 -85.4103 -84.9834 -84.8832 -19.7351 -13.9404 -13.9221 -10.9721
-10.9118 -10.6321 -10.5496 -10.4748 -10.1871 -9.8974 -3.3605 -3.3506
-3.1340 0.4557 0.6347 0.7274 0.7487 1.0576 1.0832 3.9319
4.1327 4.2264 4.5586 5.7297 5.9812 6.2709 6.3973 6.4926
6.5503 6.9034 6.9996 7.2695 7.3644 7.6488 7.7879 8.2020
8.2455 8.3821 8.5517 8.6751 8.7772 8.8946 9.0881 9.1417
9.1501 9.3346 9.3838 9.4985 9.5397 9.7531 9.8394 10.0460
10.3398 10.7610 11.3545 14.4770 15.0838 15.8710 16.1217 16.8916
16.9069 17.1483 17.4864 17.7198 17.8773 18.3422
k = 0.3750 0.0000-0.1631 (1232 PWs) bands (ev):
-134.3569-134.2259-134.1559 -86.3660 -86.1940 -86.1054 -86.0450 -85.7758
-85.6304 -85.4368 -84.9273 -84.8414 -19.7352 -13.9415 -13.9209 -10.9700
-10.9112 -10.6414 -10.5665 -10.4594 -10.1925 -9.8969 -3.3608 -3.3519

-3.1356 0.4593 0.6358 0.7190 0.7481 1.0562 1.0836 3.5234
4.1089 4.4012 4.6767 4.7264 5.3499 5.4536 6.1954 6.1984
6.2837 6.5418 6.9004 7.2167 7.5726 7.5870 7.9982 8.3515
8.4551 8.5444 8.6346 8.6618 8.7024 8.7668 8.9812 9.1006
9.1552 9.4777 9.4874 9.6300 9.7807 9.8599 10.0005 10.0212
10.0628 10.3795 10.4856 14.3597 15.1200 15.9421 16.1115 16.8248
16.8833 17.3176 17.5740 17.6192 17.6268 18.3194
k = 0.3750 0.1237 0.0000 (1225 PWs) bands (ev):
-134.3003-134.1601-134.0293 -86.2816 -86.1244 -86.0922 -85.9531 -85.5515
-85.0253 -85.0061 -84.9834 -84.8802 -19.7241 -13.9258 -13.9091 -10.9386
-10.9024 -10.6186 -10.5682 -10.4858 -10.1781 -9.9120 -3.3598 -3.3268
-3.2007 0.4592 0.5515 0.6703 0.7497 0.9401 0.9591 3.8374
4.1255 4.5468 4.7596 5.3100 5.6754 5.7859 6.2608 6.4178
6.7951 6.8482 7.3316 7.3320 7.5039 7.8722 8.0016 8.1967
8.2458 8.4050 8.4595 8.5181 8.7141 8.8042 9.0598 9.1752
9.2225 9.6795 9.7569 9.9088 9.9661 10.0523 10.1256 10.3669
10.5559 11.5911 12.5922 14.2952 15.1088 15.4109 16.4681 16.8034
17.1617 17.1877 17.5341 18.0270 18.0479 18.4507
k = 0.3750 0.1237 0.0815 (1229 PWs) bands (ev):
-134.4004-134.1774-134.0668 -86.4027 -86.2862 -86.1039 -86.0139 -85.4916
-85.2668 -85.1316 -85.0605 -84.9839 -19.7243 -13.9269 -13.9081 -10.9318
-10.9066 -10.6195 -10.5826 -10.4807 -10.1864 -9.9138 -3.3598 -3.3290
-3.2021 0.4599 0.5532 0.6709 0.7392 0.9393 0.9584 3.2664
3.7990 4.1433 4.5771 5.0111 5.4284 5.9079 6.0410 6.3314
6.4697 6.7289 7.0031 7.1232 7.1635 7.6459 7.8639 8.0390
8.2871 8.3671 8.4453 8.5940 8.7568 8.9208 9.0678 9.4345
9.4854 9.5589 9.6882 9.8358 9.9447 10.0824 10.2514 10.5556
10.8124 11.4343 11.8780 14.3221 15.0657 15.2891 16.0698 16.8729
17.0470 17.1617 17.5668 17.9407 18.0530 18.2124
k = 0.3750 0.1237-0.1631 (1222 PWs) bands (ev):
-134.2684-134.1437-133.9744 -86.2895 -86.2298 -85.7520 -85.6859 -85.6273
-85.1979 -84.8768 -84.8053 -84.7960 -19.7242 -13.9277 -13.9069 -10.9293
-10.8893 -10.6078 -10.5939 -10.4679 -10.1883 -9.8982 -3.3587 -3.3282

-3.2012 0.4646 0.5575 0.6759 0.7325 0.9419 0.9606 3.7583

4.0656 4.3039 4.9538 5.0382 5.6469 5.7455 5.8968 6.4643

6.6197 7.0080 7.2313 7.5368 7.8917 7.9652 8.1385 8.1935

8.5018 8.6293 8.7513 8.8275 8.9724 9.0164 9.4244 9.5012

9.6660 9.9618 9.9666 10.1296 10.3023 10.3533 10.8081 10.8767

11.0079 11.3924 11.6046 14.4711 15.0517 15.5678 15.6130 16.9753

17.0746 17.3098 17.6601 17.7476 17.8595 18.2586

k = 0.3750 0.2475 0.0000 (1231 PWs) bands (ev):

-134.3490-134.1897-134.1462 -86.3671 -86.3080 -85.9060 -85.8229 -85.6985

-85.5882 -85.4439 -85.0814 -84.8443 -19.6983 -13.8916 -13.8751 -10.9001

-10.8500 -10.7108 -10.5144 -10.5032 -10.1887 -9.9846 -3.3611 -3.3419

-3.2971 0.3671 0.4042 0.5540 0.6759 0.6781 0.7792 3.2720

3.8891 3.9166 4.4400 4.5479 5.1578 5.5065 5.7751 6.3684

6.5391 6.6454 6.7391 6.9399 7.0660 7.7622 7.8148 8.1000

8.3429 8.4596 8.4755 8.6028 8.7809 9.0749 9.1627 9.2519

9.3478 9.6824 9.7666 9.8117 9.9936 10.1951 10.3195 10.7542

11.1131 12.1496 12.2669 13.7815 14.5164 15.3747 16.5179 16.7061

17.1195 17.2993 17.3121 17.5708 18.1889 18.4221

k = 0.3750 0.2475 0.0815 (1228 PWs) bands (ev):

-134.3028-134.1601-134.1002 -86.3846 -86.3708 -86.0649 -85.6282 -85.5467

-85.4653 -85.2671 -84.9431 -84.7862 -19.6983 -13.8921 -13.8746 -10.8975

-10.8586 -10.7043 -10.5261 -10.4860 -10.1842 -9.9847 -3.3611 -3.3429

-3.2967 0.3673 0.4068 0.5633 0.6695 0.6838 0.7710 3.4013

3.5277 4.0389 4.5184 4.6652 5.2560 5.5391 5.7442 5.9910

6.5397 6.7726 7.1072 7.4441 7.6035 7.7659 7.8598 7.8982

8.2130 8.4622 8.6311 8.6460 8.7115 9.0699 9.1774 9.3770

9.6222 9.6820 9.9078 9.9238 10.2143 10.4390 10.6076 10.9483

11.1108 12.3469 12.8670 14.0784 14.5945 15.3617 16.0310 16.8359

17.0790 17.2409 17.4508 17.7797 18.2306 18.4108

k = 0.3750 0.2475-0.1631 (1224 PWs) bands (ev):

-134.2551-134.1143-134.0505 -86.2292 -86.0379 -85.9901 -85.7524 -85.7199

-85.4978 -84.8148 -84.8090 -84.7701 -19.6984 -13.8927 -13.8740 -10.8976

-10.8574 -10.6995 -10.5415 -10.4695 -10.1840 -9.9804 -3.3598 -3.3415

-3.2971 0.3701 0.4077 0.5725 0.6623 0.6879 0.7635 3.4589
3.6461 4.1195 4.6787 4.7666 4.7887 5.5384 5.8518 6.4917
6.6845 7.1013 7.2359 7.5799 7.5921 7.9888 8.0033 8.3596
8.5440 8.6355 8.7545 8.8000 8.8891 8.9466 9.1067 9.3718
9.6402 9.6742 9.9110 10.0682 10.2953 10.3800 10.5755 10.9465
11.9101 12.7679 13.6187 14.4530 14.5039 15.5676 15.5930 16.8599
17.1029 17.2843 17.4946 17.8159 18.3330 18.4486
k = 0.3750 0.3712 0.0000 (1223 PWs) bands (ev):
-134.2702-134.0854-134.0428 -86.1721 -85.8919 -85.5691 -85.4703 -85.4240
-85.3936 -85.2805 -85.2061 -85.1079 -19.6719 -13.8565 -13.8405 -10.9025
-10.7828 -10.7504 -10.5548 -10.3873 -10.1749 -10.0914 -3.5173 -3.3151
-3.2776 0.2159 0.2476 0.3823 0.4558 0.5543 0.8134 2.9211
3.5766 3.8541 4.0841 4.8250 5.2266 5.7576 5.9358 6.1964
6.2253 6.3248 6.7591 7.0646 7.4903 7.5966 7.8530 8.1328
8.3248 8.6981 8.7661 8.8019 9.0869 9.2948 9.6460 9.7331
9.8298 10.0147 10.2544 10.3501 10.3876 10.5599 10.6643 11.6383
12.2742 13.5856 14.3224 14.7268 14.8223 16.2786 16.4813 16.5802
16.6492 17.2713 17.4259 17.8571 18.4952 18.7671
k = 0.3750 0.3712 0.0815 (1225 PWs) bands (ev):
-134.2753-134.1084-134.0830 -86.1642 -85.8865 -85.8206 -85.7265 -85.4795
-85.4367 -85.3138 -85.1411 -84.9565 -19.6720 -13.8570 -13.8400 -10.9077
-10.7884 -10.7421 -10.5656 -10.3847 -10.1793 -10.0915 -3.5179 -3.3123
-3.2818 0.2189 0.2435 0.3840 0.4505 0.5754 0.7933 2.9267
3.4122 3.9944 4.1966 4.4939 5.4584 5.7751 5.8088 6.1460
6.3254 6.4657 6.8179 7.0562 7.2919 7.6336 8.0169 8.1495
8.3278 8.5257 8.5778 9.0244 9.1059 9.3149 9.3922 9.4419
9.7325 9.8694 10.0359 10.1127 10.2511 10.3578 10.4565 10.9701
12.6652 13.6672 13.7716 14.2909 15.4626 16.2085 16.4061 16.6249
16.8945 17.2223 17.4889 17.8871 18.5051 18.6931
k = 0.3750 0.3712-0.1631 (1214 PWs) bands (ev):
-134.1736-133.9487-133.9300 -85.9255 -85.8838 -85.7216 -85.5534 -85.2108
-85.1710 -84.9540 -84.6244 -84.5855 -19.6718 -13.8571 -13.8395 -10.9044
-10.7712 -10.7522 -10.5483 -10.3714 -10.1731 -10.0836 -3.5154 -3.3134

-3.2758 0.2229 0.2462 0.3917 0.4436 0.6044 0.7720 3.0541
3.4112 3.9858 4.5597 4.7150 5.1509 5.7300 6.2064 6.2143
6.8307 6.8310 7.1023 7.7962 8.1157 8.3794 8.5207 8.5730
8.6814 8.8268 9.1400 9.1745 9.3153 9.5414 9.7550 9.7752
10.0122 10.2706 10.3330 10.4074 10.6338 11.0535 11.1551 11.5765
13.3114 13.9836 14.0199 14.7446 15.5512 16.1998 16.4688 16.6552
17.0407 17.5288 17.6080 17.7154 18.3309 18.8906
k = 0.3750-0.4949 0.0000 (1230 PWs) bands (ev):
-134.4259-134.2605-133.9329 -86.3966 -86.2548 -86.1354 -85.9649 -85.5114
-85.4295 -85.2766 -85.1545 -84.6858 -19.6608 -13.8423 -13.8261 -10.9260
-10.8104 -10.6845 -10.6125 -10.2502 -10.2357 -10.1833 -3.5882 -3.2939
-3.2829 0.1717 0.1897 0.2107 0.3732 0.5533 0.8284 2.7054
3.3541 3.3758 3.8988 3.9431 4.2051 4.2262 5.3309 5.7741
5.8425 6.2527 6.7370 6.9096 7.5452 7.6918 7.9000 8.1741
8.2034 8.9028 8.9213 8.9557 9.3892 9.4364 9.6532 9.7198
9.9628 10.1502 10.1556 10.2693 10.4268 10.4288 10.7997 11.4997
11.8049 13.5642 13.9120 14.3817 15.1219 16.1354 16.3094 16.3979
16.8463 17.5155 17.9396 18.2894 18.3663 18.6607
k = 0.3750-0.4949 0.0815 (1222 PWs) bands (ev):
-134.3199-134.1695-133.8482 -86.0492 -86.0287 -85.9201 -85.7911 -85.5085
-85.4129 -85.0570 -84.9001 -84.5247 -19.6607 -13.8423 -13.8257 -10.9221
-10.8071 -10.6734 -10.6056 -10.2413 -10.2282 -10.1790 -3.5813 -3.2919
-3.2762 0.1688 0.2078 0.2202 0.3737 0.5794 0.8011 2.7987
3.2369 3.6008 4.2530 4.5869 4.7244 5.2765 5.5789 6.3251
6.4815 6.8776 7.0600 7.1090 7.8980 7.9864 8.2340 8.2500
8.5790 8.8870 8.9223 8.9847 9.4191 9.5034 9.6495 9.7604
9.9615 10.1125 10.3625 10.3957 10.4305 10.7115 10.9266 12.2850
12.4490 13.5683 13.9407 14.2711 15.0611 16.3337 16.4212 16.7414
16.9399 17.5876 17.6007 17.9762 17.9907 19.1528
k = 0.3750-0.4949-0.1631 (1228 PWs) bands (ev):
-134.3208-134.1450-134.0949 -86.2610 -86.1444 -85.8724 -85.6889 -85.5133
-85.3011 -85.2867 -85.2611 -85.1066 -19.6609 -13.8426 -13.8255 -10.9281
-10.8204 -10.6762 -10.6086 -10.2453 -10.2259 -10.1825 -3.5841 -3.2961

-3.2793 0.1636 0.2136 0.2140 0.3642 0.6132 0.7673 2.7533

3.0984 3.6133 4.3596 4.6003 4.8900 5.0946 5.7056 5.7755

6.1713 6.3550 6.8782 7.2834 7.5223 7.5889 7.9412 7.9687

8.3767 8.6086 8.8349 8.8626 8.9120 9.4005 9.5275 9.5313

9.7653 9.8597 10.2913 10.3278 10.5223 10.6183 10.8936 11.0247

12.4621 13.4822 13.6436 14.3726 14.8548 16.4239 16.7199 17.0481

17.0638 17.1299 17.4648 17.6435 17.6484 19.2937

k =-0.5000 0.0000 0.0000 (1202 PWs) bands (ev):

-134.0112-133.8436-133.8147 -86.0653 -85.6292 -85.3895 -85.3892 -85.0606

-84.8081 -84.7201 -84.3810 -83.7299 -19.7221 -13.9073 -13.8947 -10.9268

-10.7580 -10.6466 -10.6323 -10.5857 -10.1961 -9.8455 -3.3460 -3.3338

-3.1804 0.4632 0.5865 0.6986 0.7708 1.1044 1.1214 4.2582

4.4525 4.8053 5.3777 6.2333 6.3964 6.4189 6.8660 6.9691

7.1034 7.3339 7.4825 7.5844 7.8480 8.1594 8.5721 8.7859

8.8493 8.8542 9.1203 9.2324 9.3389 9.3805 9.5455 9.6410

9.9743 10.1176 10.2080 10.6161 10.6320 11.1100 12.0083 12.1299

12.1968 12.5563 13.1679 15.1180 15.2538 16.0277 16.1770 17.2733

17.6804 17.8932 17.9781 17.9970 18.4706 18.5962

k =-0.5000 0.0000 0.0815 (1210 PWs) bands (ev):

-134.0978-133.9927-133.8300 -86.1660 -86.0296 -85.7454 -85.6147 -85.3436

-84.9065 -84.6254 -84.3162 -83.9939 -19.7220 -13.9078 -13.8945 -10.9184

-10.7699 -10.7027 -10.5966 -10.5913 -10.1972 -9.8623 -3.3432 -3.3362

-3.1780 0.4736 0.5914 0.6936 0.7553 1.1030 1.1221 3.9869

4.3288 4.7267 4.9887 5.0842 6.1695 6.4118 6.4301 6.7181

6.7768 7.2110 7.2901 7.6116 7.8053 7.8655 8.1218 8.2804

8.6706 8.8907 8.9587 8.9602 9.0587 9.0795 9.4492 9.5036

9.6181 9.7476 9.8057 10.4559 10.5434 11.0654 11.1383 12.1043

12.2396 12.5100 12.6094 15.1632 15.1874 16.0252 16.1657 17.1986

17.4644 17.7877 18.0598 18.0662 18.1516 18.5164

k =-0.5000 0.0000-0.1631 (1208 PWs) bands (ev):

-134.0981-134.0299-133.6910 -86.0175 -85.9964 -85.9862 -85.8685 -84.9376

-84.7144 -84.3284 -84.3173 -84.0830 -19.7219 -13.9080 -13.8939 -10.8945

-10.7717 -10.7252 -10.5890 -10.5815 -10.1935 -9.8596 -3.3408 -3.3372

-3.1793 0.4851 0.5976 0.6894 0.7445 1.1012 1.1239 4.0540
4.3680 4.5481 5.0507 5.4533 6.0891 6.2118 6.4755 6.6180
6.6659 7.0935 7.4058 7.4600 7.5791 7.8260 7.9311 8.0451
8.5278 8.6622 8.9187 9.1339 9.2936 9.3468 9.3802 9.6090
9.6637 9.8023 9.8405 10.4894 10.8079 11.1531 11.2537 11.6444
12.0194 13.8613 14.2208 15.1218 15.1963 16.1275 16.1295 17.1593
17.3062 17.7701 17.8765 18.1562 18.2108 18.4322
k =-0.5000 0.1237 0.0000 (1212 PWs) bands (ev):
-134.1076-133.9563-133.9209 -86.1241 -85.7631 -85.7580 -85.5441 -85.1933
-85.0872 -84.8668 -84.8134 -83.9792 -19.7118 -13.8956 -13.8835 -10.9080
-10.7622 -10.6572 -10.6389 -10.6076 -10.1956 -9.8887 -3.3343 -3.3292
-3.2478 0.4741 0.5164 0.6318 0.7793 0.9349 0.9565 3.9353
4.0202 4.7727 4.8074 5.9502 6.1438 6.3831 6.4772 6.8492
6.8590 7.3322 7.5992 7.7635 8.0049 8.0289 8.0946 8.5801
8.7273 8.8626 8.9905 9.0215 9.0464 9.4182 9.4222 9.5829
9.6849 9.7589 9.7964 10.0816 10.2774 10.7072 10.8544 10.9545
11.5461 12.1759 12.4728 14.5942 14.7823 16.2869 16.4116 17.0239
17.6728 17.8220 18.1314 18.2458 18.2964 18.5713
k =-0.5000 0.1237 0.0815 (1214 PWs) bands (ev):
-134.1650-133.9966-133.8874 -86.2694 -86.0134 -85.7029 -85.5803 -85.3602
-85.0212 -84.8859 -84.6811 -84.0372 -19.7117 -13.8961 -13.8826 -10.9097
-10.7583 -10.6834 -10.6412 -10.5712 -10.2003 -9.8931 -3.3359 -3.3248
-3.2502 0.4846 0.5168 0.6223 0.7649 0.9340 0.9557 3.8317
4.1829 4.5567 5.2731 5.3725 5.7846 5.9541 6.3312 6.6523
7.2316 7.3784 7.5175 7.6589 7.6849 7.8366 8.1385 8.2432
8.5152 8.6535 8.8193 8.8909 8.9720 9.2204 9.3519 9.6385
9.8726 9.9196 10.0450 10.2058 10.5234 10.6539 10.7111 11.4251
11.6599 11.6993 12.3195 14.7226 14.7979 15.9820 16.2383 17.0907
17.6221 18.0117 18.0125 18.1293 18.3199 19.0170
k =-0.5000 0.1237-0.1631 (1216 PWs) bands (ev):
-134.1978-134.0791-133.8474 -86.4448 -86.4198 -85.6588 -85.6431 -85.0127
-85.0108 -84.8574 -84.5049 -84.4289 -19.7118 -13.8967 -13.8820 -10.9028
-10.7654 -10.7105 -10.6385 -10.5548 -10.2074 -9.8971 -3.3374 -3.3253

-3.2546 0.4958 0.5200 0.6158 0.7523 0.9349 0.9571 3.8628
4.1247 4.5281 5.0329 5.4565 5.9741 6.1970 6.4913 6.7049
6.8652 6.8824 7.0798 7.6187 7.6229 7.6948 7.8596 8.2295
8.3665 8.3753 8.7514 8.9409 8.9478 9.1572 9.4970 9.8139
9.9107 9.9466 9.9786 10.1514 10.3221 10.3448 10.9262 10.9809
11.6337 11.9657 12.1570 14.8065 15.3217 15.5218 16.1730 17.2168
17.5986 17.7596 17.9145 18.0714 18.4048 18.4811
k =-0.5000 0.2475 0.0000 (1230 PWs) bands (ev):
-134.4158-134.2969-133.8995 -86.6616 -86.4673 -85.8089 -85.7021 -85.5834
-85.5489 -85.5399 -85.3013 -84.1178 -19.6859 -13.8673 -13.8545 -10.9031
-10.7649 -10.7284 -10.6354 -10.5223 -10.2020 -9.9627 -3.4247 -3.3158
-3.3070 0.3310 0.4718 0.4789 0.5769 0.5778 0.8046 2.9646
3.5802 3.7786 3.9074 4.0461 4.3262 4.6134 6.1077 6.3220
6.6909 6.7061 6.7405 6.9504 6.9547 7.0471 7.1023 7.8281
8.2032 8.2428 8.7458 8.9001 8.9231 9.0530 9.1963 9.2780
9.5325 9.7818 9.8254 10.0241 10.2654 10.2842 10.5622 11.1419
12.3156 12.6798 13.6178 13.9393 14.7553 16.3685 16.7228 17.1512
17.2457 17.2683 17.5901 17.6116 18.2290 19.1288
k =-0.5000 0.2475 0.0815 (1222 PWs) bands (ev):
-134.2610-134.0529-134.0098 -86.2930 -86.2086 -86.1250 -85.4763 -85.3803
-85.1998 -85.0538 -84.7991 -84.6595 -19.6858 -13.8671 -13.8539 -10.8849
-10.7545 -10.7287 -10.6421 -10.5166 -10.1908 -9.9629 -3.4169 -3.3149
-3.3006 0.3397 0.4697 0.4961 0.5831 0.5907 0.7922 3.2930
3.5082 4.0803 4.5253 4.8961 5.4505 5.9468 6.3001 6.3880
6.4011 6.7705 7.1029 7.1705 7.6133 7.6785 7.8162 7.8497
8.2171 8.4696 8.7358 8.8298 8.9232 9.1898 9.3906 9.4035
9.8611 9.9607 9.9782 10.0747 10.2854 10.6254 10.7759 11.2603
11.4810 13.0748 13.5827 13.9790 14.4655 15.9722 16.4705 17.2203
17.2981 17.4253 17.8071 18.0298 18.4068 19.1032
k =-0.5000 0.2475-0.1631 (1220 PWs) bands (ev):
-134.2205-134.0428-134.0184 -86.3101 -86.2283 -86.1219 -85.3821 -85.2808
-85.2423 -84.9810 -84.6897 -84.6756 -19.6859 -13.8675 -13.8536 -10.8724
-10.7491 -10.7254 -10.6501 -10.5110 -10.1946 -9.9488 -3.4170 -3.3120

-3.2988 0.3420 0.4594 0.5156 0.5837 0.5851 0.7763 3.3884
3.4485 4.2190 4.4174 4.8628 5.5045 6.2203 6.5344 6.5384
6.9033 7.0188 7.0920 7.5586 7.6672 7.7612 7.9083 8.0291
8.2121 8.2441 8.7474 8.8435 8.9994 9.0661 9.3673 9.6758
9.8125 10.1821 10.2111 10.2126 10.4251 10.5674 10.6265 10.7174
11.3919 12.9356 13.6999 14.0249 14.5956 15.4840 16.3031 17.1459
17.3391 17.4095 17.9671 18.2366 18.6727 18.9172
k =-0.5000 0.3712 0.0000 (1218 PWs) bands (ev):
-134.2992-134.0934-133.8027 -86.1492 -85.8333 -85.5424 -85.5118 -85.4985
-85.2881 -85.0755 -84.9427 -84.5211 -19.6595 -13.8372 -13.8246 -10.8716
-10.8674 -10.6705 -10.5957 -10.3912 -10.1707 -10.0804 -3.5845 -3.2965
-3.2763 0.1546 0.2352 0.2652 0.3346 0.5135 0.8379 2.7489
3.4468 4.1007 4.3649 4.9830 5.1213 5.1591 5.9418 5.9712
6.1879 6.2445 6.9890 7.1756 7.6716 7.7634 8.1923 8.2771
8.4060 9.0008 9.0732 9.2784 9.4417 9.5232 9.7843 9.9069
9.9805 10.2999 10.3775 10.3843 10.3939 10.5589 11.2263 12.3794
13.2701 13.4416 14.3110 15.1952 15.8495 16.3651 16.3878 16.9736
17.1645 17.3106 17.5732 17.7619 18.4093 19.2707
k =-0.5000 0.3712 0.0815 (1222 PWs) bands (ev):
-134.3320-134.1463-133.8670 -86.3698 -86.1097 -85.6561 -85.5998 -85.5396
-85.2088 -85.0818 -84.8615 -84.8417 -19.6597 -13.8379 -13.8243 -10.8707
-10.8695 -10.6738 -10.5995 -10.3952 -10.1760 -10.0812 -3.5823 -3.2938
-3.2780 0.1608 0.2314 0.2594 0.3266 0.5416 0.8062 2.7956
3.2760 3.9758 4.2906 4.3461 4.5848 5.0963 5.7481 6.0707
6.2354 6.4644 6.6910 7.2760 7.8274 7.8923 8.1943 8.2490
8.4996 8.7550 8.8357 9.1292 9.3191 9.3653 9.5162 9.8198
9.9258 10.0495 10.2189 10.3604 10.3773 10.5275 10.9880 11.8108
12.7845 13.4696 14.1336 15.0895 15.5338 16.3654 16.4609 16.8972
17.2404 17.4314 17.5265 17.5875 18.9012 19.0806
k =-0.5000 0.3712-0.1631 (1220 PWs) bands (ev):
-134.2006-134.0297-134.0277 -86.1648 -85.8031 -85.7330 -85.4915 -85.3842
-85.2769 -85.1103 -84.9417 -84.9216 -19.6596 -13.8380 -13.8241 -10.8745
-10.8727 -10.6734 -10.6006 -10.3805 -10.1768 -10.0861 -3.5842 -3.2921

-3.2767 0.1757 0.2294 0.2707 0.3184 0.5760 0.7733 2.7673
3.1002 4.0593 4.3525 5.4625 5.5173 5.6188 5.8283 5.9301
6.2372 6.4245 6.6581 7.0128 7.3525 7.5730 8.0943 8.2013
8.6685 8.6852 8.6963 8.8356 9.2036 9.3032 9.5014 9.8700
9.9939 10.1491 10.3694 10.4293 10.4572 10.6518 10.8600 11.4818
13.4716 13.5347 13.6060 15.6839 15.7195 16.4274 16.5874 17.0548
17.2266 17.5274 17.6012 17.9184 18.6838 18.8866
k =-0.5000-0.4949 0.0000 (1204 PWs) bands (ev):
-134.2743-133.9563-133.4414 -86.0857 -85.8089 -85.4772 -85.3108 -85.1211
-85.0849 -84.2776 -84.1828 -83.9415 -19.6482 -13.8242 -13.8125 -10.9018
-10.8497 -10.6444 -10.5676 -10.2311 -10.2043 -10.1488 -3.6462 -3.2777
-3.2632 0.0870 0.1232 0.1424 0.2859 0.5194 0.8555 2.6070
3.3911 3.4033 4.0438 5.4103 6.0562 6.2727 6.9911 7.0283
7.1340 7.2284 7.2923 7.7003 8.1770 8.5252 8.5411 8.5816
8.9178 9.1801 9.2888 9.3772 9.5752 9.9706 9.9925 10.0149
10.3539 10.5817 10.6254 10.6722 11.0068 11.2935 11.8344 13.3330
14.1069 14.6926 14.8552 15.6663 16.0237 16.0352 16.5853 16.6280
16.9543 17.5908 18.2513 18.6799 18.7647 19.1001
k =-0.5000-0.4949 0.0815 (1232 PWs) bands (ev):
-134.6661-134.1620-133.8606 -86.9887 -86.4001 -86.2162 -85.6894 -85.6797
-85.2819 -85.1433 -85.0445 -84.7232 -19.6485 -13.8255 -13.8122 -10.9270
-10.8736 -10.6631 -10.5865 -10.2538 -10.2289 -10.1895 -3.6627 -3.2841
-3.2683 0.0717 0.1063 0.1435 0.2700 0.5104 0.8083 2.1381
2.5439 3.0256 3.1658 3.1897 4.0786 4.3261 4.5049 5.6351
6.1695 6.4592 6.7892 7.5761 7.5772 7.6556 8.0051 8.1807
8.2084 8.9954 9.1303 9.1460 9.3619 9.3710 9.5238 9.7423
9.7921 10.0954 10.1519 10.2962 10.7821 10.8546 10.9600 11.6514
11.9106 13.2931 13.7576 14.5508 15.9288 16.1091 16.1447 16.6240
17.1802 17.4785 17.6082 17.8354 18.6803 19.1761
k =-0.5000-0.4949-0.1631 (1248 PWs) bands (ev):
-134.9675-134.2521-134.0750 -87.3887 -87.1030 -86.6512 -85.9197 -85.7808
-85.5463 -85.4935 -85.2941 -85.2419 -19.6489 -13.8263 -13.8121 -10.9442
-10.8900 -10.6684 -10.5937 -10.2632 -10.2285 -10.2105 -3.6742 -3.2896

-3.2741 0.0650 0.0990 0.1056 0.2583 0.4755 0.7670 1.3872

2.1313 2.2754 2.6760 2.7909 2.8837 3.2397 4.2265 4.8636

6.1806 6.1852 6.6428 6.9043 7.0995 7.2999 8.0191 8.1978

8.2162 8.2871 8.4302 8.6350 8.7579 9.1017 9.1347 9.4749

9.5257 9.6841 10.0202 10.0561 10.1264 10.6776 10.6886 10.7947

12.2112 13.2425 13.3822 13.3885 14.7011 15.9959 16.5161 16.6930

16.7757 16.8452 17.5485 17.6341 18.4379 18.6886

the Fermi energy is 11.3028 ev

! total energy = -2764.62747912 Ry

estimated scf accuracy < 1.0E-09 Ry

smearing contrib. (-TS) = 0.25915693 Ry

internal energy E=F+TS = -2764.88663605 Ry

The total energy is F=E-TS. E is the sum of the following terms:

one-electron contribution = -1051.10134804 Ry

hartree contribution = 568.34837850 Ry

xc contribution = -267.25292894 Ry

ewald contribution = -864.57396587 Ry

one-center paw contrib. = -1150.30677170 Ry

convergence has been achieved in 21 iterations

Writing output data file ./tmp/BaLaCuO.save/

init_run : 32.05s CPU 32.22s WALL (1 calls)

electrons : 1536.16s CPU 1542.14s WALL (1 calls)

Called by init_run:

wfcinit : 17.90s CPU 17.95s WALL (1 calls)

potinit : 4.24s CPU 4.26s WALL (1 calls)

hinit0 : 8.16s CPU 8.18s WALL (1 calls)

Called by electrons:

c_bands : 1274.99s CPU 1275.71s WALL (21 calls)

sum_band : 164.81s CPU 167.56s WALL (21 calls)

v_of_rho : 4.35s CPU 4.45s WALL (22 calls)

newd : 36.42s CPU 38.86s WALL (22 calls)

PAW_pot : 59.56s CPU 59.62s WALL (22 calls)

mix_rho : 0.30s CPU 0.30s WALL (21 calls)

Called by c_bands:

init_us_2 : 7.27s CPU 7.30s WALL (3225 calls)

cegterg : 1220.15s CPU 1220.84s WALL (1575 calls)

Called by *egterg:

cdiaghg : 102.38s CPU 102.26s WALL (6930 calls)

h_psi : 311.95s CPU 312.56s WALL (7005 calls)

s_psi : 100.95s CPU 101.12s WALL (7005 calls)

g_psi : 0.98s CPU 1.04s WALL (5355 calls)

Called by h_psi:

h_psi:calbec : 128.43s CPU 128.66s WALL (7005 calls)

vloc_psi : 81.67s CPU 82.20s WALL (7005 calls)

add_vuspsi : 100.90s CPU 100.79s WALL (7005 calls)

General routines

calbec : 179.74s CPU 179.97s WALL (8580 calls)

fft : 1.50s CPU 1.48s WALL (284 calls)

ffts : 0.01s CPU 0.01s WALL (43 calls)

fftw : 81.29s CPU 82.15s WALL (734348 calls)

interpolate : 0.16s CPU 0.15s WALL (22 calls)

PWSCF : 26m 8.79s CPU 26m15.63s WALL

This run was terminated on: 12:14:22 22Mar2023

=--=

JOB DONE.

=--=

Appendix II: Input and Output Files for Bands

Input

```
&control
calculation = 'bands'
restart_mode='from_scratch',
prefix='BaLaCuO',
pseudo_dir ='./',
outdir='./tmp'
/
&system
ibrav= 8,
celldm(1) = 7.3962,
celldm(2) = 1.01020408163,
celldm(3) = 3.0663265,
nat=  13,
ntyp= 4,
ecutwfc =30,
nbnd= 78,
occupations='tetrahedra',smearing='marzari-vanderbilt', degauss=0.1
ecutrho=300.0,
/
&electrons
diagonalization='david'
mixing_mode = 'plain'
mixing_beta = 0.5
conv_thr =  1.0d-8
/
&ions
ion_dynamics='bfgs',
/
&cell
cell_dynamics = 'bfgs'
```

/

ATOMIC_SPECIES

Ba 137.327 Ba.pbe-spn-kjpaw_psl.1.0.0.UPF

La 138.905 La.pbe-spfn-kjpaw_psl.1.0.0.UPF

Cu 63.546 Cu_pbe_v1.2.uspp.F.UPF

O 15.99 O.pbe-n-kjpaw_psl.0.1.UPF

ATOMIC_POSITIONS (crystal)

Ba 0.5000000000 0.5000000000 0.1800261782

Ba 0.5000000000 0.5000000000 0.8199738218

Cu 0.0000000000 0.0000000000 0.0000000000

Cu 0.0000000000 0.0000000000 0.3358903234

Cu 0.0000000000 0.0000000000 0.6641096766

La 0.5000000000 0.5000000000 0.5000000000

O 0.0000000000 0.0000000000 0.1595006994

O 0.0000000000 0.0000000000 0.8404993006

O 0.0000000000 0.5000000000 0.3674702691

O 0.0000000000 0.5000000000 0.6325297309

O 0.5000000000 0.0000000000 0.3672392735

O 0.5000000000 0.0000000000 0.6327607265

O 0.0000000000 0.5000000000 0.0000000000

!CELL_PARAMETERS (angstrom)

! 3.91735712438023 -0.00000000000000 0.00000000000000

! 0.00000000000000 3.96247794916463 0.00000000000000

! 0.00000000000000 0.00000000000000 12.01828059166546

K_POINTS automatic

8 8 4 0 0 0

Output

Program DOS v.6.7MaX starts on 10Jun2024 at 11:23:26

This program is part of the open-source Quantum ESPRESSO suite for quantum simulation of materials; please cite

"P. Giannozzi et al., J. Phys.:Condens. Matter 21 395502 (2009);

"P. Giannozzi et al., J. Phys.:Condens. Matter 29 465901 (2017);

URL http://www.quantum-espresso.org",
in publications or presentations arising from this work. More details at
http://www.quantum-espresso.org/quote
Serial version
Reading XML data from the directory:
./BaLaCuO.save/
file Ba.pbe-spn-kjpaw_psl.1.0.0.UPF: wavefunction(s) 5S 6S renormalized
file La.pbe-spfn-kjpaw_psl.1.0.0.UPF: wavefunction(s) 5S 5D 4F renormalized
file O.pbe-n-kjpaw_psl.0.1.UPF: wavefunction(s) 2P renormalized

IMPORTANT: XC functional enforced from input :
Exchange-correlation= PBE
(1 4 3 4 0 0 0)
Any further DFT definition will be discarded
Please, verify this is what you really want

G-vector sticks info
---
sticks: dense smooth PW G-vecs: dense smooth PW
Sum 1313 261 89 109985 9795 1909
Check: negative core charge -0.000005
Gaussian broadening (read from file): ngauss,degauss= -1 0.100000

DOS : 13.92s CPU 14.11s WALL

This run was terminated on: 11:23:40 10Jun2024
=--=
JOB DONE.
=--=

Appendix III: KUREC Clearance Letter

KABARAK UNIVERSITY RESEARCH ETHICS COMMITTEE

Private Bag - 20157
KABARAK, KENYA
Email: kurec@kabarak.ac.ke

Tel: 254-51-343234/5
Fax: 254-051-343529
www.kabarak.ac.ke

OUR REF: KABU01/KUREC/001/04/07/24

Date: 5th July, 2024

Seville Cherotich
Reg No: GMP/M/0276/01/22
Kabarak University,

Dear Seville,

RE: FIRST PRINCIPLES COMPUTATION OF ELECTRONIC STRUCTURE, DYNAMICALAND SUPERCONDUCTING PROPERTIES OF PEROVSKITE $LABA_2CU_3O_7$

This is to inform you that ***KUREC*** has reviewed and approved your above research proposal. Your application approval number is ***KUREC-040724.*** The approval period is ***5/07/2024 – 5/07/ 2025.***

This approval is subject to compliance with the following requirements:

i. All researchers shall obtain an introduction letter to NACOSTI from the relevant head of institutions (Institute of postgraduate, School dean or Directorate of research)
ii. The researcher shall further obtain a RESEARCH PERMIT from NACOSTI before commencement of data collection & submit a copy of the permit to **KUREC.**
iii. Only approved documents including (informed consents, study instruments, MTA Material Transfer Agreement) will be used
iv. All changes including (amendments, deviations, and violations) are submitted for review and approval by ***KUREC***:
v. Death and life-threatening problems and serious adverse events or unexpected adverse events whether related or unrelated to the study must be reported to ***KUREC*** within 72 hours of notification;
vi. Any changes, anticipated or otherwise that may increase the risk(s) or affected safety or welfare of study participants and others or affect the integrity of the research must be reported to ***KUREC*** within 72 hours;
vii. Clearance for export of biological specimens must be obtained from relevant institutions and submit a copy of the permit to KUREC;
viii. Submission of a request for renewal of approval at least 60 days prior to expiry of the approval period. Attach a comprehensive progress report to support the renewal and;
ix. Submission of an executive summary report within 90 days upon completion of the study to ***KUREC***

Sincerely,

Prof. Jackson Kitetu PhD.
KUREC-Chairman

Cc Vice Chancellor
DVC-Academic & Research
Registrar-Academic & Research
Director-Research Innovation & Outreach
Institute of Post Graduate Studies

Appendix IV: NACOSTI Research Permit

REPUBLIC OF KENYA

NATIONAL COMMISSION FOR SCIENCE,TECHNOLOGY & INNOVATION

Ref No: **412186**

Date of Issue: **12/August/2024**

RESEARCH LICENSE

This is to Certify that Miss.. CHEROTICH N/A SEVILLE of Kabarak University, has been licensed to conduct research as per the provision of the Science, Technology and Innovation Act, 2013 (Rev.2014) in Kericho, Nakuru on the topic: FIRST PRINCIPLES COMPUTATION OF ELECTRONIC STRUCTURE, DYNAMICAL AND SUPERCONDUCTING PROPERTIES OF PEROVSKITE LABA2CU3O7 for the period ending : 12/August/2025.

License No: **NACOSTI/P/24/38447**

412186

Applicant Identification Number

Director General
NATIONAL COMMISSION FOR SCIENCE,TECHNOLOGY & INNOVATION

Verification QR Code

NOTE: This is a computer generated License. To verify the authenticity of this document, Scan the QR Code using QR scanner application.

See overleaf for conditions

Appendix V: Evidence of Conference Participation

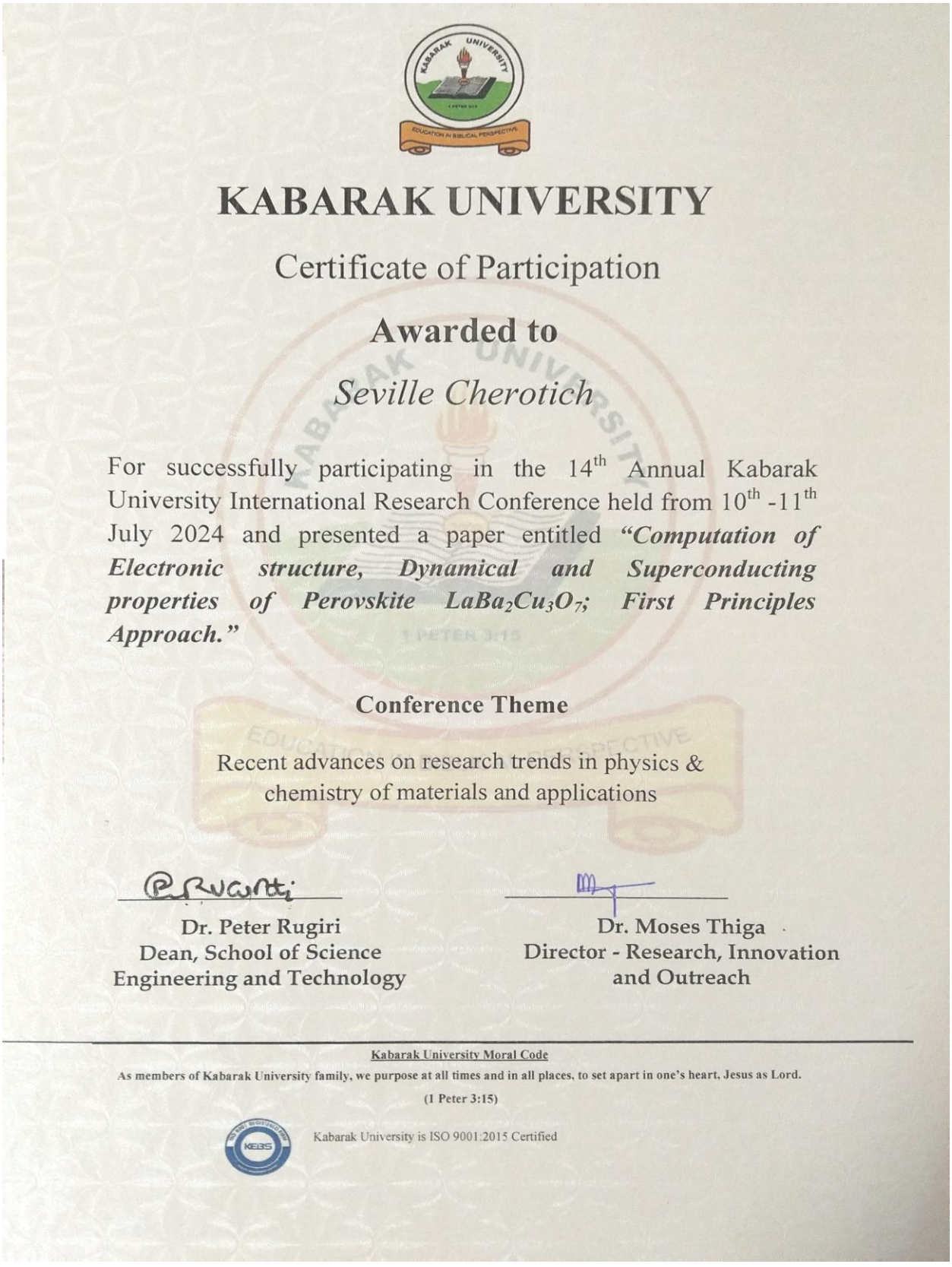

KABARAK UNIVERSITY

Certificate of Participation

Awarded to

Seville Cherotich

For successfully participating in the 14th Annual Kabarak University International Research Conference held from 10th -11th July 2024 and presented a paper entitled ***"Computation of Electronic structure, Dynamical and Superconducting properties of Perovskite $LaBa_2Cu_3O_7$; First Principles Approach."***

Conference Theme

Recent advances on research trends in physics & chemistry of materials and applications

Dr. Peter Rugiri
Dean, School of Science Engineering and Technology

Dr. Moses Thiga
Director - Research, Innovation and Outreach

Kabarak University Moral Code

As members of Kabarak University family, we purpose at all times and in all places, to set apart in one's heart, Jesus as Lord.

(1 Peter 3:15)

Kabarak University is ISO 9001:2015 Certified

Appendix VI: List of Publication

Kabarak Journal of Research & Innovation
www.kabarak.ac.ke

RESEARCH ARTICLE

First Principles Computation of Electronic Structure and Dynamical Properties of Perovskite $LaBa_2Cu_3O_7$

CHEROTICH SEVILLE[1*], Phillip OTIENO NYAWERE[1], & Peter TANUI[2]

1. Department of Physical and Biological Sciences, Kabarak University, P.O. Box Private Bag – 20157 Kabarak, Nakuru, Kenya
2. Department of Educational Sciences, Kabarak University, P.O. Box Private Bag – 20157 Kabarak, Nakuru, Kenya

Correspondence: sevillecherotich@gmail.com

Submitted 12th September, 2024, Accepted 4th October, 2024 and Published 18th February 2025

ABSTRACT

Perovskite materials have attracted research because of their ability to transition from normal metals to superconductors. This study reports electronic structure and dynamical properties of $LaBa_2Cu_3O_7$ perovskite carried out in the framework of density functional theory (DFT) using the Quantum espresso code. This is based on plane wave self-consistent field (PWscf) and ultrasoft pseudopotential (USPP) method as treated in the Perdew-Burke-Ernzerhof (PBE) generalized gradient approximation and local density approximations as implemented in Quantum Espresso Code. The electronic structure uncovers essential aspects such as bandgaps, Fermi surfaces, and density of states, offering valuable insights into the material's behaviour. Under structural properties, optimization of the material's cell dimensions, lattice parameters, k-points, and the kinetic energy cut-off values were properly checked through graphing and accurate values were obtained at the convergence of the ground state energy at minimum convergence threshold. Band structures of $LaBa_2Cu_3O_7$ are similar to that of superconducting perovskites. The results show that $LaBa_2Cu_3O_7$ is orthorhombic structure with lattice parameter calculated to be 3.925 Å which compares well with other works and a band gap of 2.043eV. The valence band is typically dominated by O 2p states, while the conduction band involves Cu 3d states. Phonon calculations shows that the compound is dynamically stable as there are no negative frequencies observed.

Keywords: *Dynamical; Electronic; Perovskite Structure*